SISSA
Scuola
Internazionale
Superiore di
Studi Avanzati

Physics Area - PhD course in
Statistical Physics

Low-energy methods in Statistical Field Theory. From interfaces to quantum quenches.

Candidate:
Marianna Sorba

Advisor:
Prof. Gesualdo Delfino

Academic Year 2023-24

Contents

Foreword

The fact that field theory provides the natural framework for the study and determination of universal properties of statistical systems is very well known. However, the universal quantities that are most often discussed arise in a regime in which the correlation length ξ – which in the study of universality is in any case much larger than the microscopic scales – is the only relevant scale. In particular, the critical exponents can be traced back to properties of the critical point, where the correlation length diverges and the mass $1/\xi$ of the collective excitation modes (particles) of the statistical system tends to zero. From the field theoretical point of view, this is an ultrarelativistic, and then high-energy, regime.

On the other hand, in statistical physics there are problems which naturally involve an additional scale much larger than ξ, so that the relevant physics occurs at low energies. In this case the framework able to provide *exact universal results* – in the limit of interest in which the additional scale is large – is that of the particle description of field theory in which the matrix elements of fields on particle states and their low-energy properties play the key role. In this thesis we will illustrate the power of this theoretical framework through original applications to a number of important and diverse problems in statistical physics.

The first problem we will consider is that of interfaces separating coexisting phases in classical three-dimensional systems at equilibrium, the Ising model providing the reference example. The separation of phases is a macroscopic phenomenon that can only be observed on scales much larger than the bulk correlation length, and then in this case the additional scale responsible for low-energy physics is the linear size R of the interface. We will show how, in the field theoretical formalism, the interface – a surface in three-dimensional systems – is generated by the propagation in imaginary time of a string made of particles (the elementary excitation modes of the bulk theory) and how this leads, among other things, to exact universal results for the order parameter profile.

We will then turn to the problem of systems with boundary conditions inducing the presence of a topological defect line, which we will investigate through the example of the $O(n)$ model in $n+1$ dimensions. Here, the scale $R \gg \xi$ is the length of the defect line, which is produced by the propagation in imaginary time of a topological excitation of the underlying quantum field theory: a kink for the 2D Ising model, a vortex for the 3D XY model, a hedgehog for the 4D Heisenberg model, and so on. We will derive,

in particular, the order parameter profile and, also comparing with the results of recent numerical simulations, we will draw conclusions about the mass of the topological quantum particle.

After these applications to classical spin systems in which the field theoretical time is taken imaginary, we will finally consider a situation in which it is kept real, namely that of non-equilibrium quantum dynamics in isolated systems. In this case the most interesting question is about the fate of the non-equilibrium evolution at large times, and it is this limit that makes low-energy excitations dominant. We will formulate the theory of quantum quenches – both homogeneous and inhomogeneous – in generic space dimensionality and will show under which conditions one-point functions of local operators (e.g. the order parameter) can exhibit oscillations that remain undamped at large times. We will also more generally study the dependence of the dynamics on the initial conditions and will exhibit the mechanisms allowing universal properties to emerge at late times.

The thesis is mainly based on the results obtained in the following research articles:

- G. Delfino, M. Sorba, and A. Squarcini, "Interface in presence of a wall. Results from field theory", *Nuclear Physics B*, vol. 967, p. 115396, 2021.
- G. Delfino and M. Sorba, "Persistent oscillations after quantum quenches in d dimensions," *Nuclear Physics B*, vol. 974, p. 115643, 2022.
- G. Delfino and M. Sorba, "Space of initial conditions and universality in nonequilibrium quantum dynamics", *Nuclear Physics B*, vol. 983, p. 115910, 2022.
- G. Delfino and M. Sorba, "Quantum quenches from an excited state", *Nuclear Physics B*, vol. 994, p. 116312, 2023.
- G. Delfino and M. Sorba, "Mass of quantum topological excitations and order parameter finite size dependence", *Journal of Physics A: Mathematical and Theoretical*, vol. 57, no. 8, p. 085003, 2024.
- G. Delfino and M. Sorba, "On unitary time evolution out of equilibrium", *Nuclear Physics B*, vol. 1005, p. 116587, 2024.

Chapter 1

Preliminary notions

The aim of this preliminary chapter is to concisely recall general concepts of statistical mechanics and field theory, in order to set the stage for the applications of the following chapters.

1.1 Symmetry and universality

In classical statistical mechanics at equilibrium [1], a system is described by the Hamiltonian $\mathcal{H}$ whose value is determined by the configuration of the system. The expectation value of a physical observable $\mathcal{O}$ is expressed by the statistical average on all possible configurations, with weights given by the Boltzmann law[1]

$$\langle \mathcal{O} \rangle = \frac{1}{Z} \sum_{\text{configurations}} \mathcal{O}\, e^{-\mathcal{H}/T}\,, \tag{1.1}$$

where $T \geq 0$ is the temperature of the system and the normalization factor Z is the partition function

$$Z = \sum_{\text{configurations}} e^{-\mathcal{H}/T}\,. \tag{1.2}$$

We focus on systems exhibiting different phases by varying the temperature, namely systems undergoing a phase transition for some critical value T_c of the temperature. To characterize a phase transition we typically use a quantity (*order parameter*) whose expectation value vanishes above T_c while it is a non-vanishing function of T below T_c. In a first order phase transition the order parameter has a discontinuity at T_c, which does not occur in a second order (or continuous) phase transition.

The order parameter of the system is closely related to the symmetry properties of its Hamiltonian. We say that the system possesses a symmetry specified by a group G

[1] We adopt natural units in which $k_B = 1$.

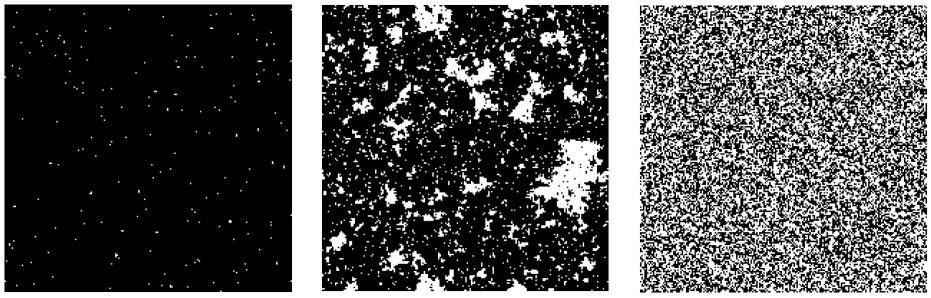

(a) (b) (c)

Figure 1.1: Bidimensional Ising model defined by the Hamiltonian (1.3) for different values of temperature: (a) $T < T_c$, (b) $T = T_c$, (c) $T > T_c$. Spins up $\sigma_i = +1$ are shown in black, spins down $\sigma_i = -1$ are in white. At criticality the system is scale invariant, in the sense that spin configurations cannot be distinguished under a scale transformation (the magnetic structure is fractal).

if $\mathcal{H}$ is left invariant by the action of G. At a temperature $T < T_c$, the order parameter can take different values related by the symmetry, and this is the manifestation of the *spontaneous* symmetry breaking below T_c. The simplest statistical model that exhibits a phase transition, associated to the spontaneous breaking of the symmetry $G = \mathbb{Z}_2$, is the Ising model (see figure 1.1). It is characterized by the Hamiltonian

$$\mathcal{H}_{\text{Ising}} = -J \sum_{\langle i,j \rangle} \sigma_i \sigma_j \,, \qquad \sigma_i = \pm 1 \,, \tag{1.3}$$

where σ_i is a spin variable associated to the i-th site of a regular lattice and the sum is performed over pairs of nearest neighboring sites. We generally refer to the ferromagnetic case for which the coupling constant $J > 0$ and the two lowest energy configurations are those with all spins pointing in the same direction. The $\mathbb{Z}_2$ symmetry of the system corresponds to the reversal of all spins $\sigma_i \to -\sigma_i$ leaving (1.3) invariant. The order parameter $\langle \sigma_i \rangle$ yields the average magnetization of the system. It vanishes above T_c (disordered phase) and can be positive or negative below T_c depending on which of the two ordered phases is selected by spontaneous symmetry breaking. The two-point correlation function $\langle \sigma_i \sigma_j \rangle$ measures the degree of relative alignment between two spins separated by a distance $|i-j|$. The two-point *connected* correlation function, defined as $\langle \sigma_i \sigma_j \rangle_c \equiv \langle \sigma_i \sigma_j \rangle - \langle \sigma_i \rangle^2$, decays as the distance between the two spins increases according to

$$\langle \sigma_i \sigma_j \rangle_c \sim e^{-|i-j|/\xi} \,, \qquad |i-j| \to \infty. \tag{1.4}$$

This asymptotic behavior defines the *correlation length* ξ of the system. At the critical point $T = T_c$ of a second order phase transition, the correlation function instead decays

with the distance between spins according to a power law, corresponding to a divergence of the correlation length as

$$\xi \sim \begin{cases} \xi_0^+ |T - T_c|^{-\nu} , & T \to T_c^+ , \\ \xi_0^- |T - T_c|^{-\nu} , & T \to T_c^- , \end{cases} \tag{1.5}$$

where ν is a critical exponent. The divergence of the correlation length at criticality implies that the system turns out to be *scale invariant*, its microscopic details become irrelevant and a universal behavior emerges. It follows that different statistical systems close to a second order phase transition point exhibit the same universal properties, if they share the symmetry group G of the Hamiltonian and the space dimensionality. We say that these systems belong to the same *universality class*. Critical exponents – of which the correlation length exponent ν is one example – are basic universal quantities. Renormalization group theory [2, 3] has clarified how the divergence of the correlation length at the critical point is responsible for the emergence of universality and how field theory describes critical phenomena.

1.2 Field theoretical formalism

Statistical models are conveniently defined on a lattice, which provides a microscopic length scale given by the lattice spacing a. As previously mentioned, when the system is close to a critical point, its correlation length diverges and, in particular, becomes much larger than the lattice spacing ($\xi \gg a$). Consequently, the universal properties exhibited at criticality are naturally described by means of variables that are smooth on many lattice spacings, in other words, continuous variables. The study of universality classes is thus captured by field theory, which provides such a continuous description (see e.g. [4, 5]).

We consider a d-dimensional statistical system and replace the lattice site i by a point $x = (x_1, ..., x_d)$ in the Euclidean space $\mathbb{R}^d$. It follows that the site-dependent lattice observables become x-dependent fields $\phi(x)$, so we pass from discrete to continuous variables. In particular, in the Ising model (1.3), we substitute the spin variable σ_i with a spin (or order) field $\sigma(x)$ and the energy density $\sum_{j \text{ n.n. of } i} \sigma_i \sigma_j$ with an energy density field $\varepsilon(x)$. The theory is specified in terms of an Euclidean action $\mathcal{A}$, that is a functional of the fields and it is invariant under the operation of the symmetry group G of the system. The action defines the Boltzmann weight of a field configuration needed to compute statistical averages as

$$\langle \mathcal{O} \rangle = \frac{1}{Z} \sum_{\substack{\text{field} \\ \text{configurations}}} \mathcal{O}\, e^{-\mathcal{A}} \sim \frac{1}{Z} \int \mathcal{D}\phi\, \mathcal{O}\, e^{-\mathcal{A}[\phi]} , \tag{1.6}$$

where the partition function now reads

$$Z = \sum_{\substack{\text{field} \\ \text{configurations}}} e^{-\mathcal{A}} \sim \int \mathcal{D}\phi \, e^{-\mathcal{A}[\phi]} \, . \tag{1.7}$$

Notice that the formalism allows to replace sums over lattice variables by functional integrals on fields. As already anticipated, the divergence of the correlation length at a second order phase transition point results into a scale invariant critical point field theory. In the language of renormalization group theory [2, 3], such a theory left invariant by scale transformations is also called *fixed point* theory and its action will be denoted by $\mathcal{A}_{FP}$. In the vicinity of the fixed point the off-critical action is written as

$$\mathcal{A} = \mathcal{A}_{FP} + \sum_i \lambda_i \int d^d x \, \phi_i(x) \, , \tag{1.8}$$

where $\phi_i(x)$ are all G-invariant fields admitted by the theory and λ_i are their conjugated coupling constants measuring the deviations from the fixed point. Since the action is dimensionless, the couplings λ_i scale close to criticality as

$$\lambda_i \sim \xi^{-(d - X_{\phi_i})} \, , \tag{1.9}$$

where X_{ϕ_i} is called *scaling dimension* of the field ϕ_i and is defined by the behavior of the two-point correlation function of the fields $\phi_i(x)$ at the fixed point as

$$\langle \phi_i(x) \phi_i(y) \rangle_{FP} = \frac{\text{constant}}{|x-y|^{2X_{\phi_i}}} \, . \tag{1.10}$$

The field theory described by (1.8) contains infinitely many G-invariant fields with growing scaling dimension. The fields having $X_{\phi_i} > d$ are called "irrelevant" because their conjugated coupling constants have the dimension of a length to a positive power, so they become negligible when the system is observed over distances much larger than the reference length ξ. Since this is the limit in which the system exhibits universal properties, the action (1.8) with all irrelevant fields omitted is called *scaling action* and characterizes the universality class. On the other hand, the fields having scaling dimension $X_{\phi_i} < d$ are named "relevant" as the correspondent coupling constants increase their value at larger distances. A theory may contain several relevant fields, with the result that more than one parameter must be tuned to reach the fixed point. This is the case, for instance, of the Ising field theory specified by the scaling action

$$\mathcal{A}_{\text{Ising}} = \mathcal{A}_{FP} + h \int d^d x \, \sigma(x) + \tau \int d^d x \, \varepsilon(x) \, , \tag{1.11}$$

where h is a magnetic field and τ measures the displacement from the critical temperature, while their conjugate relevant fields are the spin field and the energy density field

respectively. Lastly, the fields of a theory having scaling dimension $X_{\phi_i} = d$, which causes the coupling constants to be dimensionless, are said to be "marginal". In this case, if no logarithmic corrections arise, the addition of such a marginal field contribution to the scaling action preserves scale invariance, generating a line of fixed points parameterized by the coupling λ_i.

1.3 Particle description

In the usual cases we refer to, statistical systems become isotropic in the scaling limit. By means of a Wick rotation [6], one of the real Euclidean coordinates can be made purely imaginary ($x_d = it$) so that the Euclidean field theory in d spatial dimensions becomes a relativistically invariant quantum field theory in $(d-1)$ spatial and one time dimensions. We pass in this way from the Euclidean space with coordinates $x_1, ..., x_d$ to the Minkowski space with coordinates $x_1, ..., x_{d-1}, t$, but the theory keeps the same field content and correlation functions in the two cases are linked by analytic continuation from real to imaginary time. In the quantum field theory formalism, the collective excitation modes of the system above the state of minimal energy (vacuum) correspond to relativistic particles[2] [7]. If M is the mass of a particle, its energy E and momentum $\mathbf{p}$ are related by the dispersion relation $E = \sqrt{M^2 + \mathbf{p}^2}$. An initial state at $t = -\infty$ made of n particles $|\mathbf{p}_1, ..., \mathbf{p}_n\rangle_{\text{in}}$ evolves into a final state at $t = +\infty$ made of m particles $|\mathbf{q}_1, ..., \mathbf{q}_m\rangle_{\text{out}}$. Since we are assuming short range interactions, the initial and final states in which the particles are widely separated in space can be considered *asymptotic* states made of free particles. The asymptotic states are eigenstates of the Hamiltonian H and momentum $\mathbf{P}$ operators of the quantum system with eigenvalues $\sum_{i=1}^{n} E_{\mathbf{p}_i}$ and $\sum_{i=1}^{n} \mathbf{p}_i$ respectively for the incoming state and $\sum_{j=1}^{m} E_{\mathbf{q}_j}$ and $\sum_{j=1}^{m} \mathbf{q}_j$ for the outgoing state. The H and $\mathbf{P}$ operators act as generators of time and space translations, so that for a generic local operator we have

$$\mathcal{O}(\mathbf{x}, t) = e^{i\mathbf{P}\cdot\mathbf{x} + iHt}\, \mathcal{O}(0,0)\, e^{-i\mathbf{P}\cdot\mathbf{x} - iHt}\,. \tag{1.12}$$

The two-point correlation function of a local field can be expanded on the complete basis of asymptotic particles states as[3]

$$\begin{aligned}\langle \mathcal{O}(\mathbf{x}, t)\mathcal{O}(0,0)\rangle &= \langle 0|\mathcal{O}(\mathbf{x}, t)\mathcal{O}(0,0)|0\rangle \\ &= \sum_{n=0}^{\infty} \frac{1}{n!} \int_{-\infty}^{\infty} \prod_{i=1}^{n} \frac{d\mathbf{p}_i}{(2\pi)^{d-1} E_{\mathbf{p}_i}} \left|F_n^{\mathcal{O}}(\mathbf{p}_1, ..., \mathbf{p}_n)\right|^2 e^{-i\left(\sum_{i=1}^{n} E_{\mathbf{p}_i} t + \sum_{i=1}^{n} \mathbf{p}_i \cdot \mathbf{x}\right)},\end{aligned} \tag{1.13}$$

[2] They are sometimes referred to as "quasiparticles" in order to emphasize their character of *collective* excitations for the statistical system.

[3] We adopt the following normalization of asymptotic particle states $\langle \mathbf{q}|\mathbf{p}\rangle = (2\pi)^{d-1} E_{\mathbf{p}} \delta(\mathbf{p} - \mathbf{q})$.

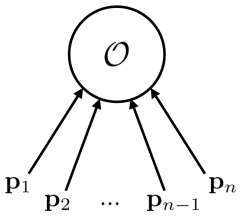

Figure 1.2: Graphical representation of the form factor defined in (1.14).

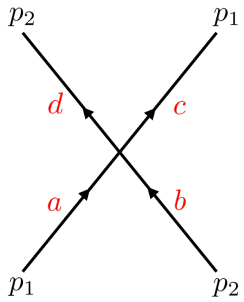

Figure 1.3: Two-particle elastic scattering process in $(1+1)$ dimensions. The indices a, b, c, d denote particle species.

where $|0\rangle$ is the vacuum state and the functions

$$F_n^{\mathcal{O}}(\mathbf{p}_1, ..., \mathbf{p}_n) = \langle 0|\mathcal{O}(0,0)|\mathbf{p}_1, ..., \mathbf{p}_n\rangle \tag{1.14}$$

are called *form factors*. These are, by definition, matrix elements of an operator placed at the origin of the system between an asymptotic particle state and the vacuum state (see figure 1.2). If $F_1^{\mathcal{O}}(\mathbf{p}) = \langle 0|\mathcal{O}(0,0)|\mathbf{p}\rangle \neq 0$ we say that the operator $\mathcal{O}$ creates the particle. In the large spacetime distance limit, (1.13) is dominated by the contribution of the excitation with lowest energy (a single particle at rest). Going in Euclidean space and recalling the definition (1.4) of the correlation length, this leads to the identification

$$M = 1/\xi\,. \tag{1.15}$$

1.3.1 Analytic scattering theory

The probability amplitude that an incoming particle state at $t = -\infty$, defined by a set of energies $\{E_{\mathbf{p}_i}\}$, momenta $\{\mathbf{p}_i\}$ and internal quantum numbers $\{a_i\}$ $(i = 1, ..., n)$, evolves into an outgoing state at $t = +\infty$, characterized by $\{E_{\mathbf{q}_j}\}$, $\{\mathbf{q}_j\}$ and $\{b_j\}$ $(j = 1, ..., m)$, is given by the matrix element

$$\mathcal{S}^{b_1,...,b_m}_{a_1,...,a_n}(\mathbf{q}_1, ..., \mathbf{q}_m|\mathbf{p}_1, ..., \mathbf{p}_n) = {}_{b_1,...,b_m}\langle \mathbf{q}_1, ..., \mathbf{q}_m|\mathcal{S}|\mathbf{p}_1, ..., \mathbf{p}_n\rangle_{a_1,...,a_n}\,. \tag{1.16}$$

The operator $\mathcal{S}$ is named *scattering operator* and the matrix element (1.16) is an element of the so called S-matrix. Since the square modulus of the amplitude (1.16) describes the probability to pass from an initial state $|i\rangle$ to a final state $|f\rangle$ and $\sum_f |\mathcal{S}_{i\to f}|^2 = 1$, it follows that the S-matrix is *unitary*; in operator form, it means

$$\mathcal{S}\mathcal{S}^\dagger = 1\,. \tag{1.17}$$

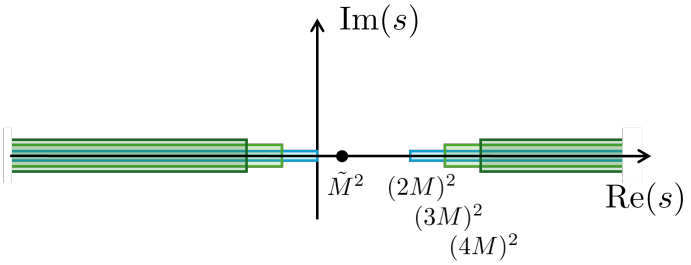

Figure 1.4: Analytic structure of the elastic two-particle scattering amplitude in the complex s-plane. Its singularities are shown on the real axis: branch cuts (the ones relative to unitarity are on the right, those relative to crossing are on the left) and simple poles.

The particle description of a quantum field theory is conveyed by the S-matrix theory [8], which represents the relativistic generalization of the scattering theory in quantum mechanics. In a generic relativistic scattering process, total energy and momentum are conserved, but the number of particles may change after their interaction ($n \neq m$). A scattering process is called "elastic" if it preserves the number of particles and their masses.

We will now illustrate the properties of the S-matrix focusing on the case of scattering theories in (1+1) dimensions, where the analytic structure of the S-matrix becomes simpler. Let us consider, in particular, the two-particle elastic scattering process depicted in figure 1.3, which is the simplest possible scattering event. We consider for simplicity that the two colliding particles have the same mass M. The conservation of total energy and momentum forces the momenta p_1 and p_2 to be individually conserved by the scattering, while any total internal quantum number (such as the total charge) may be redistributed. The scattering amplitude (1.16) is relativistically invariant, so it will be an analytic function of the single relativistic invariant quantity that can be built out of the two energies and momenta, which is the Mandelstam variable

$$s = (E_{p_1} + E_{p_2})^2 - (p_1 + p_2)^2 \,. \tag{1.18}$$

In the reference frame of the center of mass, $p_1 + p_2 = 0$ so that s corresponds to the square of the total energy of the system. The scattering amplitude of the process in fig. 1.3 is denoted $\mathcal{S}_{ab}^{cd}(s)$ and satisfies the following properties [8]:

- The amplitude $\mathcal{S}_{ab}^{cd}(s)$ is an analytic function of the – formally complex – variable s, up to singularities that have a physical meaning. Indeed, in the complex s-plane, there are branch cuts[4] corresponding to the opening of scattering channels and simple poles identifying particle bound states. The branch cuts start at $s = (kM)^2$ with $k = 2, 3, ...$, which are branch points associated to the threshold energy needed for

[4]The branch cuts ultimately originate from the unitarity condition of the S-matrix.

the production of a final state made of k particles with mass M. These cuts originate a nested structure along the real axis of the s-plane (see figure 1.4) and the physical values of the amplitude correspond to the limit

$$\mathcal{S}_{ab}^{cd}(s+i\epsilon) \qquad s\,\text{real}\,,\epsilon\to 0^+\,. \tag{1.19}$$

These paths lie on the "physical" sheet of the Riemann surface associated to the s-plane, while the other "non-physical" sheets are defined by the crossing of one or more cuts. Any simple pole $s=\tilde{M}^2$ located in the interval $0<s<(2M)^2$ corresponds instead to a particle of mass $\tilde{M}$ appearing as a stable bound state of the two particles in the process of figure 1.3.

- A relativistic scattering process satisfies the property of *crossing invariance*. It states that exchanging the role of space and time in figure 1.3, which is possible for a relativistic theory, corresponds to an analytic continuation of the scattering amplitude. More specifically, when passing from the "direct" channel (time running upwards in fig. 1.3) to the "crossed" channel (time running from left to right in fig. 1.3), the particles labeled by b,d become antiparticles $\bar{b},\bar{d}$ with energy and momentum reversed $(-E_{p_2},-p_2)$. Therefore the variable s becomes $4M^2-s$ and the crossing relation reads

$$\mathcal{S}_{ab}^{cd}(s+i\epsilon)=\mathcal{S}_{\bar{d}a}^{\bar{b}c}(4M^2-s-i\epsilon) \qquad s\,\text{real}\,,\epsilon\to 0^+\,. \tag{1.20}$$

  As a consequence of the crossing symmetry, the scattering amplitude acquires on the negative real axis of the s-plane images of the branch cuts and bound state poles already present along the positive real axis.

- The unitarity condition of the S-matrix coming from probability conservation (1.17) translates, in particular, into the following relation for the amplitude of the two-particle elastic scattering

$$\sum_{e,f}\mathcal{S}_{ab}^{ef}(s+i\epsilon)[\mathcal{S}_{ef}^{cd}(s+i\epsilon)]^*=\delta_{ac}\delta_{bd} \qquad (2M)^2<s<(3M)^2\,. \tag{1.21}$$

  Since the values of the scattering amplitude on the upper and lower edge of a branch cut are related by complex conjugation $\mathcal{S}_{ab}^{cd}(s+i\epsilon)=[\mathcal{S}_{ab}^{cd}(s-i\epsilon)]^*$ (a property called *real analyticity*), the unitarity condition can be rewritten as

$$\sum_{e,f}\mathcal{S}_{ab}^{ef}(s+i\epsilon)\mathcal{S}_{ef}^{cd}(s-i\epsilon)=\delta_{ac}\delta_{bd} \qquad (2M)^2<s<(3M)^2\,. \tag{1.22}$$

  From the real analyticity of the scattering amplitude we conclude, in particular, that the amplitude must be real along the uncut segment of the real axis.

Part I

Inhomogeneous systems

Chapter 2

Interfaces in three dimensions

In this chapter we show how low-energy methods of field theory allow to determine universal properties of interfaces in three-dimensional systems, focusing on the paradigmatic example of the Ising model.

2.1 Interface in the Ising model

2.1.1 Introduction

The concept of interface is crucial in different areas of physics. In statistical systems, the spatial separation of different phases is characterized through the formation of an interface. In particle physics, confinement is described in terms of a flux tube (a string) that connects quarks inside hadrons and whose time propagation spans an interface. Lattice discretization directly links these two problems through duality, which relates a spin model to a lattice gauge theory, with the Ising model serving as a fundamental example [9]. Effective descriptions that use interfacial fluctuations as the main degrees of freedom lead to capillary wave theory [10] on one side, and effective string actions [11, 12] on the other.

An important problem in the theory of statistical systems close to criticality is that of providing a fundamental treatment of phenomena involving different length scales. The divergence of the correlation length ξ as the critical temperature T_c is approached is at the origin of universality, namely the existence of quantities such as critical exponents whose values only depend on global properties (internal symmetries and space dimensionality). Field theory then emerges as the natural framework for the quantitative study of universality classes (see e.g. [4, 9]). In particular, the scaling dimensions of the fields, which determine the critical exponents, are related to the behavior of correlation functions at distances much smaller than ξ. On the other hand, below T_c, in a system with discrete internal symmetry, suitable boundary conditions lead to the presence of an interface separating two coexisting phases. The phenomenon requires a length scale R – the linear size of the interface – which is much larger than ξ, since on shorter scales bulk fluctuations do

not allow the emergence of the two distinct phases. There is no doubt that slightly below T_c the full description of the system with the interface should be obtained supplementing with the required boundary conditions the field theory of the bulk (i.e. homogeneous) system. In practice, however, it is far from obvious how to derive analytical results that simultaneously encode scaling and interfacial properties, which are related to short and large distance effects, respectively. It was shown in [13, 14] how the problem can be dealt with in three dimensions within the particle description of field theory.

2.1.2 General setting and interfacial tension

The reduced Hamiltonian of the three-dimensional Ising model is

$$\mathcal{H} = -\frac{1}{T}\sum_{\langle i,j\rangle} s_i s_j \,, \tag{2.1}$$

where the spin variable located at site i of a cubic lattice takes the values $s_i = \pm 1$, and $\langle i, j\rangle$ means that the sum is performed over all pairs of nearest-neighbor sites. We consider values of the temperature T below the critical value T_c, namely in the regime in which the spin reversal $\mathbb{Z}_2$ symmetry of the Hamiltonian (2.1) is spontaneously broken and the absolute value of the magnetization is $|\langle s_i\rangle| = M > 0$, where $\langle\cdots\rangle$ denotes the average over all spin configurations weighted by $e^{-\mathcal{H}}$. More precisely, we consider temperatures only slightly below T_c, in such a way that the large correlation length (it diverges as $\xi \simeq |T - T_c|^{-\nu}$ as $T \to T_c$) allows to take the continuum limit. The latter defines an Euclidean (translationally and rotationally invariant in the three dimensions) field theory that we call the bulk field theory [4, 9]. This Euclidean field theory can also be seen as the analytic continuation to imaginary time of a quantum field theory defined in two space and one time dimensions. Denoting by $r = (x, y, z)$ a point in Euclidean space, we will identify z as the imaginary time direction. In the continuum, the discrete spin variables s_i are replaced by the spin field $s(r)$.

We consider the case in which the system is finite in the z direction, with $|z| < R/2$ and R is much larger than the bulk correlation length ξ, while the size in the x and y directions is infinite in the theoretical analysis. The spin variables at $z = \pm R/2$ are fixed to the values $s_i = 1$ for $x < 0$ and $s_i = -1$ for $x > 0$, whereas they are left unconstrained for $x = 0$. Denoting by $\langle\cdots\rangle_{+-}$ configurational averages with these boundary conditions, it follows that for $z = 0$ and R large we have $\lim_{x\to-\infty}\langle s(r)\rangle_{+-} = M$ and $\lim_{x\to+\infty}\langle s(r)\rangle_{+-} = -M$, being M the bulk magnetization. The two pure phases for $x \to -\infty$ and $x \to +\infty$ are then separated at $x = 0$ by a region spanned by the fluctuations of an interface running between the pinning lines $z = \pm R/2$ and $x = 0$ (figure 2.1).

In order to study the interface, we will exploit the fact that, as we recalled in the introductory chapter, the bulk field theory admits a particle description [7, 15]. The particles correspond to the excitations modes with respect to the ground state (vacuum) of the quantum field theory, and should not be confused with the molecules of a fluid. Since the

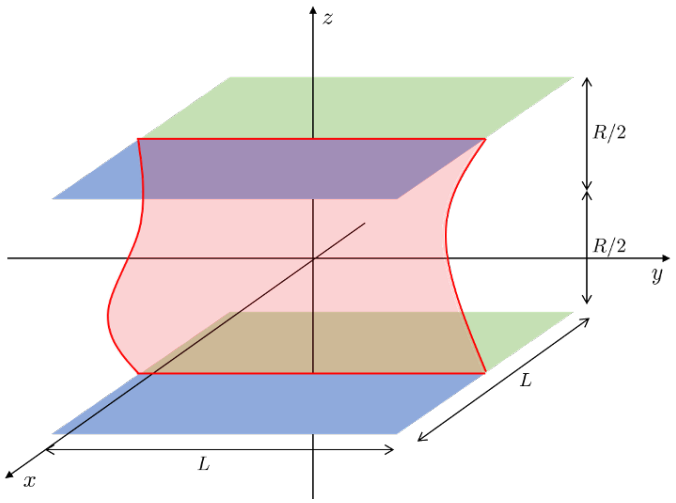

Figure 2.1: Geometry considered in the theoretical derivation, with $L \to \infty$ and R much larger than the bulk correlation length ξ. Boundary spins at $z = \pm R/2$ are fixed to 1 (green) for $x < 0$, -1 (blue) for $x > 0$ and left free for $x = 0$. This induces the presence of an interface (one configuration is shown here) between the axes $x = 0$ on the top and bottom surfaces.

rotational invariance of the bulk Euclidean theory is mapped into relativistic invariance of the quantum theory in $(2+1)$ dimensions, the energy $E_{\mathbf{p}}$ of a particle mode with mass m and momentum $\mathbf{p} = (p_x, p_y)$ obeys the relativistic dispersion relation $E_{\mathbf{p}} = \sqrt{\mathbf{p}^2 + m^2}$. A complete basis onto which generic excitations can be expanded is provided by the asymptotic n-particle states $|\mathbf{p}_1, \mathbf{p}_2, \ldots, \mathbf{p}_n\rangle$ of the bulk theory. These states are eigenstates of the energy and momentum operators H and $\mathbf{P}$ of the quantum theory, with eigenvalues $\sum_{i=1}^n E_{\mathbf{p}_i}$ and $\sum_{i=1}^n \mathbf{p}_i$, respectively. The operators H and $\mathbf{P}$ also act as generators of spacetime translations, and for a generic field $\Phi(r)$ we have

$$\Phi(r) = e^{ixP_x + iyP_y + zH}\, \Phi(0)\, e^{-ixP_x - iyP_y - zH} \,. \tag{2.2}$$

In field theory, interfaces are produced by the propagation of particles between the pinning points [16–18], in the present case the lines $z = \pm R/2$ at $x = 0$. Translation invariance in the y direction implies that the number N of propagating particles is extensive in that direction, and is therefore infinite. In order to regulate our expressions, we will denote by L the size of the system in the y direction, always understanding that $N \propto L \to \infty$. The interface is then spanned by the propagation in the imaginary time direction z of an excitation (a string) containing N/L particles per unit length. The propagation occurs between the states $|B(\pm R/2)\rangle = e^{\pm \frac{R}{2} H} |B(0)\rangle$, called boundary states and corresponding

in the field theory to the boundary conditions that we have imposed at $z = \pm R/2$. They can be expanded over the basis of particle states of the bulk theory in the form [13]

$$|B(\pm R/2)\rangle = \frac{1}{\sqrt{N!}} \int \prod_{i=1}^{N} \frac{d\mathbf{p}_i}{(2\pi)^2\, E_{\mathbf{p}_i}}\, f(\mathbf{p}_1, ..., \mathbf{p}_N)\, e^{\pm \frac{R}{2} \sum_{i=1}^{N} E_{\mathbf{p}_i}}\, \delta\left(\sum_{i=1}^{N} p_{y,i}\right)\, |\mathbf{p}_1, ..., \mathbf{p}_N\rangle + ... \,, \tag{2.3}$$

where $f(\mathbf{p}_1, ..., \mathbf{p}_N)$ is an amplitude, the delta function enforces translation invariance in the y direction and the state normalization $\langle \mathbf{p}|\mathbf{q}\rangle = (2\pi)^2\, E_{\mathbf{p}}\, \delta(\mathbf{p} - \mathbf{q})$ is adopted. For reasons that will become clear in a moment, the contribution that we write explicitly in (2.3) is that of the particles with the lowest mass. The latter is denoted by m and determines the large distance decay of the bulk spin-spin correlation function as $\langle s(r)s(0)\rangle \sim e^{-m|r|}$, a relation that implies

$$\xi = 1/m \,. \tag{2.4}$$

States involving heavier particles enter the expansion (2.3) in the part that we do not write explicitly and, as we will discuss later, they produce only subleading corrections in the large R limit we are interested in.

The partition function Z_{+-} corresponding to our boundary conditions is related to the sum over all configurations of particles propagating between the bottom and top surfaces. It is hence given by the overlap between the two boundary states, namely

$$\begin{aligned} Z_{+-} &= \langle B(R/2)|B(-R/2)\rangle = \langle B(0)|e^{-R\,H}|B(0)\rangle \\ &\sim \frac{L}{2\pi} \int \prod_{i=1}^{N} \frac{d\mathbf{p}_i}{(2\pi)^2\, m}\, |f(\mathbf{p}_1, ..., \mathbf{p}_N)|^2\, \delta\left(\sum_{i=1}^{N} p_{y,i}\right)\, e^{-R\left(Nm + \sum_{i=1}^{N} \frac{\mathbf{p}_i^2}{2m}\right)} \,, \end{aligned} \tag{2.5}$$

where in the last line we exploited the fact that the limit of large R forces all momenta to be small, and used the regularization $\delta(0) = L/2\pi$ following from $2\pi\delta(p) = \int e^{ipy} dy$. Here and in the following the symbol $\sim$ indicates omission of terms subleading for large R. In this limit, the amplitude $f(\mathbf{p}_1, ..., \mathbf{p}_N)$ is projected to a constant defined as

$$f(\mathbf{p}_1, ..., \mathbf{p}_N) \simeq f(0, ..., 0) \equiv f_0 \,, \qquad \mathbf{p}_i, \ldots, \mathbf{p}_N \to 0 \,. \tag{2.6}$$

Therefore we obtain for the partition function (2.5) the expression

$$Z_{+-} \sim \frac{L\, |f_0|^2\, e^{-RNm}}{(2\pi)^{2(N+1)}} \left(\frac{2\pi}{R}\right)^N \sqrt{\frac{2\pi R}{Nm}} \,. \tag{2.7}$$

This result shows, in particular, how a state with a particle of mass m replaced by one of mass $m' > m$ contributes to the large R expansion a term further suppressed by a factor $e^{-(m'-m)R}$.

The interfacial tension σ is the free energy per unit area contributed by the interface $-\ln Z_{+-}/LR$, for both L and R going to infinity. Since the limit $L \to \infty$ is understood, we have

$$\sigma = -\lim_{R\to\infty} \frac{1}{LR} \ln Z_{+-} = \kappa\, m^2 = \frac{\kappa}{\xi^2}\,, \tag{2.8}$$

where

$$\kappa = \frac{N\xi}{L} \tag{2.9}$$

is dimensionless, and then universal, meaning that near criticality it is the same number for different lattice realizations. Notice that our regulators to infinity N and L can enter the measurable quantity (2.9) only in the form of a finite ratio. The number of particles per unit length along the string can be written as $N/L = \sigma\xi = \kappa/\xi$. It follows that there are κ particles per correlation length in the y direction of the string. Since, due to (2.6), in the large R limit required for phase separation, the partition function (2.5) retains no information about the interaction among the particles, we deduce that the large R limit selects weakly interacting and then, in average, widely separated particles. This conclusion perfectly matches with the Monte Carlo determination $\sigma\xi^2 = \kappa = 0.1084(11)$ [19] corresponding to an average interparticle distance $L/N = \xi/\kappa$ in the y direction of about 10 correlation lengths, which means that the interparticle interaction is negligible. It is remarkable that the particle description is able to provide insight on a measurable and universal quantity like κ.

2.1.3 Order parameter profile

The expectation value of a field $\Phi(r)$ at $z = 0$ is given by

$$\begin{aligned} G_\Phi(x) \equiv \langle \Phi(x,y,0)\rangle_{+-} &= \frac{1}{Z_{+-}} \langle B(R/2)|\Phi(x,y,0)|B(-R/2)\rangle \\ &\sim \frac{|f_0|^2}{Z_{+-}N!} \int \prod_{i=1}^{N} \left(\frac{d\mathbf{p}_i}{(2\pi)^2\, m} \frac{d\mathbf{q}_i}{(2\pi)^2\, m} \right) \delta\left(\sum_{i=1}^{N} p_{y,i} \right) \delta\left(\sum_{i=1}^{N} q_{y,i} \right) \\ &\times e^{-\frac{R}{2}\left(2Nm + \sum\limits_{i=1}^{N} \left(\frac{\mathbf{p}_i^2}{2m} + \frac{\mathbf{q}_i^2}{2m} \right) \right) + ix \sum\limits_{i=1}^{N} (p_{x,i} - q_{x,i})} F_\Phi(\mathbf{p}_1, ..., \mathbf{p}_N|\mathbf{q}_1, ..., \mathbf{q}_N)\,, \end{aligned} \tag{2.10}$$

where we used (2.2) to extract the coordinate dependence, the large R limit has again been taken, and the matrix element

$$\begin{aligned} &F_\Phi(\mathbf{p}_1, \ldots, \mathbf{p}_N|\mathbf{q}_1, \ldots, \mathbf{q}_N) = \langle \mathbf{p}_1, \ldots, \mathbf{p}_N|\Phi(0)|\mathbf{q}_1, \ldots, \mathbf{q}_N\rangle \\ &= \langle \mathbf{p}_1, \ldots, \mathbf{p}_N|\Phi(0)|\mathbf{q}_1, \ldots, \mathbf{q}_N\rangle_c + (2\pi)^2 m\, \delta(\mathbf{p}_1 - \mathbf{q}_1) \langle \mathbf{p}_2, \ldots, \mathbf{p}_N|\Phi(0)|\mathbf{q}_2, \ldots, \mathbf{q}_N\rangle_c \\ &+ \ldots \end{aligned} \tag{2.11}$$

is evaluated for small momenta. The second equality in (2.11) expresses the decomposition of the matrix elements into connected (subscript c) and disconnected parts produced by

annihilations of particles on the left with particles on the right [15]; the dots indicate that one has to take into account all possible annihilations. Since the form of (2.10) implies that each power of momentum contributes a factor $R^{-1/2}$, and each annihilation in (2.11) yields a delta function $\delta(\mathbf{p}_i - \mathbf{q}_j)$, and then a factor R, the leading contribution to (2.10) for large R is produced by the maximal number of annihilations. On the other hand, N annihilations just leave a constant C_Φ, so that the leading x-dependence is obtained from $N-1$ annihilations, which can be performed in $N!N$ ways. Taking all this into account, we arrive at the expression [13]

$$G_\Phi(x) \sim C_\Phi + \frac{\kappa\, R}{(2\pi)^2\, m} \int d\mathbf{p}\, d\mathbf{q}\, \delta(p_y - q_y)\, F^c_\Phi(\mathbf{p}|\mathbf{q})\, e^{-\frac{R}{4m}\,(\mathbf{p}^2+\mathbf{q}^2)+ix\,(p_x-q_x)}\,, \tag{2.12}$$

where $F^c_\Phi(\mathbf{p}|\mathbf{q}) \equiv \langle \mathbf{p}|\Phi(0)|\mathbf{q}\rangle_c$. In particular, we see that, if $F^c_\Phi(\mathbf{p}|\mathbf{q})$ behaves for small momenta as a momentum to the power α_Φ, the x-dependent part of (2.12) i.e. $G_\Phi(x) - C_\Phi$ will behave as $R^{-(1+\alpha_\Phi)/2}$. Notice also that the integral term in (2.12) is even (respectively odd) in x when $F^c_\Phi(\mathbf{p}|\mathbf{q})|_{p_y=q_y}$ is even (resp. odd) under exchange of p_x and q_x.

For the spin field $s(r)$ the functional form

$$F^c_s(\mathbf{p}|\mathbf{q})|_{p_y=q_y} = \frac{c_s}{p_x - q_x}\,, \qquad p_x, q_x \to 0 \tag{2.13}$$

was deduced in [13]. When inserting this expression in (2.12) it is convenient to get rid of the pole by differentiating with respect to x. Performing the momentum integrations and integrating back in x with the boundary conditions $\lim_{x\to\pm\infty} G_s(x) = \mp M$ then gives the order parameter (or magnetization) profile

$$G_s(x) \sim -M \mathrm{erf}(\eta)\,, \tag{2.14}$$

with

$$\eta = \sqrt{\frac{2}{R\xi}}\, x \tag{2.15}$$

and $c_s = -2iM/\kappa$. Using (2.2) the calculation can be straightforwardly extended to a generic $z \in (-R/2, R/2)$. The effect is that in (2.14) η is replaced by $\chi = \eta/\sqrt{1-(2z/R)^2}$. The error function in (2.14) already appears in the exact result of the magnetization profile in two dimensions (i.e. in absence of the y axis in figure 2.1), which was obtained from the lattice solution of the Ising model in [20,21] and more recently in field theory in [16]. Despite the overall similarity between the magnetization profiles in two and three dimensions, it must be noted that the factor $\sqrt{2}$ in (2.15) is absent in the two-dimensional result. This is due to the fact that in two dimensions the elementary excitations of the Ising model below T_c are kinks [15] and therefore have a topological nature. Since the spin field is topologically neutral, the lightest state to which it couples is a two-particle one (kink-antikink state [22, 23]) having mass equal to $2m$. It follows that in two dimensions the

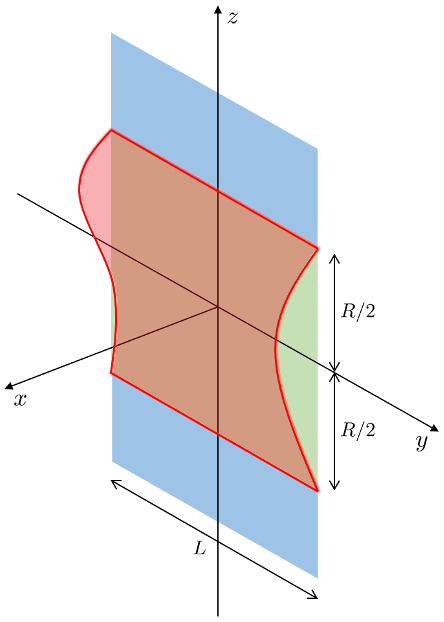

Figure 2.2: Geometry considered for the Ising model below T_c, with $L \to \infty$ in the theoretical analysis and $R \gg \xi$. Spins on the wall $x = 0$ are fixed to 1 (green) for $|z| < R/2$, -1 (blue) for $|z| > R/2$ and left free for $|z| = R/2$. One configuration of the interface running between the boundary condition changing axes $z = \pm R/2$ is shown.

relation (2.4) has to be replaced by $\xi = 1/2m$ and this difference propagates in the results expressed in terms of the correlation length.

The theoretical prediction of the magnetization profile (2.14) was perfectly confirmed by comparison with Monte Carlo data in Ref. [13], in absence of any adjustable parameter. The numerical values of the magnetization were obtained from simulations of the Ising model on a cubic lattice for different values of T and R, while L was taken sufficiently larger than R so to reproduce the infinite L analytical results.

2.2 Interface in presence of a wall

2.2.1 Order parameter profile

We now turn to the case in which the interface can only fluctuate in the half-volume due to the presence of an impenetrable wall. More precisely, we consider the Ising model of the previous section in the half-volume $x \geq 0$, with the spins on the wall $x = 0$ fixed to the values $s_i = 1$ for $|z| < R/2$ and $s_i = -1$ for $|z| > R/2$, where $R \gg \xi$ with ξ being the bulk correlation length defined by (2.4). Denoting by $\langle \cdots \rangle_{+-}$ configurational averages

with these boundary conditions, it is clear that $\lim_{x\to+\infty}\langle s(x,y,0)\rangle_{+-}$ is $-M$ for R finite and M for R infinite. Hence, one expects the presence of an interface pinned along the boundary-condition-changing lines $z=\pm R/2$ on the wall (figure 2.2), separating an inner phase with positive magnetization from an outer phase with negative magnetization, and whose average distance from the wall at $z=0$ diverges with R. In the following we will show how this result indeed emerges within the field theoretical description of the problem.

It is our goal to determine the expectation value $\langle\Phi(x,y,0)\rangle_{+-}$ of a field $\Phi(r)$ in this geometry. As in the previous section, we write the configurational sums in momentum space and interpret the interface and its fluctuations as due to the propagation of particle modes distributed along a string with a density related to the interfacial tension. The string extending for all values of y and whose propagation in the z direction spans the interface corresponds in the field theory to the boundary states (2.3). Correlation functions of fields located in the region $|z|<R/2$ of the system with the interface will be computed between the states $|B(-R/2)\rangle$ and $|B(R/2)\rangle$. It follows that the partition function is given by (2.5), where the required condition $R\gg\xi$ has projected the calculation to a low-energy limit.

So far we took into account that the interface runs between the pinning axes, but not the presence at $x=0$ of a wall that the interface cannot cross. This information has to be carried by the function $f(\mathbf{p}_1,...,\mathbf{p}_N)$, which plays the role of emission/absorption amplitude of the particles at the pinning axes. We then impose that none of the particles stays at $x=0$, namely that $f(\mathbf{p}_1,...,\mathbf{p}_N)$ vanishes when at least one of the momentum components $p_{x,i}$ vanishes. Taking into account that the particles in (2.3) play a symmetric role, and that $f(\mathbf{p}_1,...,\mathbf{p}_N)$ should be analytic in the limit of small momenta required for the calculations at large R, we write

$$f(\mathbf{p}_1,...,\mathbf{p}_N)\simeq f_0\prod_{i=1}^{N}p_{x,i}\,,\qquad \mathbf{p}_i,\ldots,\mathbf{p}_N\to 0\,, \tag{2.16}$$

where f_0 is a constant. Plugging this expression in (2.5) we obtain

$$Z_{+-}\sim\frac{L\,|f_0|^2\,e^{-RNm}}{(2\pi)^{2(N+1)}}\left(\frac{2\pi m}{R^2}\right)^N\sqrt{\frac{2\pi R}{Nm}}\,. \tag{2.17}$$

As it was in (2.7), it again appears from (2.17) how the contribution of a state in which a particle of mass m is replaced by one of larger mass $m'>m$ is suppressed at large R by a factor $e^{-(m'-m)R}$.

The interfacial tension σ is again defined as the free energy per unit area provided by an interface whose size is infinite in both the y and the z directions. Having understood the limit $L\to\infty$, we have

$$\sigma=-\lim_{R\to\infty}\frac{1}{LR}\ln Z_{+-}=\kappa\,m^2=\frac{\kappa}{\xi^2}\,, \tag{2.18}$$

where κ is the universal number (2.9). We notice that the presence of the wall does not affect the interfacial tension since we obtained the same result as (2.8). As we will show in the next section, this is due to the fact that the average distance of the interface from the wall increases with R. Hence, the Monte Carlo determination obtained for the three-dimensional Ising model in absence of the wall [19] continues to hold, resulting in a weak interparticle interaction. This is nicely consistent with our finding that in the large R limit the particle propagation between the pinning axes is only subject to translation invariance in the y direction (delta function in (2.3)) and to the presence of the wall (expression (2.16)).

The one-point functions at $z = 0$ are given by

$$\begin{aligned} G_\Phi(x) \equiv \langle \Phi(x,y,0)\rangle_{+-} &= \frac{1}{Z_{+-}} \langle B(R/2)|\Phi(x,y,0)|B(-R/2)\rangle \\ &\sim \frac{|f_0|^2\, e^{-RNm}}{Z_{+-}N!} \int \prod_{i=1}^{N} \left(\frac{d\mathbf{p}_i}{(2\pi)^2\, m} \frac{d\mathbf{q}_i}{(2\pi)^2\, m}\, p_{x,i}\, q_{x,i} \right) \delta\left(\sum_{i=1}^{N} p_{y,i} \right) \delta\left(\sum_{i=1}^{N} q_{y,i} \right) \\ &\times e^{-\frac{R}{4m} \sum\limits_{i=1}^{N} (\mathbf{p}_i^2 + \mathbf{q}_i^2) + ix \sum\limits_{i=1}^{N} (p_{x,i} - q_{x,i})} F_\Phi(\mathbf{p}_1, ..., \mathbf{p}_N | \mathbf{q}_1, ..., \mathbf{q}_N)\,, \end{aligned} \tag{2.19}$$

where we again consider the large R limit and the matrix elements (2.11) is evaluated for small momenta. It is worth stressing that the matrix element (2.11) refers to the bulk field theory and therefore does not depend on the geometry considered for the interfacial problem. It follows that the observations made in section 2.1 still apply, giving the result

$$G_\Phi(x) \sim C_\Phi + \frac{\kappa\, R^2}{(2\pi)^2\, m^2} \int d\mathbf{p}\, d\mathbf{q}\, p_x\, q_x\, \delta(p_y - q_y)\, F_\Phi^c(\mathbf{p}|\mathbf{q})\, e^{-\frac{R}{4m}(\mathbf{p}^2 + \mathbf{q}^2) + ix\,(p_x - q_x)}\,, \tag{2.20}$$

where $F_\Phi^c(\mathbf{p}|\mathbf{q}) \equiv \langle \mathbf{p}|\Phi(0)|\mathbf{q}\rangle_c$. Using for the spin field the expression (2.13), we again conveniently cancel the pole in $p_x - q_x$ by differentiation with respect to x. Performing then the momentum integrations and integrating back in x with the boundary conditions $\lim\limits_{x\to+\infty} G_s(x) = -M$ and $G_s(0) = M$ we obtain

$$G_s(x) \sim M + 2M \left[\frac{2}{\sqrt{\pi}}\, \eta\, e^{-\eta^2} - \mathrm{erf}(\eta) \right], \tag{2.21}$$

with (2.15) and $c_s = 4iM/\kappa$.

2.2.2 Probabilistic interpretation

The result (2.21) admits a simple probabilistic interpretation once we look at this leading contribution in the large R expansion as due to an interface that sharply separates two pure phases. Then the magnetization at a point $r = (x, 0, 0)$ within a configuration in which the interface intersects the x-axis at a point u can be written as

$$s(x|u) = M\, \theta(u - x) - M\, \theta(x - u)\,, \tag{2.22}$$

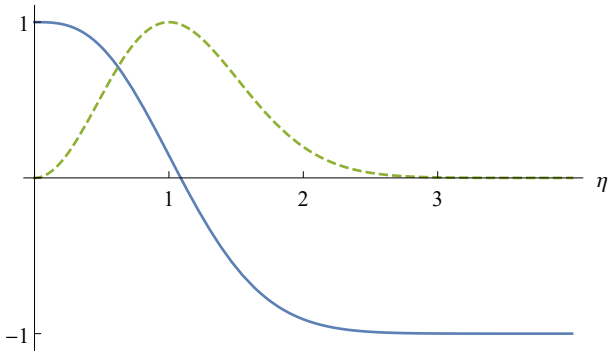

Figure 2.3: Order parameter profile $G_s(x)/M$ (eq. (2.21), continuous blue curve) and passage probability $p(x)/p(\sqrt{R\xi/2})$ (eq. (2.24), dashed green curve).

where $\theta(x)$ is the step function that vanishes for $x < 0$ and equals 1 for $x > 0$. If $p(u)\,du$ is the probability that the interface intersects the x-axis in the interval $(u, u + du)$, then the average magnetization can be written as

$$\overline{s(x)} = \int_0^{+\infty} du\, p(u)\, s(x|u) = M \int_x^{+\infty} du\, p(u) - M \int_0^x du\, p(u)\,. \tag{2.23}$$

This expression coincides with (2.21) for a passage probability density

$$p(x) = 4\sqrt{\frac{2}{\pi R\xi}}\,\eta^2\, e^{-\eta^2}\,, \tag{2.24}$$

which correctly satisfies $p(x) \geq 0$ and $\int_0^{+\infty} dx\, p(x) = 1$. $p(x)$ is maximal at $\eta = 1$ (figure 2.3), showing that the average distance of the interface from the wall increases as $\sqrt{R}$. In addition, $p(0) = 0$ verifies in real space the impenetrability of the wall that we imposed in momentum space through the condition (2.16).

The probabilistic interpretation also illustrates that the fluctuations of the interface in the y direction do not affect the leading term of the local magnetization in the large R expansion. Then it is not surprising that the profile (2.21) is analogous to that known in two dimensions [21, 24, 25], i.e. in absence of the y direction[1]. Once again, however, the factor $\sqrt{2}$ in (2.15) is absent in two dimensions for the reason explained in the case of the full volume.

It must also be observed that the impenetrability of the wall is the only boundary effect that we took into account in our theoretical derivation. In actual measurements (in particular in simulations on the lattice) the value of the order parameter close enough to

[1]The fluctuations in the y direction should show up at leading order in the large R expansion of the spin-spin correlation function, which in two dimensions was obtained in [26].

the wall will be affected by the specific nature of the interaction between the wall and the bulk degrees of freedom. Hence, the results (2.21) and (2.24) hold for x larger than few correlation lengths. Since the main interfacial effects occur around $x \propto \sqrt{R}$, and $R \gg \xi$, they are not affected by boundary details, unless we consider the generalization of the next section.

2.2.3 Binding transition

The system setting considered so far leads to an interface whose average distance from the wall diverges as $\sqrt{R}$. On the other hand, the introduction of a tunable boundary field can lead to a wall-interface interaction sufficiently attractive to determine a binding of the interface to the wall. Conversely, the passage from the binding to the fluctuating regime corresponds to a transition that is most often referred to as "wetting" transition (see [27–29] for reviews). This terminology refers to a liquid-vapor interface, the liquid phase being that internal to the interface.

As we now explain, the particle formalism naturally accounts also for the binding transition. We saw that in the limit relevant for phase separation (linear size of the interface much larger than the bulk correlation length ξ) the interfacial properties are determined by low-energy particle modes whose mutual interaction is negligible due to a large average separation. The interaction of a particle with the wall can be characterized within the scattering framework, in which an incoming particle has momentum $\mathbf{p} = (p_x < 0, p_y)$. At low energy the interaction with the wall is elastic and the particle bounces back with momentum $\mathbf{p} = (-p_x, p_y)$, the component p_y being conserved due to translation invariance in the y direction. The relation $E^2 = \mathbf{p}^2 + m^2$ defines the parameter β such that

$$E = m \cosh \beta \,, \tag{2.25}$$

$$|\mathbf{p}| = m \sinh \beta \,. \tag{2.26}$$

If the particle-wall interaction is sufficiently attractive, the particle will bind to the wall and, as usual in scattering theory [8,30], the bound state corresponds to a value $E_0 < m$ of the energy, namely to $\mathbf{p}^2 < 0$, or $\beta = i\theta_0$ with $\theta_0 \in (0, \pi)$. It follows that in the bound regime the contribution of the interface to the energy per unit length is $\frac{N}{L} m \cos\theta_0 = \sigma \cos\theta_0$, where we used (2.18) and (2.9). Hence, if e is the energy per unit length associated to the wall, the energy per unit length of the wall-interface bound state is

$$\tilde{e} = e + \sigma \cos\theta_0 \,. \tag{2.27}$$

The value of the binding angle θ_0 depends on the strength of the particle-wall interaction, and the unbinding transition occurs at $\theta_0 = 0$, when the binding energy per unit length $\sigma(1 - \cos\theta_0)$ vanishes.

Remarkably, (2.27) accounts for the basic relation of the phenomenological wetting theory [27], namely the equilibrium condition for a liquid drop on the wall, in which $\tilde{e}$ and

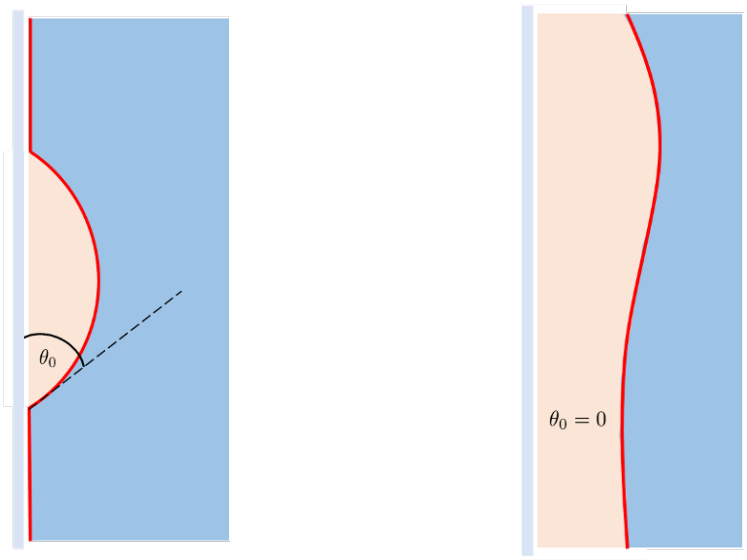

Figure 2.4: In field theory a drop on the wall corresponds to the unbinding and recombination of a wall-interface bound state. The contact angle θ_0 vanishes at the unbinding transition.

e are the wall-vapor and wall-liquid surface tensions, respectively, and θ_0 is the angle that the drop forms with the wall (figure 2.4). The wetting transition occurs at $\theta_0 = 0$, when the drop spreads on the wall.

Consider now the dependence of θ_0 on the parameters of the system. The wall contributes to the Euclidean action of the theory a term $h \int dydz\, \Phi_B(0, y, z)$. Since the action is dimensionless, if X_B is the scaling dimension of the boundary field Φ_B, the coupling h has the dimension of a mass (or inverse length) to the power $2-X_B$. Hence, θ_0 is a function of the dimensionless combination h/m^{2-X_B}, where $m = 1/\xi \sim (T_c - T)^\nu$. For h fixed, the condition $\theta_0 = 0$ determines the unbinding (or wetting) transition temperature $T_w(h) < T_c$. It is clear that for T sufficiently close to T_c, namely for a mass m sufficiently small, the near-critical fluctuations become too strong and the particles have to be unbounded, so that the bound regime corresponds to $T < T_w$. We also see that the interface is unbound for $h = \infty$, which corresponds to the boundary field considered in the previous sections.

It is customary (see [28, 29]) to characterize the transition through the exponent α_S defined for $T \to T_w^-$ by

$$(1 - \cos\theta_0) \propto (T_w - T)^{2-\alpha_S}\,, \tag{2.28}$$

and the transition is said to be continuous if $\alpha_S < 1$. The terminology refers to the continuity of the first derivative of (2.28) at T_w, taking into account that the contact angle θ_0 is phenomenologically set to zero in the unbound regime $T_w < T < T_c$. We can get insight on the exponent α_S recalling that, as usual in scattering theory, the bound state

corresponds to a pole at $E = E_0$ in the scattering amplitude of the particle on the wall (see chapter 1). Then general analytical properties of the amplitude [8,30] tell us that when we move from the bound to the unbound regime, namely when T increases through T_w, the pole does not disappear, but slides through a square root branch point at $E = m$ into a second sheet of the complex energy plane. Within the parametrization $E = m\cos\theta_0$ this corresponds to a continuation from positive to negative values[2] of θ_0, namely to

$$\theta_0 \propto (T_w - T)^{2n+1}\,, \qquad n = 0, 1, 2, \ldots \tag{2.29}$$

in the vicinity of T_w. Comparison with (2.28) then yields

$$\alpha_S = -4n\,. \tag{2.30}$$

Clearly, the generic case is expected to correspond to $n = 0$, and then to $\alpha_S = 0$. As reviewed in [29], this value agrees with numerical simulations within the Ising model[3] [32, 33].

A second exponent $\beta_S < 0$ describes the divergence of the distance of the interface from the boundary,

$$l \propto (T_w - T)^{\beta_S}\,, \tag{2.31}$$

as $T \to T_w^-$. In the scattering framework l is related to the decay $e^{-x/l}$ of the wave function for a distance $x \to \infty$ from the wall in the bound regime. Such a behavior can be seen as originating from the plane wave $e^{ip_x x}$ and the imaginary value of the momentum in the bound regime: $|\mathbf{p}| = im\sin\theta_0$ from (2.26). Close to T_w, where θ_0 is small, one could naively argue $l \propto 1/m\theta_0$, and infer $\beta_S = \alpha_S/2 - 1$ from comparison with (2.28) and (2.31). $\alpha_S = 0$ then leads to $\beta_S = -1$, a value that has been observed experimentally [34]. However, experimental systems include long range interactions that are not present in our framework. The safest comparison is that with simulations within the nearest-neighbor Ising model[4], which are consistent with $l \propto |\ln(T_w - T)|$ (see [32, 33] and the discussion in [36]). This indicates that the fact that $p_x \to 0$ does not imply $|\mathbf{p}| \to 0$ cannot be forgotten. The implication holds instead in two dimensions [37] (i.e. in absence of the y direction), where the values $\alpha_S = 0$ and $\beta_S = -1$ indeed correspond to the exact Ising lattice solution of [21, 38].

[2] Such a continuation is regularly exploited in the context of exact scattering solutions, see [31].

[3] We also notice that the value $\alpha_S \approx -5$ deduced from a phenomenological renormalization group approach (see [29] and references therein) is reminiscent of the case $n = 1$, i.e. $\alpha_S = -4$.

[4] It can be noted that the value $\alpha_S = 0$, which agrees with simulations in the Ising model, is also consistent with the experiment of [35].

Chapter 3

Topological defect lines

In this chapter we consider the spontaneously broken phase of the $O(n)$ vector model in $(n+1)$ dimensions with boundary conditions enforcing the presence of a topological defect line. We derive the exact expression for one-point functions such as the order parameter, in the limit in which the length of the defect line is large, and discuss the implications for the mass of the topological excitation in the underlying quantum field theory.

3.1 Introduction

Some quantum field theories allow for a nontrivial mapping between the ground state manifold and the spatial boundary, and then for topological excitations. These are among the most fascinating objects in quantum field theory [7,39]. Topological excitations correspond to extended configurations of the fields entering the action, a feature which requires nonperturbative methods for their characterization as quantum particles. It is well known that these methods have been available in the case of spacetime dimension $d = 2$, as illustrated by sine-Gordon solitons: on one hand fermionization maps them onto the fundamental fields of the massive Thirring model [40, 41], on the other integrability provides the exact soliton scattering amplitudes [42].

In the last years it has been pointed out that the correspondence – through analytic continuation to imaginary time – between relativistic and Euclidean field theories can be exploited to gain insight into the case $d > 2$ [43, 44]. For this purpose one works in the spontaneously broken phase of the Euclidean theory, with boundary conditions enforcing the presence of a topological defect, and with a finite size R in the imaginary time direction. Then the large R asymptotics of one-point functions such as the order parameter are determined by the state with a single topological particle, and can be obtained analytically [43]. In addition, comparison between these analytical results and their determination in numerical simulations of the corresponding spin system allows the measurement of basic parameters of the theory such as the mass of the topological particle; this program

was illustrated in [44] for the case of the scalar $O(2)$ theory in $d = 3$, which describes the universality class of the superfluid transition (see [45]) and possesses quantum vortex excitations.

More recently, the program of [44] has been carried through in [46,47] for the $O(3)$ scalar theory in $d = 4$. Intriguingly, the numerical simulations showed a scaling dependence on the parameters – the finite size R and the deviation from criticality – markedly different from that observed in [44]. It was shown in [48] that the theory of [43] accounts for both cases, with the difference arising from the fact that the mass of the topological particle is finite in the three-dimensional $O(2)$ model and infinite in the four-dimensional $O(3)$ model. This is due to the passage from the nontrivial renormalization group fixed point of the first case to the Gaussian fixed point of the second. All this is discussed in detail below.

3.2 General setting and partition function

We consider the universality class of $O(n)$-symmetric ferromagnets, whose simplest representative (see e.g. [5]) is the vector model defined by the reduced Hamiltonian

$$\mathcal{H} = -\frac{1}{T} \sum_{<i,j>} \mathbf{s}_i \cdot \mathbf{s}_j \,, \tag{3.1}$$

where T is the temperature, $\mathbf{s}_i$ is a n-component unit vector located at site i of a regular lattice, and the sum is performed over all pairs of nearest neighboring sites. Denoting by T_c the critical temperature, we focus on the regime $T < T_c$ in dimension

$$d = n + 1 \geq 2 \,. \tag{3.2}$$

Then the $O(n)$ symmetry of the Hamiltonian is spontaneously broken, i.e. $\langle \mathbf{s}_i \rangle \neq 0$, with $\langle \cdots \rangle$ denoting the average over spin configurations weighted by $e^{-\mathcal{H}}$.

Close to T_c, where the intrinsic length scale becomes much larger than lattice spacing, the system is described by an $O(n)$-invariant Euclidean scalar field theory, which in turn is the continuation to imaginary time of a quantum field theory in n space and one time dimensions. Switching to notations of the continuum, we denote by $(\mathbf{x}, y)$ a point in Euclidean space, with y the imaginary time and $\mathbf{x} = (x_1, \ldots, x_n)$, and by $\mathbf{s}(\mathbf{x}, y)$ the order parameter field, namely the continuous version of the lattice spin variable $\mathbf{s}_i$. Then the Landau-Ginzburg field theory takes the usual form specified by the action

$$\mathcal{A} = \int d^d x \left\{ [\partial_\mu \mathbf{s}(x)]^2 + g_2 \, \mathbf{s}^2(x) + g_4 [\mathbf{s}^2(x)]^2 \right\} \,, \tag{3.3}$$

with the $O(n)$ critical point reachable tuning the couplings (see e.g. [5]). Since the ground state manifold and the space boundary both correspond to the sphere S^{n-1}, the quantum theory possesses particle excitations associated with extended field configurations, with

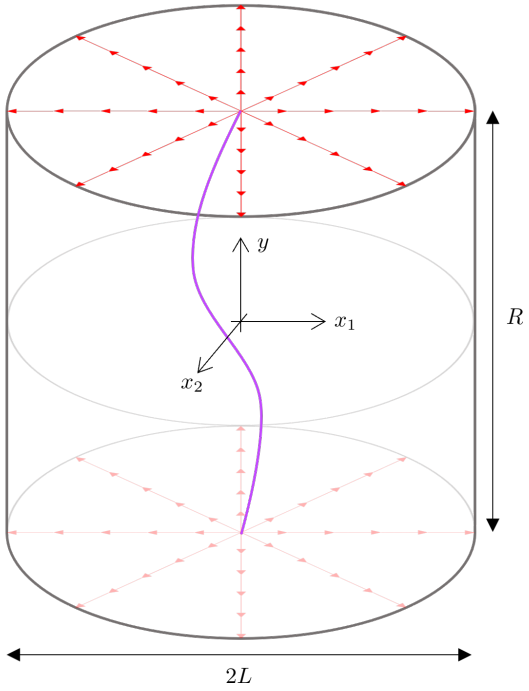

Figure 3.1: Geometry considered in the text ($n = 2$), where it is understood that $L \to \infty$. The spins on the top and bottom surfaces are fixed to point radially outwards, so that a topological defect line (one configuration is shown) runs between the central points of these surfaces.

different points on the space boundary mapped onto different ground states. Such topological excitations are kinks in the 2D Ising model ($n = 1$), vortices in the 3D XY model ($n = 2$), hedgehogs in the 4D Heisenberg model ($n = 3$), and so on. The propagation of these particles in imaginary time generates topological defect lines for the Euclidean system.

We consider the system in the hypercylinder $|\mathbf{x}| \leq L$, $|y| \leq R/2$, with $L \to \infty$ and R large but finite. The boundary conditions are chosen in such a way that the spin field $\mathbf{s}(\mathbf{x}, y)$ points outwards in the radial direction $\mathbf{x}/|\mathbf{x}| \equiv \hat{\mathbf{x}}$ on the hypersurfaces $|\mathbf{x}| = L$, $|y| < R/2$, and $0 < |\mathbf{x}| \leq L$, $y = \pm R/2$. This leads to the formation of a topological defect on each section with constant y, with the defect center spanning as y varies a line (particle trajectory) running between the endpoints at $\mathbf{x} = 0$, $y = \pm R/2$. The system geometry and boundary conditions[1] are illustrated in fig. 3.1 for the case $n = 2$.

[1] As long as the topology is preserved and the $L \to \infty$ limit is considered, the system geometry does not need to be cylindrical for comparison with our subsequent analytical results in the continuum limit; see [44] for a parallelepiped realization which is equivalent for our purposes.

The boundary conditions at $y = \pm R/2$ act as boundary states $|B(\pm R/2)\rangle = e^{\pm\frac{R}{2}H}|B(0)\rangle$ of the Euclidean time evolution, where H denotes the Hamiltonian of the relativistic quantum system. These boundary states can be expanded on the basis of asymptotic particle states of the quantum field theory[2], and will contain the topological particle τ as the contribution with minimal energy, namely

$$|B(\pm R/2)\rangle = \int \frac{d\mathbf{p}}{(2\pi)^n E_{\mathbf{p}}}\, a_{\mathbf{p}}\, e^{\pm\frac{R}{2}E_{\mathbf{p}}}\, |\tau(\mathbf{p})\rangle + \cdots\,, \tag{3.4}$$

where $\mathbf{p}$ is the n-component momentum of the particle, $E_{\mathbf{p}} = \sqrt{\mathbf{p}^2 + m_\tau^2}$ its energy, m_τ its mass, $a_{\mathbf{p}}$ an amplitude, and we normalize the states by $\langle\tau(\mathbf{p}')|\tau(\mathbf{p})\rangle = (2\pi)^n E_{\mathbf{p}}\,\delta(\mathbf{p}-\mathbf{p}')$. In the calculations performed with the boundary conditions we have chosen (which we will indicate with a subscript $\mathcal{B}$) the contribution in (3.4) with one topological particle determines the asymptotics for $m_\tau R \gg 1$. In the following, the symbol $\sim$ will indicate omission of terms subleading in the large R limit. To begin with we have

$$\begin{aligned} Z_{\mathcal{B}} &\equiv \langle B(R/2)|B(-R/2)\rangle = \langle B(0)|e^{-RH}|B(0)\rangle \\ &\sim |a_0|^2 \int \frac{d\mathbf{p}}{(2\pi)^n m_\tau}\, e^{-\left(m_\tau + \frac{\mathbf{p}^2}{2m_\tau}\right)R} = \frac{|a_0|^2}{m_\tau}\left(\frac{m_\tau}{2\pi R}\right)^{n/2} e^{-m_\tau R}\,. \end{aligned} \tag{3.5}$$

3.3 One-point functions

The expectation value of a scalar field Φ is given by[3]

$$\begin{aligned} \langle\Phi(\mathbf{x},0)\rangle_{\mathcal{B}} &= \frac{1}{Z_{\mathcal{B}}}\,\langle B(R/2)|\Phi(\mathbf{x},0)|B(-R/2)\rangle \\ &\sim \left(\frac{2\pi R}{m_\tau}\right)^{n/2} \int \frac{d\mathbf{p}_1 d\mathbf{p}_2}{(2\pi)^{2n} m_\tau}\, F_\Phi(\mathbf{p}_1|\mathbf{p}_2)\, e^{-\frac{R}{4m_\tau}(\mathbf{p}_1^2+\mathbf{p}_2^2)+i\mathbf{x}\cdot(\mathbf{p}_1-\mathbf{p}_2)}, \end{aligned} \tag{3.6}$$

where

$$F_\Phi(\mathbf{p}_1|\mathbf{p}_2) = \langle\tau(\mathbf{p}_1)|\Phi(0,0)|\tau(\mathbf{p}_2)\rangle\,, \qquad \mathbf{p}_1, \mathbf{p}_2 \to 0 \tag{3.7}$$

is the matrix element on the topological particle state, evaluated in the low-energy limit enforced by the large R expansion. It decomposes as

$$F_\Phi(\mathbf{p}_1|\mathbf{p}_2) = F_\Phi^c(\mathbf{p}_1|\mathbf{p}_2) + (2\pi)^n E_{\mathbf{p}_1}\delta(\mathbf{p}_1-\mathbf{p}_2)\,\langle\Phi\rangle\,, \tag{3.8}$$

where $\langle\Phi\rangle$ is the bulk expectation value, and we see that only the connected part F_Φ^c contributes to the $\mathbf{x}$-dependence of (3.6). If F_Φ^c behaves for small momenta as momentum

[2] We refer here to the bulk theory, namely the fully translation invariant theory.

[3] We consider for simplicity $y = 0$, the extension to y generic being straightforward (see [44]).

to the power α_Φ, rescaling of momentum components by $\sqrt{R}$ shows that the $\mathbf{x}$-dependent part of (3.6) is suppressed at large R as

$$R^{-(n+\alpha_\Phi)/2}\,. \tag{3.9}$$

The order parameter $\langle \mathbf{s}(\mathbf{x},0)\rangle_{\mathcal{B}}$ is an odd function of $\mathbf{x}$ which interpolates between zero at $\mathbf{x}=0$ and the asymptotic value

$$\lim_{|\mathbf{x}|\to\infty} \langle \mathbf{s}(\mathbf{x},0)\rangle_{\mathcal{B}} \sim v\,\hat{\mathbf{x}}\,, \tag{3.10}$$

where

$$v = |\langle \mathbf{s}(\mathbf{x},y)\rangle| \tag{3.11}$$

is the modulus of the bulk magnetization. This interpolation is not suppressed as $R\to\infty$ and requires $\alpha_{\mathbf{s}} = -n$, and it was seen in [43] that $F^c_{\mathbf{s}}(\mathbf{p}_1|\mathbf{p}_2)$ is proportional to

$$\frac{\mathbf{p}_1-\mathbf{p}_2}{|\mathbf{p}_1-\mathbf{p}_2|^{n+1}}\,. \tag{3.12}$$

Upon insertion in (3.6) this leads to [43]

$$\langle \mathbf{s}(\mathbf{x},0)\rangle_{\mathcal{B}} \sim v\,\frac{\Gamma\left(\frac{n+1}{2}\right)}{\Gamma\left(1+\frac{n}{2}\right)}\,{}_1F_1\left(\frac{1}{2},1+\frac{n}{2};-z^2\right) z\,\hat{\mathbf{x}}\,, \tag{3.13}$$

where ${}_1F_1(\alpha,\gamma;z)$ is the confluent hypergeometric function, and

$$z \equiv \sqrt{\frac{2m_\tau}{R}}\,|\mathbf{x}|\,. \tag{3.14}$$

For $n=1$ the result (3.12) is the low-energy limit of the matrix element known exactly [49] from 2D Ising field theory, which is integrable (see [23] for a review). On the other hand, (3.13) reduces to $v\,\mathrm{erf}(z)$; this result, which describes the separation of phases in the 2D Ising model, was obtained from the exact lattice solution in [20,21] and from field theory in [16,17] (see [13,14] and chapter 2 for the relation with phase separation in $d=3$).

It is interesting to extend the analysis to the energy density field $\varepsilon \propto \mathbf{s}^2$. Recalling (3.9) and (3.14), the result of (3.6) for this field will take the form

$$\langle \varepsilon(\mathbf{x},0)\rangle_{\mathcal{B}} \sim \left[\frac{f_\varepsilon(z)}{(m_\tau R)^{(n+\alpha_\varepsilon)/2}}+1\right]\langle\varepsilon\rangle\,, \tag{3.15}$$

where f_ε depends on the specific form of the connected matrix element $F^c_\varepsilon(\mathbf{p}_1|\mathbf{p}_2)$ for small momenta. It follows from (3.6) and (3.8) that the $|\mathbf{x}|$-dependent term in (3.15) is the contribution to the energy density on the hyperplane $y=0$ coming from the propagation of the topological particle between the endpoints $(\mathbf{x},y)=(0,\pm R/2)$ of its trajectories.

Hence, the dimensionless function $f_\varepsilon(z)$ is proportional to the probability of finding the particle at a distance $|\mathbf{x}|$ from the origin on that hyperplane, and monotonically decreases from $f_\varepsilon(0)$ to $f_\varepsilon(\infty) = 0$; the limit

$$\lim_{|\mathbf{x}|\to\infty} \langle \varepsilon(\mathbf{x}, 0) \rangle_{\mathcal{B}} \sim \langle \varepsilon \rangle \,, \tag{3.16}$$

with $\langle \varepsilon \rangle$ the bulk energy density, is the expected one.

3.4 Mass of the topological particle

As anticipated above, the large R leading expression of the order parameter (3.13) for $n = 1$, i.e. in the 2D Ising model, coincides with the exact lattice solution obtained in [20, 21] and with the result from field theory given in [16, 17].

For $n = 2$ the result (3.13) was successfully tested against Monte Carlo simulations of the 3D XY model in [44]. In particular, this allowed to numerically determine the mass m_τ of the vortex particle, which was the only unknown parameter involved in the simulations. This finding is particularly relevant in view of Derrick's theorem [50] (see also [39]), which prevents the existence of finite energy topological configurations in theories of *classical* self-interacting scalar fields in $d > 2$. The finite value of m_τ measured in [44] provided the first direct verification that this obstruction does not in general persist at the quantum level. In particular, a result of classical field theory such as Derrick's theorem has no special reason to hold in presence of the nontrivial fixed point of the renormalization group exhibited by the 3D XY model.

At the same time, the last observation suggests that something might change for $n \geq 3$. Indeed, $d = 4$ is the upper critical dimension d_c of the theory (3.3), meaning that for $d \geq d_c$ the fixed point ruling the critical behavior is the Gaussian one, the role of fluctuations is suppressed and the critical exponents take mean field values (see e.g. [5]). Derrick's result might persist in this case and it is relevant to see what the above analysis predicts for $m_\tau \to \infty$. In this case, for any finite R, (3.14) yields $z \to \infty$ as long as $\mathbf{x} \neq 0$, and the result (3.13) for the order parameter becomes

$$\lim_{m_\tau\to\infty} \langle \mathbf{s}(\mathbf{x}, 0) \rangle_{\mathcal{B}} \sim \begin{cases} v\,\hat{\mathbf{x}}\,, & \mathbf{x} \neq 0\,, \\ \\ 0\,, & \mathbf{x} = 0\,. \end{cases} \tag{3.17}$$

It is worth stressing how $m_\tau = \infty$ does not mean that the topological particle is absent: the result (3.17) is entirely due to this particle. In other words, the infinitely massive particle does not contribute to fluctuations but provides the topological charge required when the boundary conditions enforce the presence of a topological defect.

It follows from (3.17) that, if the topological particle has an infinite mass, the order parameter becomes R-independent in the large R limit we consider. The absence of an

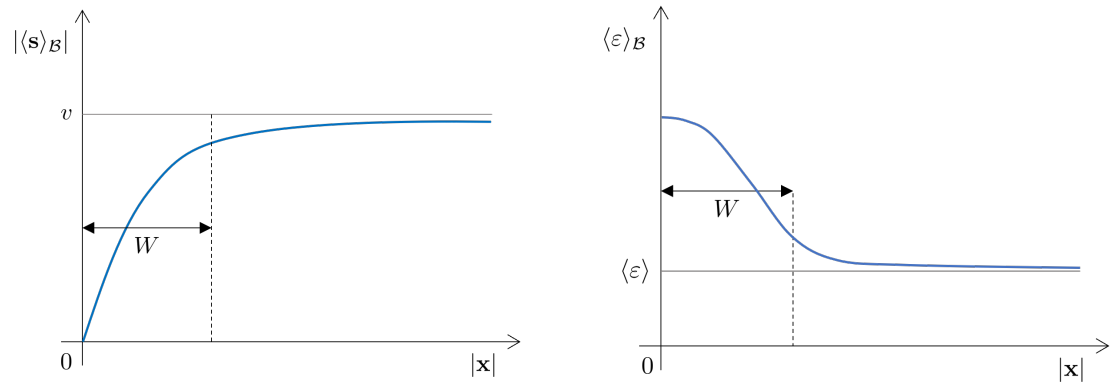

Figure 3.2: Qualitative profiles at $y = 0$ for the modulus of the order parameter (left) and the energy density (right) as a function of the distance from the center. The width W (eq. (3.18)) of the pre-asymptotic region is replaced by $\tilde{W}$ (eq. (3.20)) when the mass of the topological particle becomes infinite ($n \geq 3$).

appreciable R-dependence of the one-point functions is the key difference observed in the numerical simulations of [46,47] for $n = 3$ with respect to those of [44] for $n = 2$. We now see that this difference is explained by the theory and indicates that the topological mass m_τ is infinite for $n = 3$, i.e. for $d = 4$. The same is then expected to hold more generally for $d \geq d_c = 4$, namely in presence of a Gaussian critical point. Spontaneous symmetry breaking around a Gaussian point is taken into account already at the classical level, and $m_\tau = \infty$ means that Derrick's result of classical field theory persists in the mean field regime.

Consider now the result (3.15) for the energy density. The form (3.14) of the scaling variable z shows that the width W of the peak of (3.15) around $\mathbf{x} = 0$ (fig. 3.2) depends on the parameters as

$$W \propto \sqrt{R/m_\tau} \propto \sqrt{(T_c - T)^{-\nu} R}\,, \tag{3.18}$$

where ν is the correlation length critical exponent. Hence, (3.15) becomes flat as $R \to \infty$, and (3.16) requires $\alpha_\varepsilon > -n$. The dependence (3.15) of the energy density for large R is known in full detail for $n = 1$ [16,17,51], and has been confirmed numerically for $n = 2$ [44]. Passing to the case $n \geq 3$, we know by now that it requires the limit $m_\tau \to \infty$. Knowing that $f_\varepsilon(\infty) = 0$ and $\alpha_\varepsilon > -n$, (3.15) yields

$$\lim_{m_\tau \to \infty} \langle \varepsilon(\mathbf{x}, 0) \rangle_{\mathcal{B}} \sim \langle \varepsilon \rangle\,. \tag{3.19}$$

This result explains, in particular, why no appreciable R-dependence of the energy density was observed in the simulations of [46] for $n = 3$.

3.5 Residual fluctuations

An additional element which complicated the interpretation of the numerical results of [46, 47] for $n = 3$ is that, in spite of the R-independence that we have now explained, the overall qualitative $\mathbf{x}$-dependence of the one-point functions was found to be quite analogous to that observed in [44] for $n = 2$. In particular, $\langle \mathbf{s}(\mathbf{x}, 0)\rangle_{\mathcal{B}}$ was found to exhibit a smooth interpolation between zero at $\mathbf{x} = 0$ and $v\,\hat{\mathbf{x}}$ at $|\mathbf{x}| = \infty$, at variance with the step-like interpolation of (3.17). The energy density $\langle \varepsilon(\mathbf{x}, 0)\rangle_{\mathcal{B}}$ was observed to display a bell shape centered in $\mathbf{x} = 0$ and approaching the bulk value $\langle \varepsilon\rangle$ for $|\mathbf{x}|$ large enough.

These corrections to (3.17) and (3.19) should come from contributions not considered in the previous discussion. In the Ising case ($n = 1$) it is known [16, 17] that the leading corrections to (3.13) and (3.15) expand in powers of $R^{-1/2}$ and are due to the subleading terms of the expansion for small momenta associated to the state $|\tau\rangle$ itself[4] in (3.6). For $n \geq 3$, however, this type of corrections are eliminated by the divergence of m_τ, and we should consider the states contributing to the dots in (3.4). These are of the type τ (which provides the required topological charge) plus Goldstone bosons associated to the spontaneous breaking of the continuous symmetry. The analytical evaluation of the contribution of these states to the one-point functions would require information about the matrix elements of the fields on these states, which is not available. Remarkably, however, we now show that implications sufficient for our purposes can be obtained from the following considerations. For $n \geq 3$ the nonzero width $\tilde{W}$ of the pre-asymptotic region in the profiles of fig. 3.2 – i.e. the deviation from the results (3.17) and (3.19) – is due to the Goldstone fluctuations. Since $m_\tau = \infty$ suppresses the R-dependence[5], the width $\tilde{W}$ can only depend on the temperature and scales in the way expected for a length,

$$\tilde{W} \propto (T_c - T)^{-\nu}\,, \tag{3.20}$$

where the critical exponent ν takes the mean field value $1/2$ around the Gaussian fixed point relevant for $n \geq 3$. If one tries to explain the scaling observed in simulations performed for $n \geq 3$ through the formulae which apply to the case of m_τ finite ($n = 1, 2$), this means reproducing the behavior (3.20) using (3.18), namely writing $(T_c - T)^{-\nu} \propto \sqrt{R/m_\tau}$. One is then led to the *formal* identification $m_\tau \propto (T_c - T)^{2\nu} R = (T_c - T)R$. This is precisely what was observed using (3.13) for the fits of [46, 47] at $n = 3$. We now see why the R-dependence of m_τ obtained in this way is artificial and, at the same time, how the data of [46, 47] confirm $m_\tau = \infty$ and (3.20).

[4] See [51] for an accurate comparison between theoretical predictions and the results of numerical simulations.

[5] It cannot be excluded that the cumulative effect of Goldstone bosons results in a residual, very weak – e.g. logarithmic – R-dependence which was not detected within the numerical accuracy of the simulations in [46, 47]. For the purpose of explaining the data of [46, 47], this possibility can be consistently ignored.

3.6 Final remarks

In this chapter we considered the $O(n)$ vector model in $d = n + 1$ dimensions in its spontaneously broken phase, with boundary conditions giving rise to a topological defect line. Recent Monte Carlo simulations for the cases $n = 2$ [44] and $n = 3$ [46,47] showed different scaling dependence of one-point functions (e.g. the order parameter) on the parameters of the theory, namely the finite size R and the deviation from critical temperature. We showed that the theory of [43] accounts for both cases, the difference being produced by a mass m_τ of the topological particle which is finite for $n = 2$ and infinite for $n = 3$. We argued that this is due to the fact that $d = 4$ is the upper critical dimension of the $O(n)$ model. For $d \geq 4$ the critical behavior is controlled by the Gaussian fixed point, namely the fixed point explicitly present in the Landau-Ginzburg action (3.3). This action belongs to the class covered by Derrick's theorem [39,50] of *classical* field theory, which states that static solutions in self-interacting scalar theories in $d > 2$ have infinite energy. The Monte Carlo data of [46, 47] and their present theoretical interpretation indicate that Derrick's result gets through to the mean field regime $d \geq 4$, in the sense that topological particles have infinite mass. For $d < 4$, instead, the critical behavior is controlled by a nontrivial fixed point, for which arguments of classical field theory have no reason to remain quantitatively reliable. In particular, the R-dependence of one-point functions observed numerically in [44] for $n = 2$ showed that the quantum vortex has a finite mass which was estimated from the comparison between theory and Monte Carlo data. It is worth recalling that this is a particularly relevant result in view of the long debate concerning the definition of a mass of vortices in superfluids (see [44] and references therein), a debate in which the transposition of considerations of classical field theory (Derrick's theorem) to the quantum case plays a substantial role. Our analysis gives concrete evidence that such a transposition is possible only in the mean field regime $d \geq d_c$. It is remarkable that this insight could be obtained comparing considerations of quantum field theory with numerical simulations performed in the Euclidean case, thus providing a very fruitful operative illustration of the interplay between real and imaginary time.

Part II

Non-equilibrium quantum dynamics

Chapter 4

Quantum quenches in d dimensions

In this chapter we obtain analytical results for the time evolution of local observables in systems undergoing quantum quenches in d spatial dimensions. For homogeneous systems we show that oscillations undamped in time occur when the state produced by the quench includes single-quasiparticle modes and the observable couples to those modes. For the more general case in which the quench is performed only in a subregion of the whole d-dimensional space occupied by the system, the time evolution occurs inside a lightcone spreading away from the boundary of the quenched region as time increases. The additional condition for undamped oscillations is that the volume of the quenched region is extensive in all dimensions.

4.1 Introduction

Recent advances in experiments with cold atomic gases have sparked significant interest in the non-equilibrium dynamics of quantum many body systems (see e.g. [52] for a review), leading to extensive numerical and theoretical investigations [53, 54]. A main question is whether time evolution eventually leads to some form of relaxation or can produce a different behavior. The problem of the fate at large times of an extended and isolated quantum system out of equilibrium was addressed analytically in [55] for the case of non-interacting fermions in one dimension. Understanding the case of interacting quasiparticles turned out to be a difficult problem that could be faced through the perturbative approach introduced in [56] and further developed in [57–60]. The perturbative analysis applies to the basic way of dynamically generating non-equilibrium evolution, which has been called "quantum quench" [61,62] in analogy with thermal quenches of classical statistical systems: the system is in a stationary state until the sudden change of an interaction parameter leads to the new Hamiltonian that rules the unitary time evolution thereafter. The theory is perturbative in the quench size, while the interaction among the quasiparticles can be arbitrarily strong. It allows to actually *determine* the non-equilibrium state generated

by the quench and to follow analytically the time evolution. One result is that, in any spatial dimension, interaction leads to persistent oscillations of one-point functions (e.g. the order parameter) when the state produced by a homogeneous quench includes a one-quasiparticle mode and no internal symmetry prevents the observable to couple to that mode [56]. It was argued in [58] that, if undamped oscillations are present at finite order in perturbation theory, they will remain as a feature of the non-perturbative result, a prediction that found a remarkable confirmation in [63], where no decay of the oscillations was observed in a simulation of the Ising chain reaching times several orders of magnitude larger than the perturbative timescale. The undamped oscillations of [56] have also been observed in simulations and experiments performed on shorter time intervals, see [64–68] for a non-exhaustive list and [58, 59] for a discussion of the different instances.

In this chapter we perform the study of quantum quenches in d spatial dimensions for both the homogeneous and inhomogeneous cases. We consider a d-dimensional system occupying the whole space $\mathbb{R}^d$. Before the quench the system is translation invariant and in the ground state $|0\rangle$ of the Hamiltonian H_0. We perform the theoretical analysis exploiting the complete basis of asymptotic quasiparticle states $|\mathbf{p}_1, \dots, \mathbf{p}_n\rangle$ of the pre-quench theory, with $\mathbf{p}_i$ denoting the d-dimensional momenta of the quasiparticles. The asymptotic states are eigenstates of H_0 with eigenvalues equal to the sum of the quasiparticle energies $E_{\mathbf{p}_i} = \sqrt{M^2 + \mathbf{p}_i^2}$. $M > 0$ is the quasiparticle mass and measures the distance from a quantum critical point. In order to simplify the notation we refer to the case of a single quasiparticle species; generalizations are straightforward and will be discussed when relevant.

We will show that for a translation invariant system with post-quench Hamiltonian

$$H = H_0 + \lambda \int d\mathbf{x}\, \Psi(\mathbf{x})\,, \tag{4.1}$$

the large time limit of the one-point function of an operator Φ takes the form

$$\langle \Phi(\mathbf{x}t)\rangle = \langle \Phi\rangle_\lambda^{\rm eq} + \lambda \left[\frac{2}{M^2} F_1^\Psi F_1^\Phi \cos Mt + O(t^{-\alpha})\right] + O(\lambda^2)\,, \tag{4.2}$$

where $\langle \Phi\rangle_\lambda^{\rm eq}$ is the equilibrium expectation value in the theory with the Hamiltonian H, $F_1^{\mathcal{O}}$ the matrix element of $\mathcal{O}$ between $|0\rangle$ and the single-quasiparticle state, and

$$\alpha \geq d/2\,. \tag{4.3}$$

In case of systems possessing several quasiparticle species the term in the square bracket is summed over the species. The result (4.2) shows, in particular, the presence of undamped oscillations under the same conditions determined in [56] for the case $d = 1$ (for which α is generically $3/2$), namely when the excitations produced by the quench include a single-quasiparticle mode[1] ($F_1^\Psi \neq 0$) and the observable couples to this mode ($F_1^\Phi \neq 0$).

[1] This in turn requires interacting quasiparticles, otherwise Ψ creates only quasiparticle pairs.

In turn, (4.2) is a particular case ($\mathcal{D} = \mathbb{R}^d$) of the more general situation that we are going to consider, namely that of a quench performed only in a subregion $\mathcal{D}$ of the full space $\mathbb{R}^d$ occupied by the system. For such an inhomogeneous quench, corresponding to the post-quench Hamiltonian

$$H = H_0 + \lambda \int_{\mathcal{D}} d\mathbf{x}\, \Psi(\mathbf{x})\,, \tag{4.4}$$

we will show that the large time limit (4.2) generalizes to

$$\begin{aligned}\langle \Phi(\mathbf{x},t)\rangle = {} & \langle \Phi(\mathbf{x})\rangle_\lambda^{\rm eq} \\ & + \lambda \left[\frac{2F_1^\Psi F_1^\Phi}{(2\pi)^d} \int_{\mathcal{D}} d\mathbf{y} \int d\mathbf{p}\, \frac{\cos(\sqrt{\mathbf{p}^2+M^2}\, t + (\mathbf{x}-\mathbf{y})\cdot\mathbf{p})}{\mathbf{p}^2+M^2} + O(t^{-\alpha-\beta_{\mathcal{D}}}) \right] \\ & + O(\lambda^2)\,,\end{aligned} \tag{4.5}$$

where α is the same entering (4.2), while

$$\beta_{\mathcal{D}} \in [0, d/2] \tag{4.6}$$

rules the large time behavior $t^{-\beta_{\mathcal{D}}}$ of the integral term. If L^d, with $L \to \infty$, is the volume of $\mathbb{R}^d$, there are undamped oscillations ($\beta_{\mathcal{D}} = 0$) when the volume of $\mathcal{D}$, vol($\mathcal{D}$), is of order L^d, a condition weaker than $\mathcal{D} = \mathbb{R}^d$. On the other hand, $\beta_{\mathcal{D}} = d/2$ when vol($\mathcal{D}$) is finite. Intermediate values of $\beta_{\mathcal{D}}$ occur depending on the number of dimensions in which vol($\mathcal{D}$) is extensive. We will also show that the effect of the quench is appreciable only inside a lightcone that at time t contains $\mathcal{D}$ and the external region within distance t from the boundary $\partial\mathcal{D}$. More specifically, the oscillations propagate inside a lightcone and are sustained by the energy produced in the quench and carried by the quasiparticles. In order the oscillations to stay undamped, a nonzero energy density inside the lightcone is needed at late times (besides $F_1^\Psi F_1^\Phi \neq 0$). Since the energy produced by the quench and conserved by the time evolution is proportional to vol($\mathcal{D}$), and since the volume enclosed by the lightcone becomes L^d as $t \to \infty$, a nonzero energy density at late times requires that vol($\mathcal{D}$) is of order L^d, and this is the case corresponding to $\beta_{\mathcal{D}} = 0$.

4.2 Post-quench state and one-point functions

The quench at $t = 0$ is performed changing the Hamiltonian H_0 to (4.4) and for $\mathcal{D} \neq \mathbb{R}^d$ breaks translation invariance. Since the quench excites quasiparticle modes, the pre-quench state $|0\rangle$ evolves into the state $|\psi_0\rangle = S_\lambda |0\rangle$, where

$$S_\lambda = T\, \exp\left(-i\lambda \int_0^\infty dt \int_{\mathcal{D}} d\mathbf{x}\, \Psi(\mathbf{x},t) \right) \tag{4.7}$$

(T denotes chronological ordering) is the operator whose matrix elements $\langle n|S_\lambda|0\rangle$ give the probability amplitude that the quench induces the transition from $|0\rangle$ to $|n\rangle$. Here we adopt the compact notation $|n\rangle = |\mathbf{p}_1, \dots, \mathbf{p}_n\rangle$. To first order in the quench parameter λ we have

$$|\psi_0\rangle \simeq |0\rangle + \lambda \sum\!\!\!\!\!\!\int_{n,\mathbf{p}_i} \frac{g_{\mathcal{D}}(\mathbf{P})}{E} [F_n^\Psi]^* |n\rangle \,, \tag{4.8}$$

where we defined

$$E = \sum_{i=1}^n E_{\mathbf{p}_i} \,, \qquad \mathbf{P} = \sum_{i=1}^n \mathbf{p}_i \,, \tag{4.9}$$

$$g_{\mathcal{D}}(\mathbf{P}) = \int_{\mathcal{D}} d\mathbf{x}\, e^{i\mathbf{P}\cdot\mathbf{x}} \,, \tag{4.10}$$

$$F_n^{\mathcal{O}}(\mathbf{p}_1, ..., \mathbf{p}_n) = \langle 0|\mathcal{O}(0,0)|\mathbf{p}_1, ..., \mathbf{p}_n\rangle \,, \tag{4.11}$$

introduced the notation

$$\sum\!\!\!\!\!\!\int_{n,\mathbf{p}_i} = \sum_{n=1}^\infty \frac{1}{n!} \int_{-\infty}^\infty \prod_{i=1}^n \frac{d\mathbf{p}_i}{(2\pi)^d E_{\mathbf{p}_i}} \,, \tag{4.12}$$

and used

$$\mathcal{O}(\mathbf{x}, t) = e^{i\mathcal{P}\cdot\mathbf{x} + iH_0 t}\, \mathcal{O}(0,0)\, e^{-i\mathcal{P}\cdot\mathbf{x} - iH_0 t} \,, \tag{4.13}$$

with $\mathcal{P}$ the momentum operator and $\mathcal{O}$ a generic local operator. An infinitesimal imaginary part is given to the energy to make the time integral in (4.7) convergent[2]. The result (4.8) shows that the quench produces excitation modes with any number of quasiparticles and all possible momenta. Only when the quasiparticles do not interact, so that H_0 and H are quadratic in the quasiparticle modes and $F_n^\Psi \propto \delta_{n,2}$, a post-quench state with quasiparticles organized in pairs is obtained.

The one-point function of a local observable Φ is given by the expectation value $\langle\Phi(\mathbf{x}, t)\rangle$ on the post-quench state (4.8). In the formalism of asymptotic states the spacetime dependence is carried by the operator and is extracted exploiting (4.13). The variation $\delta\langle\Phi(\mathbf{x}, t)\rangle$ of the one-point function of a hermitian observable with respect to the pre-quench value is given, at first order in λ, by

$$\begin{aligned} \delta\langle\Phi(\mathbf{x}, t)\rangle &= \langle\psi_0|\Phi(\mathbf{x}, t)|\psi_0\rangle - \langle 0|\Phi(0,0)|0\rangle + C_\Phi(\mathbf{x}) \\ &\simeq 2\lambda \sum\!\!\!\!\!\!\int_{n,\mathbf{p}_i} \frac{1}{E} \,\mathrm{Re}\left\{ g_{\mathcal{D}}(\mathbf{P})\, [F_n^\Psi]^* F_n^\Phi\, e^{-i(Et + \mathbf{P}\cdot\mathbf{x})} \right\} + C_\Phi(\mathbf{x}) \,, \end{aligned} \tag{4.14}$$

[2]The sum in (4.12) starts from $n = 1$ rather than from $n = 0$ because the $O(\lambda)$ contribution to (4.8) with $n = 0$ (corresponding to $E = \mathbf{P} = 0$) diverges and must be subtracted. Such a term corresponds to vacuum energy renormalization and can be canceled through a counterterm in the Hamiltonian [56].

where we took into account that normalizing by $\langle\psi_0|\psi_0\rangle = 1 + O(\lambda^2)$ is immaterial at first order, and added the term

$$C_\Phi(\mathbf{x}) \simeq -2\lambda \sum\!\!\!\!\!\!\int_{n,\mathbf{p}_i} \frac{1}{E} \,\mathrm{Re}\left\{ g_{\mathcal{D}}(\mathbf{P})\, [F_n^\Psi]^* F_n^\Phi \, e^{-i\mathbf{P}\cdot\mathbf{x}} \right\} \tag{4.15}$$

to ensure continuity at $t = 0$, namely the condition $\delta\langle\Phi(\mathbf{x}, 0)\rangle = 0$, which has no reason to be automatically satisfied.

4.3 Large time behavior

We can use (4.10) to rewrite (4.14) as

$$\delta\langle\Phi(\mathbf{x}, t)\rangle \simeq 2\lambda \sum\!\!\!\!\!\!\int_{n,\mathbf{p}_i} \int_{\mathcal{D}} d\mathbf{y}\, \frac{1}{E} \,\mathrm{Re}\left\{ [F_n^\Psi]^* F_n^\Phi \, e^{-i[Et + \mathbf{P}\cdot(\mathbf{x}-\mathbf{y})]} \right\} + C_\Phi(\mathbf{x})\,.$$

For t large the rapid oscillation of the exponential suppresses the integrals over momenta unless the phase is stationary, namely unless

$$\nabla_{\mathbf{p}_i}[E_{\mathbf{p}_i} t + \mathbf{p}_i \cdot (\mathbf{x} - \mathbf{y})] = \mathbf{v}_i t + \mathbf{x} - \mathbf{y} = 0\,, \qquad i = 1, 2, \ldots, n\,, \tag{4.16}$$

where we introduced the quasiparticle velocities

$$\mathbf{v}_i = \nabla_{\mathbf{p}_i} E_{\mathbf{p}_i} = \frac{\mathbf{p}_i}{\sqrt{M^2 + \mathbf{p}_i^2}}\,. \tag{4.17}$$

Since[3] $|\mathbf{v}_i| < 1$, the stationarity condition (4.16) is satisfied when

$$|\mathbf{x} - \mathbf{y}| < t\,. \tag{4.18}$$

This means that, for any point $\mathbf{y} \in \mathcal{D}$, the effect of the quench is appreciable only within a distance t from $\mathbf{y}$, namely the maximal distance that the quasiparticles excited by the quench at the point $\mathbf{y}$ could reach at time t. Hence, the time evolution takes place inside a lightcone[4] containing $\mathcal{D}$ and the external region within distance t from $\partial\mathcal{D}$ (figure 4.1).

For $\mathcal{D}$ finite, $\mathbf{x}$ fixed and t large enough, the stationarity condition $\mathbf{v}_i = (\mathbf{y} - \mathbf{x})/t$ implies that the time dependence in (4.14) receives a significant contribution only when all momenta $\mathbf{p}_i$ are small, and then can be evaluated with $g_{\mathcal{D}} \to \mathrm{vol}(\mathcal{D})$ and $E_{\mathbf{p}_i} \to M + \mathbf{p}_i^2/2M$. The matrix elements (4.11) do not diverge at small momenta (see e.g. [70]),

[3] We adopt natural units in which the maximal velocity of the quasiparticles is $v_{\max} = 1$.

[4] See [69] for the derivation of the lightcone associated to the spreading of two-point correlations in the translation invariant case, which involves the connectedness properties of matrix elements as an additional ingredient.

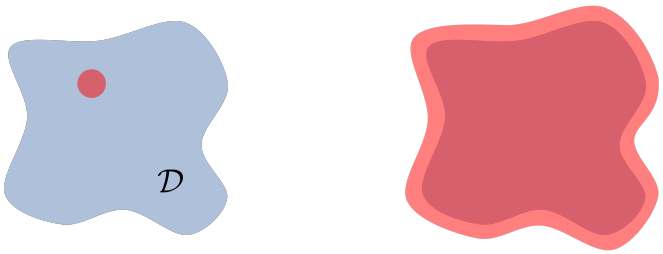

Figure 4.1: Implications of the stationarity condition (4.16) for a quench in a region $\mathcal{D}$ of the space $\mathbb{R}^d$ occupied by the system. **Left:** The quench operator Ψ acting at a point $\mathbf{y} \in \mathcal{D}$ creates excitations that at time t have spread inside a sphere of radius t. **Right:** Since Ψ acts at all points of $\mathcal{D}$, the effect of the quench is appreciable only inside the lightcone containing $\mathcal{D}$ and the region within distance t from its boundary.

and in such a limit $[F_n^\Psi]^* F_n^\Phi$ will behave as momentum to a power $2\alpha_n \geq 0$. In particular $\alpha_1 = 0$, since $F_1^\mathcal{O}$ is a real constant for the scalar hermitian operators that we consider. With this information, it is easy to rescale the momenta and see that the n-quasiparticle contribution in (4.14) behaves at large times as $t^{-(nd/2+\alpha_n)}$.

More generally, suppose that $\mathcal{D}$ goes from $-\infty$ to $+\infty$ in k of the d spatial dimensions (say $x_1, x_2, \ldots, x_k$). Now $g_\mathcal{D} \propto \delta(P_1) \cdots \delta(P_k)$, and this gives an extra contribution $-k$ to the counting of the powers of momentum, so that the large time behavior is modified to $t^{-[(nd-k)/2+\alpha_n]}$. As long as $F_1^\Psi F_1^\Phi \neq 0$ the leading contribution comes from the single-quasiparticle mode $n = 1$ and goes as $t^{-(d-k)/2}$. For an homogeneous quench ($\mathcal{D} = \mathbb{R}^d$, i.e. $k = d$) we have undamped oscillations and the result in the square bracket of (4.2), with the lower bound (4.3) coming from $n = 2$. A generic k gives the time dependence in the square bracket of (4.5), behaving as $t^{-\beta_\mathcal{D}}$, with $\beta_\mathcal{D} = (d-k)/2$ that satisfies (4.6).

On the other hand, suppose that $\mathcal{D}$ differs from $\mathbb{R}^d$ for the subtraction of a finite region, namely $\mathcal{D} \cup \tilde{\mathcal{D}} = \mathbb{R}^d$ with $\tilde{\mathcal{D}}$ finite. In this case $g_\mathcal{D} = g_{\mathbb{R}^d} - g_{\tilde{\mathcal{D}}}$, and the dependence at large times corresponds to the difference of the previous cases $k = d$ and $k = 0$. Hence, we have $\beta_\mathcal{D} = 0$ and undamped oscillations at sufficiently large times produced by the integral in (4.5). The conclusion that in general there are undamped oscillations when

$$\rho_\mathcal{D} = \text{vol}(\mathcal{D})/\text{vol}(\mathbb{R}^d) \tag{4.19}$$

is nonzero corresponds to the physical picture anticipated in the introduction: the energy produced by the quench is proportional to vol($\mathcal{D}$) and spreads in time inside the lightcone, so that the energy density will be asymptotically proportional to $\rho_\mathcal{D}$; a nonzero $\rho_\mathcal{D}$ is able to keep the oscillations undamped. The amplitude of the undamped oscillations goes to zero if $\rho_\mathcal{D}$ goes to zero. The condition $\rho_\mathcal{D} > 0$ amounts to vol($\mathcal{D}$) extensive in all dimensions.

We finally explain the origin of the time-independent term in (4.2) and (4.5). For this purpose observe that in the equilibrium theory with Hamiltonian (4.4) the first order contribution in λ to the one-point function $\langle\Phi(\mathbf{x})\rangle_\lambda^{\rm eq}$ is[5]

$$\begin{aligned}\delta\langle\Phi(\mathbf{x})\rangle_\lambda^{\rm eq} &\simeq -i\lambda\int_{-\infty}^{+\infty} dt\int_{\mathcal{D}} d\mathbf{y}\,\langle 0|T\,\Psi(\mathbf{y},t)\Phi(\mathbf{x},0)|0\rangle_c \\ &= -2\lambda\sum\!\!\!\!\!\!\int_{n,\mathbf{p}_i}\frac{1}{E}\,\mathrm{Re}\left\{[F_n^\Psi]^* F_n^\Phi\int_{\mathcal{D}} d\mathbf{y}\,e^{-i\mathbf{P}\cdot(\mathbf{x}-\mathbf{y})}\right\} \\ &= C_\Phi(\mathbf{x})\,, \end{aligned} \tag{4.20}$$

where we used (4.13), expanded over asymptotic states, and finally compared with (4.15). Hence, recalling what we just concluded about the time-dependent part, we have

$$\lim_{t\to\infty}\langle\Phi(\mathbf{x},t)\rangle = \langle\Phi(\mathbf{x})\rangle_\lambda^{\rm eq} + O(\lambda^2) \tag{4.21}$$

when $\beta_{\mathcal{D}}\neq 0$. When $\beta_{\mathcal{D}}=0$, namely when $\mathrm{vol}(\mathcal{D})$ is extensive in all dimensions, the r.h.s. of (4.21) is the value around which the undamped oscillations take place.

4.4 Time evolution

We rewrite (4.5) in the form

$$\langle\Phi(\mathbf{x},t)\rangle = \langle\Phi(\mathbf{x})\rangle_\lambda^{\rm eq} + \lambda\left[\frac{2}{M^2}\,F_1^\Psi F_1^\Phi\,f(\mathbf{x},t) + O(t^{-(\alpha+\beta_{\mathcal{D}})})\right] + O(\lambda^2)\,, \tag{4.22}$$

where

$$f(\mathbf{x},t) = \frac{M^2}{(2\pi)^d}\int d\mathbf{p}\,\frac{1}{\mathbf{p}^2+M^2}\,\mathrm{Re}\left\{g_{\mathcal{D}}(\mathbf{p})\,e^{-i(\sqrt{\mathbf{p}^2+M^2}\,t+\mathbf{p}\cdot\mathbf{x})}\right\} \tag{4.23}$$

is a dimensionless function. For $F_1^\Psi F_1^\Phi\neq 0$, $f(\mathbf{x},t)$ determines the large time behavior of the one-point function for small quenches, until a time scale t_λ that goes to infinity as λ is reduced[6]. On the other hand, the analysis of the previous section does not allow to neglect the terms with $n>1$ in (4.14) when t is *not* large. However, it is known that in $d=1$ [57, 58] the contribution of the n-quasiparticle state is normally rapidly suppressed as n increases, so that $f(\mathbf{x},t)$ provides a good approximation also for short times. If this is true also for $d>1$ we should expect, recalling (4.20) and (4.15), that the first order contribution to the equilibrium expectation value is well approximated as

$$\delta\langle\Phi(\mathbf{x})\rangle_\lambda^{\rm eq} \approx -\lambda\,\frac{2}{M^2}\,F_1^\Psi F_1^\Phi\,f(\mathbf{x},0)\,. \tag{4.24}$$

We will soon explicitly illustrate that (4.24) indeed yields the result expected for $\delta\langle\Phi(\mathbf{x})\rangle_\lambda^{\rm eq}$,

[5] The subscript c indicates the connected part of the two-point function.

[6] The expression of t_λ was given in [56] for $d=1$. Its generalization to the present d-dimensional case is $t_\lambda\sim 1/\lambda^{1/(d+1-X_\Psi)}$, where $X_\Psi<d+1$ is the scaling dimension of Ψ at the quantum critical point.

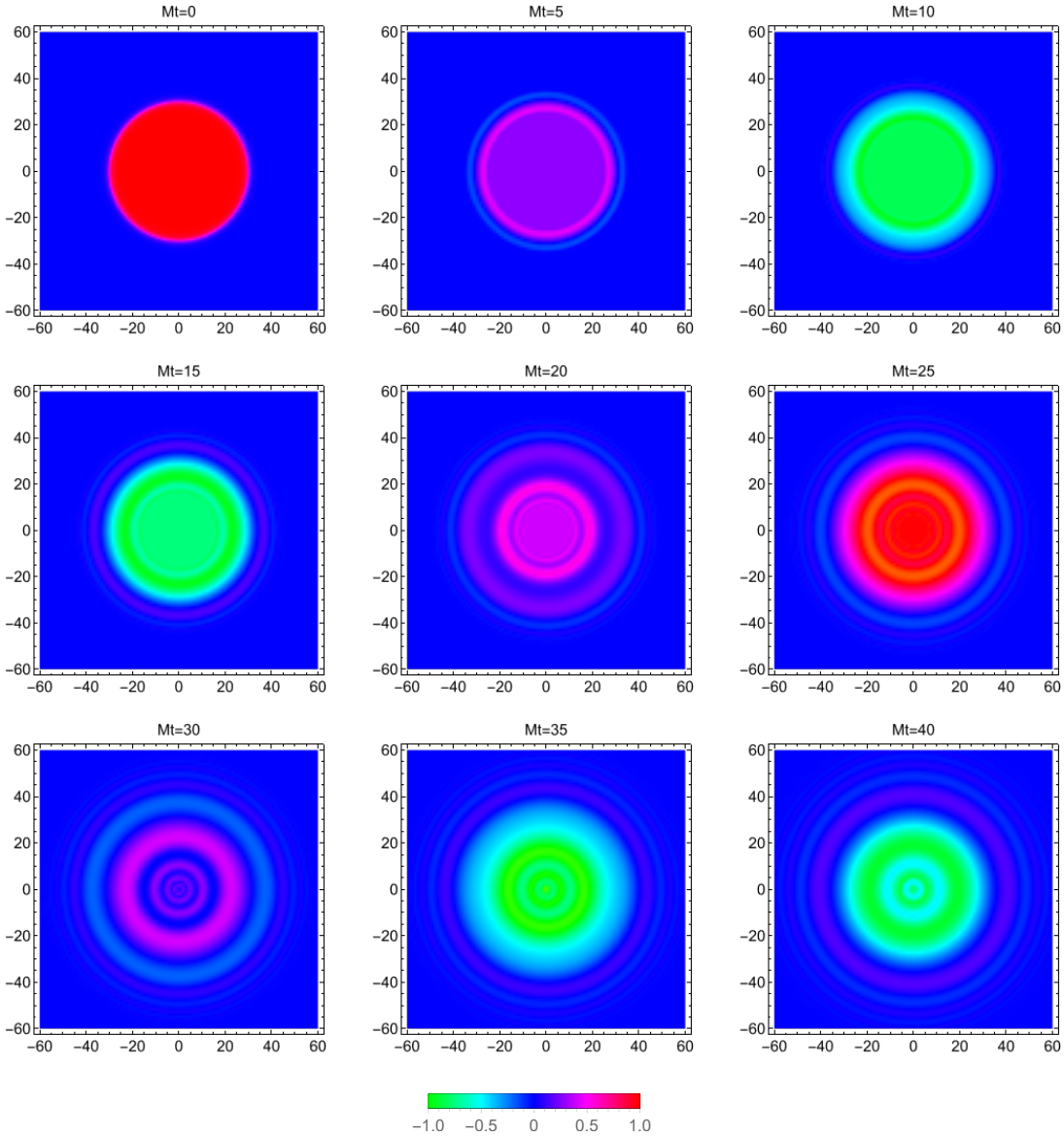

Figure 4.2: $f(\mathbf{x}, t)$ at different times in the plane Mx_1-Mx_2 for a quench in $d = 2$ with $\mathcal{D}$ a disk of radius $b = 30/M$.

namely a function that is essentially constant for $\mathbf{x} \in \mathcal{D}$ and zero otherwise. With this anticipation, we see that (4.22) (without the term $O(t^{-\alpha-\beta_{\mathcal{D}}})$) can be used not only for large times but, with good approximation, also for short times, meaning that the function (4.23) yields a global view of the time evolution for small quenches. We now consider this

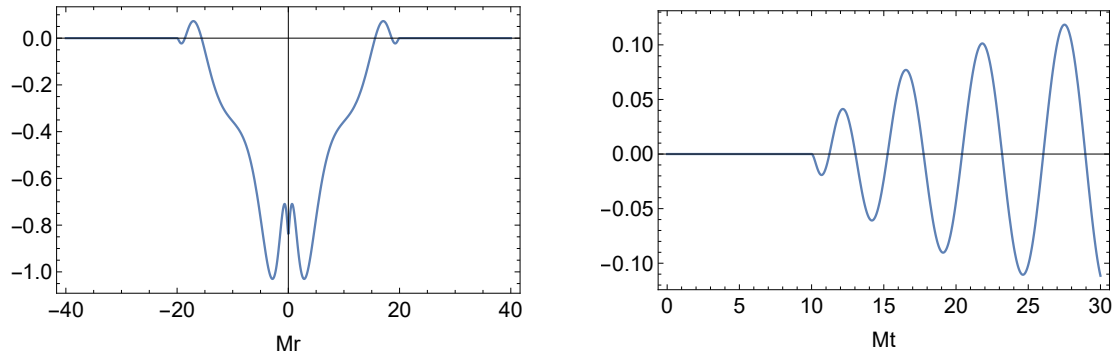

Figure 4.3: $f(\mathbf{x}, t)$ for a quench in $d = 2$ with $\mathcal{D}$ a disk of radius $b = 10/M$. **Left:** $Mt = 10$. The function is essentially zero outside the edges of the lightcone located at distance $r = b + t$ from the origin. **Right:** $Mr = 20$. Time evolution becomes appreciable only after that the lightcone is reached at time $t = r - b$.

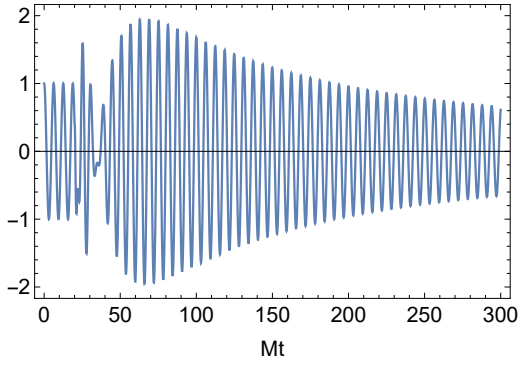

Figure 4.4: $f(0, t)$ for a quench in $d = 2$ with $\mathcal{D}$ a disk of radius $b = 20/M$. The oscillations in the origin stay undamped until the arrival at time $t = b$ of the modes originating from $\partial\mathcal{D}$. Eventually, the damping factor $t^{-d/2}$ prescribed by (4.5) with $\mathcal{D}$ finite sets in for large times.

function for a number of quenching domains $\mathcal{D}$.

4.4.1 Rotationally invariant quenched domains

If $\mathcal{D}$ is the d-dimensional sphere of radius b centered in the origin, (4.10) and (4.23) yield

$$g_{\text{sphere}}(\mathbf{P}) = \left(\frac{2\pi b}{|\mathbf{P}|}\right)^{\frac{d}{2}} J_{\frac{d}{2}}(|\mathbf{P}|b)\,, \tag{4.25}$$

and

$$f(\mathbf{x},t) = \frac{M^2\, b^{\frac{d}{2}}}{r^{\frac{d}{2}-1}} \int_0^\infty dp\, J_{\frac{d}{2}}(pb) J_{\frac{d}{2}-1}(pr)\, \frac{\cos(\sqrt{M^2+p^2}\, t)}{M^2+p^2}\,, \tag{4.26}$$

respectively, with $J_\alpha(z)$ the Bessel function and $r = |\mathbf{x}|$. The function (4.26) is plotted at different times in $d = 2$ ($\mathcal{D}$ = disk) in figure 4.2. The result for $t = 0$ confirms what we anticipated about (4.24) and the ability of $f(\mathbf{x}, t)$ to give an accurate view of the time evolution also for short times. As t increases the figure clearly shows the spreading of the lightcone located at distance t from the boundary of the disk. The boundary modes propagate also inside the disk, but for $t < b$ they leave unaffected the central region with $r < b - t$. Here the function essentially behaves as for a homogeneous quench, namely is spatially constant with undamped oscillations in time. The presence of the lightcone is also illustrated in figure 4.3. Figure 4.4 shows the damping of the oscillations at large times, with the suppression $t^{-d/2}$ expected for the case $\mathcal{D}$ finite.

A straightforward generalization is that of a quench with $\mathcal{D}$ the d-dimensional spherical shell $b_1 < r < b_2$, which yields

$$f(\mathbf{x},t) = \frac{M^2}{r^{\frac{d}{2}-1}} \int_0^\infty dp\, \left[b_2^{\frac{d}{2}}\, J_{\frac{d}{2}}(pb_2) - b_1^{\frac{d}{2}}\, J_{\frac{d}{2}}(pb_1) \right] J_{\frac{d}{2}-1}(pr)\, \frac{\cos(\sqrt{p^2+M^2}\, t)}{p^2+M^2}\,. \tag{4.27}$$

The time evolution is illustrated in figures 4.5 and 4.6 for b_2 finite, and in figure 4.7 for b_2 infinite.

4.4.2 Quenched domains with corners

If the quenched domain is a d-dimensional box, $\mathcal{D} = [-b_1, b_1] \times \cdots \times [-b_d, b_d]$, we have

$$g_{\rm box}(\mathbf{P}) = \prod_{k=1}^{d} \frac{2}{P_k}\, \sin(P_k b_k)\,. \tag{4.28}$$

Figure 4.8 shows the corresponding function $f(\mathbf{x}, t)$ at different times in $d = 2$ for a square domain. Again, the image at $t = 0$, with the function essentially constant inside the square and vanishing outside, illustrates (through (4.24)) that the time evolution is described with good approximation also at short times. For $t > 0$, the general result that the lightcone is located at distance t from the boundary of $\mathcal{D}$ leads to a rounding in correspondence of the corners of the square. This example gives an idea of the patterns that can be expected when $\partial\mathcal{D}$ increasingly deviates from a smooth surface.

4.5 Ising model

The model-dependent information for the use of (4.2) and (4.5) is whether the matrix elements F_1^Ψ and F_1^Φ vanish or not. They are generically nonzero, unless a symmetry

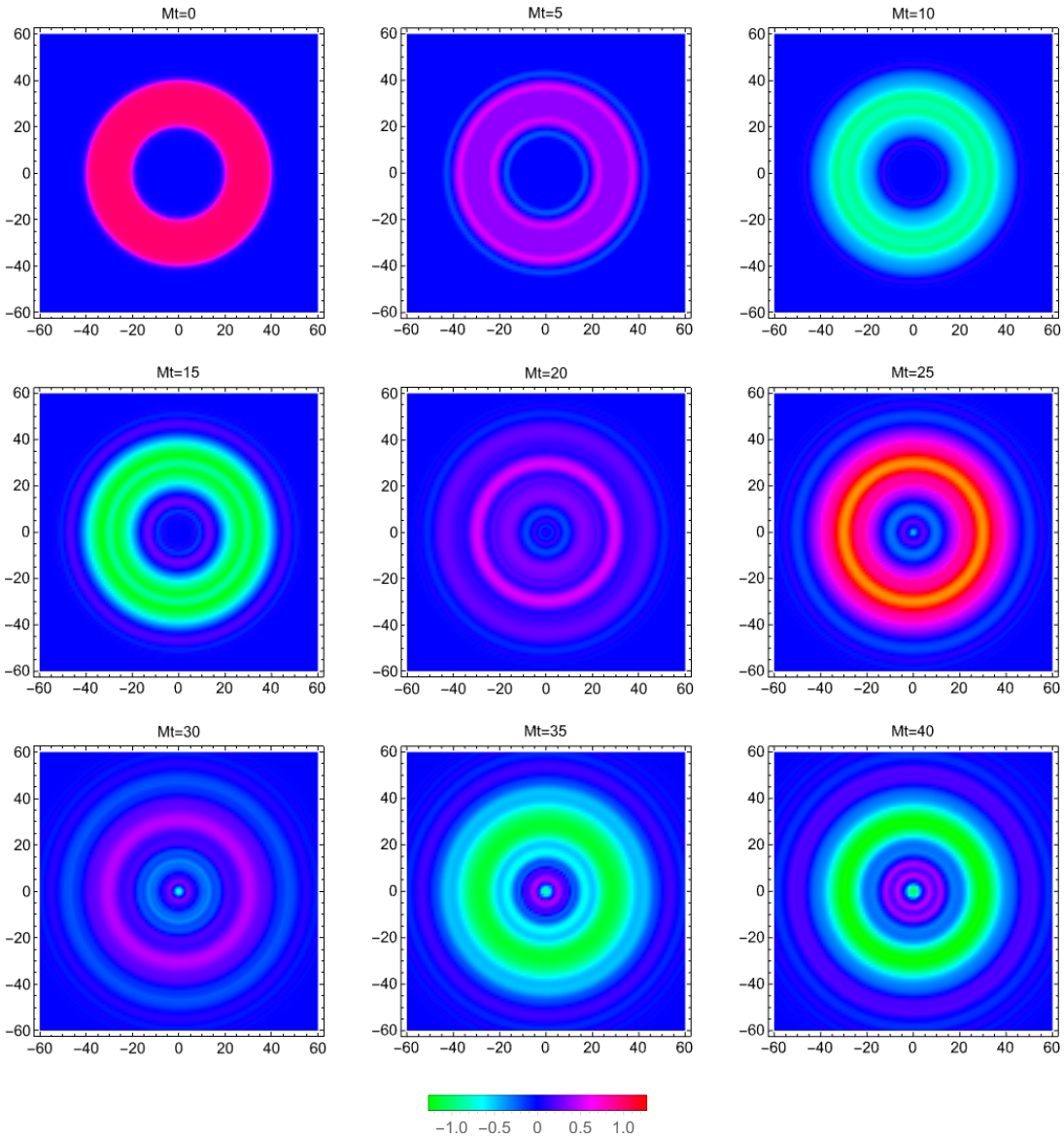

Figure 4.5: $f(\mathbf{x}, t)$ at different times in the plane Mx_1-Mx_2 for a quench in $d = 2$ with $\mathcal{D}$ an annulus occupying the region $20 < Mr < 40$. The initial central gap in the lightcone closes when the boundary modes reach $r = 0$ at $Mt = Mb_1 = 20$. See also figure 4.6.

forces them to vanish. In this section we illustrate the role of symmetries through the basic example of the d-dimensional quantum Ising ferromagnet. This is defined by the

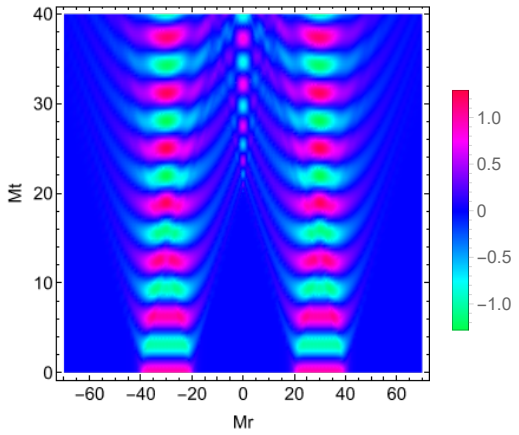

Figure 4.6: $f(\mathbf{x}, t)$ for the same quench of figure 4.5.

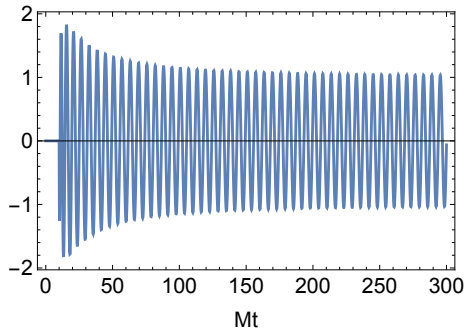

Figure 4.7: $f(0, t)$ for a quench in $d = 3$ with $\mathcal{D}$ extending everywhere except a sphere of radius $b = 10/M$ centered in the origin. The time evolution in the origin starts at $t = b$, with oscillations that become undamped at large time, as for the general case of vol($\mathcal{D}$) extensive in all dimensions.

Hamiltonian

$$H_{\rm Ising} = -J \sum_{\langle i,j \rangle} \sigma_i^x \sigma_j^x - h_z \sum_i \sigma_i^z - h_x \sum_i \sigma_i^x \,, \tag{4.29}$$

where $\sigma_i^{x,y,z}$ are Pauli matrices at site i, $\langle i, j \rangle$ denotes a pair of nearest-neighbor sites, J is positive, and h_z and h_x are the transverse and longitudinal magnetic fields, respectively. For $h_x = 0$ and $|h_z| = h_z^c$ the system possesses a quantum critical point associated to the spontaneous breaking of spin reversal ($\mathbb{Z}_2$) symmetry in the x direction and belonging to the universality class of the classical Ising model in $(d + 1)$ dimensions. The operator σ_i^z (σ_i^x) is $\mathbb{Z}_2$-even (odd). The paramagnetic (ferromagnetic) phase corresponds to $h_x = 0$ and $|h_z| > h_z^c$ ($|h_z| < h_z^c$).

We will consider quenches in which the system, which for $t < 0$ is in the ground state $|0\rangle$ of the Hamiltonian H_0 given by (4.29) with $h_x = 0$, evolves for $t > 0$ with the Hamiltonian (4.4) with[7] $\lambda\, \Psi(\mathbf{x})$ equal to $\delta h_z\, \sigma^z(\mathbf{x})$ ($\delta h_z \ll h_z$) or to $h_x\, \sigma^x(\mathbf{x})$. Depending on the fact that we start from the paramagnetic or ferromagnetic phase, we have the four quenches depicted in figure 4.9.

The specialization of (4.2) and (4.5) to the different quenches proceeds through symmetry considerations in the pre-quench theory. In the paramagnetic phase, the fundamental quasiparticle excitation is created by the order parameter operator $\sigma^x(\mathbf{x})$ and then is $\mathbb{Z}_2$-

[7] Our theory is formulated in the continuum, which in the present case is accessed working not too far from the critical point.

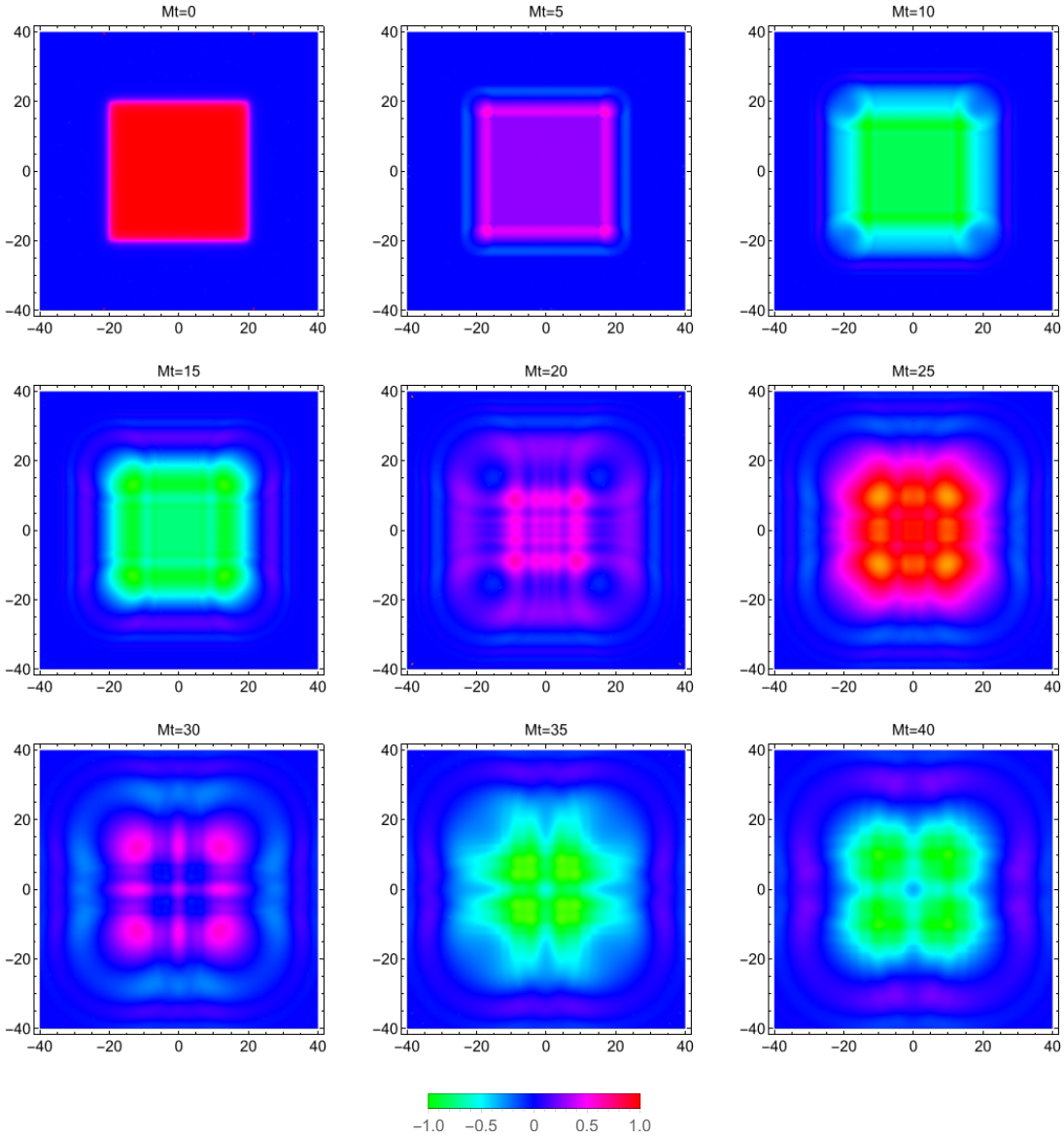

Figure 4.8: $f(\mathbf{x}, t)$ at different times in the plane Mx_1-Mx_2 for a quench in $d = 2$ with $\mathcal{D}$ a square of side $40/M$.

odd; it follows that $F_1^{\sigma^z} = 0$ and $F_1^{\sigma^x} \neq 0$. In the ferromagnetic phase the symmetry is spontaneously broken and both $F_1^{\sigma^z}$ and $F_1^{\sigma^x}$ are nonzero in $d > 1$. The case $d = 1$ is special because the excitations in the ferromagnetic phase have a topological nature (they are kinks, see [23] for a review) and can couple to σ^x and σ^z only in topologically neutral

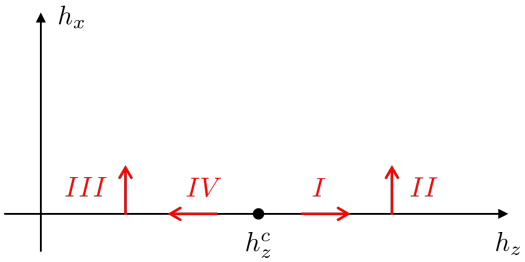

Figure 4.9: The different quenches in the quantum Ising model considered in the text. The critical point is located at $(h_z^c, 0)$. With reference to the Hamiltonian (4.29), each arrows goes from the pre-quench to the post-quench values of the parameters.

Quench	λ	Ψ	$F_1^\Psi F_1^{\sigma^x}$	
			$d=1$	$d>1$
I	δh_z	σ^z	0	0
II	h_x	σ^x	$\neq 0$	$\neq 0$
III	h_x	σ^x	0	$\neq 0$
IV	δh_z	σ^z	0	$\neq 0$

Table 4.1: Quenches in the d-dimensional quantum Ising ferromagnet indicated in figure 4.9. The information about $F_1^\Psi F_1^{\sigma^x}$ determines the time evolution of the order parameter $\langle \sigma^x \rangle$ for homogeneous quenches through (4.2), and for quenches in the subregion $\mathcal{D}$ through (4.5). The peculiarities of the case $d = 1$ are discussed in the text.

pairs, with the consequence that $F_1^{\sigma^z} = F_1^{\sigma^x} = 0$.

This information about $F_1^{\sigma^z}$ and $F_1^{\sigma^x}$ determines the time evolution of $\langle \sigma^x \rangle$ and $\langle \sigma^z \rangle$ through (4.2) when the quenches[8] I-IV are performed in the whole space $\mathbb{R}^d$, and through (4.5) when they are performed only in a subregion $\mathcal{D}$. In particular we saw that, if vol($\mathcal{D}$) is extensive in all dimensions, undamped oscillations at large time occur when $F_1^\Psi F_1^\Phi \neq 0$, and we explicitly provide this information in table 4.1 for the case $\Phi = \sigma^x$. The peculiarity of the cases III and IV in $d = 1$ follows from the previous observation about kinks.

The topological nature of the excitations of the ferromagnetic phase in $d = 1$ gives rise to an additional caveat about quench III in the Ising chain. While (4.2) and (4.5) hold also in this case and do not yield undamped oscillations at first order in $\lambda = h_x$, the longitudinal field makes kinks unstable and confines them into topologically neutral pairs [22, 23, 71], thus generating non-perturbatively the single-quasiparticle modes able to produce undamped oscillations of the order parameter on a time scale that becomes

[8] For quench I the symmetry implies $\langle \sigma^x \rangle = 0$ at all orders in λ.

accessible for h_x not too small[9]. These oscillations have indeed been observed numerically in [65]. Hence, we see that for quench III kink confinement in $d = 1$ produces for h_x large enough the undamped oscillations that in $d > 1$ are already present at first order in h_x. For quench IV, instead, the stability of the kinks precludes in $d = 1$ the undamped oscillations that arise in $d > 1$. It is worth recalling that the presence of kinks in the spontaneously broken phase of systems with discrete symmetry, as well as their confinement under explicit symmetry breaking, are generic in $d = 1$ (see [74, 75]), so that considerations analogous to those we made for Ising apply more generally.

In $d = 1$ the theory (4.29) possesses a single species of quasiparticles at $h_x = 0$, so that (4.2) and (4.5) hold as they are. In $d > 1$, on the other hand, more species may be present, in which case the term $2M^{-2}F_1^\Psi F_1^\Phi \cos Mt$ in (4.2) is replaced by $\sum_a 2M_a^{-2}F_{1,a}^\Psi F_{1,a}^\Phi \cos M_a t$, where a labels the different species; a similar generalization occurs in (4.5). For the ferromagnetic phase in $d = 2$ there is numerical consensus [76–81] about the existence, besides the lightest quasiparticle with mass M_1, of a second stable quasiparticle with mass $M_2 \approx 1.8M_1$. A spectral analysis of the undamped oscillations expected for quench IV should provide an alternative, possibly more accurate, way of determining this mass ratio.

It was also observed in [58] that in presence of several quasiparticle species oscillation frequencies $M_a - M_b$ can arise at order λ^2. In addition, the comparison performed in [57] with the result of [73] for non-interacting fermions indicates that corrections of order λ^2 and higher lead to the replacement of the pre-quench masses with the post-quench ones, and numerical evidence in this sense for interacting quasiparticles was given in [63, 82]. By post-quench masses we mean the masses of the equilibrium theory with the post-quench values of the couplings; their difference from the pre-quench masses is of order λ. The mass ratio M_2/M_1 to be observed in quench IV in $d = 2$ does not depend on λ in the scaling region.

The time evolution of the order parameter $\langle \sigma^x \rangle$ (in our notations) following a homogeneous quench in the Ising ferromagnetic phase has been numerically investigated in $d = 2$ in [83, 84], for a pre-quench value $h_z^i = 0$ that maximizes the distance from the continuum limit of our analytical study. Still, confirming a robustness of our results, the plots show undamped oscillations, at least for post-quench values h_z^f not too close to h_z^c. When h_z^f approaches h_z^c the correlation length becomes large, the long cylinder with a six-site circumference used in the simulation no longer approximates the plane, and a crossover to one-dimensional behavior (with damping of the oscillations) can be expected. In perspective, it would be very interesting to have numerical results for small quenches to perform the first quantitative comparison with analytical results in $d = 2$.

[9] As recalled above, the results at first order in λ quantitatively hold until a time scale that goes to infinity as λ goes to zero. Ref. [57] contains a more detailed discussion of Ising quenches in $d = 1$, including the agreement with other analytical results [72, 73] available for quenches I and IV (non-interacting fermions) when $\mathcal{D} = \mathbb{R}$. More generally, for $d = 1$ one can exploit the exact knowledge of all matrix elements (4.11) when the pre-quench theory is integrable [56].

4.6 Final remarks

In the present chapter we studied quantum quenches of systems in d spatial dimensions that are initially in the ground state of a spatially homogeneous Hamiltonian H_0. The quench is performed instantaneously changing an interaction parameter inside a spatial region $\mathcal{D}$. The analytical results that we derived provide unique benchmarking for numerical and experimental methods, as well as a general picture of the time evolution of local observables. In the first place the evolution takes place inside a lightcone that originates from the boundary of $\mathcal{D}$ at the moment of the quench and spreads outwards as time increases. Inside the lightcone the observable undergoes oscillations with frequency equal to the quasiparticle mass, which persist undamped at late times under two types of conditions. The first type, of dynamical nature, requires that the state produced by the quench includes single-quasiparticle modes and that the observable couples to them. These requirements are generically fulfilled when the quasiparticles interact, unless internal symmetries of the system cause the vanishing of some matrix elements, a mechanism that we illustrated through the paradigmatic example of the quantum Ising model. The second condition, of geometrical type, is that the energy density does not tend to zero at large times, and is fulfilled when the volume of $\mathcal{D}$ is extensive in all dimensions. The wavefronts spreading from the boundary of $\mathcal{D}$ are increasingly structured as the boundary deviates from a smooth surface. Our formulae apply to any choice of $\mathcal{D}$, and we provided explicit illustrations of these features through some examples.

Chapter 5

Quantum quenches from an excited state

Here we show how the theory of quantum quenches can be extended to the case in which before the quench the system is in an excited state.

5.1 Introduction

Determining the role of initial conditions in the late time evolution is a key issue for the theory of non-equilibrium dynamics of isolated quantum systems. In this chapter we investigate the dependence on initial conditions for the case of a non-equilibrium state that is generated dynamically by a change of an interaction parameter at time $t = 0$, i.e. after a quantum quench. It was shown in [56] that for a homogeneous one-dimensional system with Hamiltonian

$$H = \begin{cases} H_0\,, & t < 0\,, \\ H_0 + \lambda \int dx\, \Psi(x)\,, & t > 0\,, \end{cases} \tag{5.1}$$

which for $t < 0$ is in the ground state $|0\rangle$ of the pre-quench Hamiltonian H_0, it is possible to obtain *general* results perturbatively in the quench size λ, for the different quench operators $\Psi(x)$ and independently of the strength of the interaction among the quasiparticles. In particular, the result[1]

$$\langle \Phi(x,t) \rangle_0 = \langle \Phi \rangle_\lambda^{\rm eq} + \lambda \left[\frac{2}{M^2}\, F_1^\Psi F_1^\Phi\, \cos Mt + O(t^{-3/2}) \right] + O(\lambda^2) \tag{5.2}$$

is obtained for the one-point function of an operator Φ at large time (this coincides with the result (4.2) of the previous chapter with $d = 1$ and $\alpha = 3/2$). Here $\langle \Phi \rangle_\lambda^{\rm eq}$ is the

[1] The subscript 0 in (5.2) refers to the number of quasiparticle excitations in the pre-quench state, which is zero for the ground state.

equilibrium expectation value in the theory with the post-quench Hamiltonian [57], M the quasiparticle mass, and $F_1^{\mathcal{O}}$ the matrix element of $\mathcal{O}$ between the ground state $|0\rangle$ and the one-quasiparticle state[2]. As a particularly interesting feature, the result (5.2) first revealed that undamped oscillations are present whenever an internal symmetry does not cause the vanishing of the product $F_1^{\Psi}F_1^{\Phi}$ of the one-quasiparticle matrix elements [56]. In particular, the undamped oscillations of one-point functions are absent in the case of non-interacting quasiparticles – for which $F_1^{\Psi} = 0$ – thus showing that interaction makes a qualitative difference in non-equilibrium quantum dynamics.

The extension of the analytical results of [56] to higher spatial dimensions was given in [59], where it was shown, in particular, that $F_1^{\Psi}F_1^{\Phi} \neq 0$ continues to be the condition for undamped oscillations in a homogeneous quench[3]. It is natural to ask to which extent the presence of persistent oscillations depends on the initial conditions. Answering this question, however, proved to be quite difficult. Indeed, changing the initial condition for the homogeneous quench (5.1) means starting with a pre-quench state other than the ground state of H_0, and then with a non-normalizable state whose direct use leads to undetermined expressions.

Here we show how to overcome these technical difficulties considering an infinite and homogeneous system in one spatial dimension which before the quench (i.e. for $t < 0$) is in the first excited state, namely the one-quasiparticle state $|q\rangle$. The latter is an eigenstate of the pre-quench Hamiltonian H_0 with momentum q and energy

$$E_q = \sqrt{M^2 + q^2}\,, \tag{5.3}$$

and is normalized as

$$\langle p|q\rangle = 2\pi E_q \delta(p-q)\,. \tag{5.4}$$

A direct use of the pre-quench state $|q\rangle$ for the determination of the post-quench dynamics, however, is complicated by the appearance of singular factors such as $\langle q|q\rangle$. These factors, appearing in the numerator and denominator of the expressions for the observables, lead to indeterminate expressions. It is then necessary to first prevent the singularities introducing a regulator R to be removed at the end of the calculations, leaving a finite result for the observables. We do so starting with a pre-quench state in the form of the wave packet

$$\int_{-\infty}^{\infty} dq\, f(q)\, |q\rangle\,, \tag{5.5}$$

with

$$f(q) = \frac{R}{\sqrt{2\pi}}\, e^{-\frac{R^2}{2}\, q^2}\,. \tag{5.6}$$

[2]We refer for simplicity to the case of a single species of quasiparticles. Otherwise, the square bracket in (5.2) is summed over species [56].

[3]For the more general case of inhomogeneous quenches there is an additional condition about the extensiveness of the quenched domain [59], see also the previous chapter.

The results corresponding to the pre-quench state[4] $|q=0\rangle$ are obtained taking the limit $R\to\infty$ in the final expressions for observable quantities.

5.2 Post-quench state and one-point functions

The state $|\psi_1\rangle$ produced by the quench is given by

$$|\psi_1\rangle = S_\lambda \int dq\, f(q)\,|q\rangle = T\exp\left(-i\lambda\int_0^{+\infty} dt\int_{-\infty}^{+\infty} dx\,\Psi(x,t)\right)\int dq\, f(q)\,|q\rangle\,, \tag{5.7}$$

where T denotes chronological order and S_λ is the operator whose matrix elements $\langle n|S_\lambda|q\rangle$ give the probability amplitude that the quench induces the transition from $|q\rangle$ to $|n\rangle$. Here we adopt the compact notation $|n\rangle = |p_1,...,p_n\rangle$ for the n-quasiparticle states of the pre-quench theory, having energy and momentum

$$E=\sum_{i=1}^n E_{p_i}\,,\qquad P=\sum_{i=1}^n p_i\,, \tag{5.8}$$

respectively. To first order in the quench parameter λ we have

$$|\psi_1\rangle \simeq \int dq\, f(q)\,|q\rangle + 2\pi\lambda \sum\!\!\!\!\!\!\int_{n,p_i} dq\, f(q)\,\delta(P-q)\,\frac{[F^\Psi_{1,n}(q\,|\{p_i\})]^*}{E-E_q}\,|n\rangle\,, \tag{5.9}$$

where we defined the matrix elements

$$F^{\mathcal{O}}_{1,n}(q\,|\{p_i\}) = \langle q|\mathcal{O}(0,0)|p_1,...,p_n\rangle \tag{5.10}$$

for a generic operator $\mathcal{O}(x,t)$, introduced the notation

$$\sum\!\!\!\!\!\!\int_{n,p_i} = \sum_{n\neq 1}\frac{1}{n!}\int_{-\infty}^{+\infty}\prod_{i=1}^n\frac{dp_i}{2\pi E_{p_i}}\,, \tag{5.11}$$

and used

$$\mathcal{O}(x,t) = e^{i\mathcal{P}x+iH_0t}\,\mathcal{O}(0,0)\,e^{-i\mathcal{P}x-iH_0t}\,, \tag{5.12}$$

with $\mathcal{P}$ the momentum operator. An infinitesimal imaginary part was given to the energy to make the time integral in (5.7) convergent. The sum (5.11) is taken on the non-negative integers with the exclusion of $n=1$, which in (5.9) corresponds to $-iLT_+\lambda\int dq\, f(q)\,F^\Psi_{1,1}(q|q)$, where LT_+ is the infinite post-quench spacetime volume; this contribution is due to mass renormalization and is subtracted by a corresponding counterterm in the Hamiltonian[5].

[4] A state $|q_0\rangle$ can be obtained centering the Gaussian in q_0. Since we will only consider scalar operators, the results for $R\to\infty$ do not depend on q_0, and setting it to zero involves no loss of generality.

[5] See [71] for an analogous subtraction in the equilibrium context.

In an interacting theory, the matrix elements $F^{\Psi}_{1,n}$ entering (5.9) are nonzero for any n, so that the state produced by the quench is a superposition of states containing any number of quasiparticles with all possible momenta. It is worth emphasizing that it is our ability to deal with this structure in its full complexity that allows us to obtain general analytical results about quantum quench dynamics.

The result (5.9) gives in particular

$$\langle\psi_1|\psi_1\rangle = \int dpdq\, f(p)f(q)\langle p|q\rangle \, + O(\lambda^2) \sim \sqrt{\pi}MR + O(\lambda^2)\,. \tag{5.13}$$

Here and below the symbol $\sim$ indicates omission of terms subleading for $R \to \infty$.

The one-point function of a scalar hermitian operator $\Phi(x,t)$ after a quench from the single-quasiparticle state is given by

$$\begin{aligned}\langle\Phi(x,t)\rangle_1 &= \frac{\langle\psi_1|\Phi(x,t)|\psi_1\rangle}{\langle\psi_1|\psi_1\rangle} + D_\Phi \\ &\sim \frac{1}{\langle\psi_1|\psi_1\rangle}\int dp\, dq\, f(p)f(q)\Big[F^{\Phi}_{1,1}(p|q) \\ &+ 2\pi\lambda \sum\!\!\!\!\!\!\int_{n,p_i} \frac{\delta(P-q)}{E-E_P}\, 2\mathrm{Re}\left\{[F^{\Psi}_{1,n}(P\,|\{p_i\})]^* F^{\Phi}_{1,n}(p\,|\{p_i\})\, e^{i(E_p-E)t}\right\}\Big] \\ &+ D_\Phi + O(\lambda^2)\,.\end{aligned} \tag{5.14}$$

Here and below the limit $R \to \infty$ is understood. Then the limit $p, q \to 0$ is enforced by the Gaussian $f(p)f(q)$, so that the factors $e^{i(p-q)x}$ and $e^{i(E_p-E_q)t}$ produced by (5.12) can be omitted at leading order for large R; this yields the x-independence expected for the homogeneous system, as well as the t-independence of the pre-quench value

$$A_\Phi = \frac{\int dp\, dq\, f(p)f(q)\, F^{\Phi}_{1,1}(p|q)}{\int dp\, dq\, f(p)f(q)\langle p|q\rangle}\,. \tag{5.15}$$

The term D_Φ is added to ensure continuity at $t = 0$, namely to impose that $\langle\Phi(x,0)\rangle_1$ is equal to (5.15). Defining

$$B_\Phi(t) = \frac{2\pi}{\langle\psi_1|\psi_1\rangle} \sum\!\!\!\!\!\!\int_{n,p_i} \int dp\, \frac{f(p)f(P)}{E-E_P}\, 2\mathrm{Re}\left\{[F^{\Psi}_{1,n}(P\,|\{p_i\})]^* F^{\Phi}_{1,n}(p\,|\{p_i\})\, e^{i(E_p-E)t}\right\}, \tag{5.16}$$

we have

$$D_\Phi = -\lambda\, B_\Phi(0) + O(\lambda^2)\,, \tag{5.17}$$

and

$$\langle\Phi(x,t)\rangle_1 = A_\Phi + \lambda\,[B_\Phi(t) - B_\Phi(0)] + O(\lambda^2)\,. \tag{5.18}$$

5.3 Large time behavior

The time dependence of the one-point function (5.18) is contained in the term (5.16). For $t \to \infty$ the integrand rapidly oscillates due to the factor $e^{i(E_p - E)t}$ and the leading contribution to the integral is obtained when all the momenta $p, p_1, \ldots, p_n$ are small. Notice that this is true also in case of cancellation of energy terms in the exponent. Indeed, p is in any case made small by the large R limit, so that $E_p \simeq M + p^2/2M$ can only be canceled by a single energy term E_{p_i}, with the consequence that $p_i = p$ is also small.

The matrix elements in (5.16) can be rewritten in terms of the form factors

$$F_n^{\mathcal{O}}(p_1, \ldots, p_n) = \langle 0|\mathcal{O}(0,0)|p_1, \ldots, p_n\rangle \tag{5.19}$$

by crossing the quasiparticle on the left. For $p, p_1, \ldots, p_n \to 0$ this gives

$$\begin{aligned} F_{1,n}^{\mathcal{O}}(p|p_1, \ldots, p_n) &= F_{n+1}^{\mathcal{O}}(\bar{p}, p_1, ..., p_n) \\ &\quad + \sum_{i=1}^{n} 2\pi E_{p_i} \delta(p_i - p)\, (-1)^{i-1}\, F_{n-1}^{\mathcal{O}}(p_1, ..., p_{i-1}, p_{i+1}, ..., p_n)\,, \end{aligned} \tag{5.20}$$

where $\bar{p}$ corresponds to the crossed quasiparticle with momentum $-p$ and energy $-E_p$, the first term on the r.h.s. is the connected part, and the terms with the delta function are the disconnected parts produced by the annihilation between the crossed quasiparticle and the quasiparticle with momentum p_i. In writing (5.20) we took into account that for small momenta interacting theories in one spatial dimension exhibit fermionic statistics; this produces the factor $(-1)^{i-1}$ when the crossed quasiparticle reaches the quasiparticle to be annihilated. It follows that the product of matrix elements in (5.16) is given by

$$\begin{aligned} &[F_{1,n}^{\Psi}(P|\{p_i\})]^* F_{1,n}^{\Phi}(p|\{p_i\}) = [F_{n+1}^{\Psi}(\bar{P}, p_1, ..., p_n)]^* F_{n+1}^{\Phi}(\bar{p}, p_1, ..., p_n) \\ &+ [F_{n+1}^{\Psi}(\bar{P}, p_1, ..., p_n)]^* \sum_{i=1}^{n} 2\pi E_{p_i} \delta(p_i - p)\, (-1)^{i-1}\, F_{n-1}^{\Phi}(p_1, ..., p_{i-1}, p_{i+1}, ..., p_n) \\ &+ F_{n+1}^{\Phi}(\bar{p}, p_1, ..., p_n) \sum_{i=1}^{n} 2\pi E_{p_i} \delta(p_i - P)\, (-1)^{i-1}\, \left[F_{n-1}^{\Psi}(p_1, ..., p_{i-1}, p_{i+1}, ..., p_n)\right]^* \\ &+ \sum_{i=1}^{n}\sum_{j=1}^{n} (2\pi)^2 E_{p_i} E_{p_j} \delta(p_i - P)\delta(p_j - p)\, (-1)^{i+j-2}\, \left[F_{n-1}^{\Psi}(p_1, ..., p_{i-1}, p_{i+1}, ..., p_n)\right]^* \\ &\times F_{n-1}^{\Phi}(p_1, ..., p_{j-1}, p_{j+1}, ..., p_n)\,. \end{aligned} \tag{5.21}$$

We call the four terms in the r.h.s. connected-connected ($c_\Psi c_\Phi$), connected-disconnected ($c_\Psi d_\Phi$), disconnected-connected ($d_\Psi c_\Phi$) and disconnected-disconnected ($d_\Psi d_\Phi$), respectively. For the latter we further distinguish the terms with $i = j$ ($d_\Psi^i d_\Phi^i$) from those with $i \neq j$ ($d_\Psi^i d_\Phi^j$). Inserting (5.21) back into (5.16), the exponential factor in the integrand for each type of contribution reads

- $c_\Psi c_\Phi : e^{-\frac{R^2}{2}(p+P^2)+i[M(1-n)t-\frac{t}{2M}\sum_{i=1}^n p_i^2]}$
- $c_\Psi d_\Phi : e^{-\frac{R^2}{2}(p_i+P^2)+i[M(1-n)t-\frac{t}{2M}\sum_{k\neq i}^n p_k^2]}$
- $d_\Psi c_\Phi : e^{-\frac{R^2}{2}(p+p_i^2)+i[M(1-n)t-\frac{t}{2M}\sum_{k\neq i}^n p_k^2]}$
- $d^i_\Psi d^i_\Phi : e^{-R^2p_i^2+i[M(1-n)t-\frac{t}{2M}\sum_{k\neq i}^n p_k^2]}$
- $d^i_\Psi d^j_\Phi : e^{-\frac{R^2}{2}(p_i^2+p_j^2)+i[M(1-n)t-\frac{t}{2M}\sum_{k\neq i,j}^n p_k^2]}$.

Due to the delta functions, some energies can cancel in $e^{i(E_p-E)t}$ and no longer couple to t; as already observed, however, the corresponding momenta are still made small by the large R limit. Moreover, if p_i^2 coming from $E_{p_i} \simeq M + p_i^2/2M$ couples in the exponential both to R^2 and t, we have $(R^2 \pm it/M)p_i^2 \to R^2 p_i^2$ in the limit $R \to \infty$, which must be taken before that of large times.

For small momenta the form factors F^Φ_{n+1} in (5.21) behave as

$$\prod_{i=1}^n \frac{1}{p-p_i} \prod_{1\leq i<j\leq n} (p_i - p_j)\,, \tag{5.22}$$

where the numerator accounts for the fermionic statistics and the denominator for the annihilation poles[6]; the same is true for F^Ψ_{n+1} after replacing p with P. On the other hand, the form factors F^Φ_{n-1} and F^Ψ_{n-1}, which are the products of the annihilations, behave as $\prod_{k<l\,(k,l\neq i)}(p_k - p_l)$. The large time behavior of the different contributions to (5.18) is now easily determined rescaling the momenta which couple to t in the exponent. Up to the oscillating factor $e^{-i(n-1)Mt}$ we have

- $c_\Psi c_\Phi : t^{-n(n-1)/2}$
- $c_\Psi d_\Phi, d_\Psi c_\Phi, d^i_\Psi d^i_\Phi : t^{-n(n-2)/2}$
- $d^i_\Psi d^j_\Phi : t^{-(n-2)^2/2}$.

We see that the leading contribution at large time comes from $n = 0$ ($c_\Psi c_\Phi$) and $n = 2$ ($c_\Psi d_\Phi, d_\Psi c_\Phi, d^i_\Psi d^i_\Phi, d^i_\Psi d^j_\Phi$), and is purely oscillatory[7]. It is easily checked in a similar way that the term $d^i_\Psi d^j_\Phi$ with $n = 3$ actually vanishes as $R \to \infty$, so that the first subleading contribution at large t comes from $c_\Psi c_\Phi$ with $n = 2$ and is suppressed as t^{-1}.

Concerning the explicit calculation of the leading large time behavior of (5.16), it is straightforward for the $n = 0$ contribution. For the $n = 2$ contributions we know from (5.22) that

$$F^\Phi_3(\bar p, p_1, p_2)\big|_{p,p_1,p_2\to 0} \simeq a_\Phi\, \frac{p_1 - p_2}{(p-p_1)(p-p_2)}\,, \tag{5.23}$$

[6] See [85] for explicit illustrations in the case of integrable theories.

[7] We recall that $n \neq 1$ and that $n = 0$ produces no disconnected part.

and similarly

$$F_3^{\Psi}(\bar{P}, p_1, p_2)\big|_{P,p_1,p_2\to 0} \simeq a_{\Psi}\,\frac{p_1 - p_2}{p_1 p_2}\,. \tag{5.24}$$

The fermionic statistics at low energies yields the expression

$$\operatorname*{Res}_{q_1=q_2} F_{k+2}^{\mathcal{O}}(\bar{q}_1, q_2, p_1, ..., p_k) = iM\left[1-(-1)^k\right]\, F_k^{\mathcal{O}}(p_1, ..., p_k)\,, \tag{5.25}$$

for the residue on an annihilation pole in the limit $q_1, q_2, p_1, ..., p_k \to 0$ of our present interest. This in turn determines the coefficients

$$a_{\Phi} = 2iMF_1^{\Phi}\,, \tag{5.26}$$

$$a_{\Psi} = 2iMF_1^{\Psi}\,. \tag{5.27}$$

The integrals in (5.16) are then computed using the expressions (5.23) and (5.24) with the prescription

$$\frac{1}{p - i\epsilon} = i\pi\delta(p) + \text{p.v.}\left(\frac{1}{p}\right) \tag{5.28}$$

for the poles. The results for the leading contributions are[8]

- $n = 0$
  - $c_{\Psi}c_{\Phi} : -\frac{2\sqrt{2}\lambda}{M^2}\, F_1^{\Psi}F_1^{\Phi}\, \cos Mt$
- $n = 2$
  - $c_{\Psi}d_{\Phi} : \frac{2\lambda}{M^2}(1-\sqrt{2})\, F_1^{\Psi}F_1^{\Phi}\, \cos Mt$
  - $d_{\Psi}c_{\Phi} : \frac{2\lambda}{M^2}(1+\sqrt{2})\, F_1^{\Psi}F_1^{\Phi}\, \cos Mt$
  - $d_{\Psi}^i d_{\Phi}^i : \frac{2\lambda}{M^2}\, F_1^{\Psi}F_1^{\Phi}\, \cos Mt$
  - $d_{\Psi}^i d_{\Phi}^j : -\frac{2\sqrt{2}\lambda}{M^2}\, F_1^{\Psi}F_1^{\Phi}\, \cos Mt\,,$

where we took into account that for scalar hermitian operators $F_1^{\mathcal{O}}$ is a real constant. Putting all together we obtain

$$B_{\Phi}(t) = \frac{F_1^{\Psi}F_1^{\Phi}}{M^2}\,(6 - 4\sqrt{2})\, \cos Mt + O(t^{-1})\,, \qquad t \to \infty\,. \tag{5.29}$$

We see from (5.18) and (5.29) that for $t \to \infty$ the one-point function $\langle\Phi(x,t)\rangle_1$ tends to (if $F_1^{\Psi}F_1^{\Phi} = 0$) or oscillates around (if $F_1^{\Psi}F_1^{\Phi} \neq 0$) the asymptotic offset $A_{\Phi} + D_{\Phi}$. The

[8] They come only from the delta function terms in the pole prescription, since the principal values turn out to be subleading for $R \to \infty$.

pre-quench value A_Φ is given by (5.15) and involves $F^\Phi_{1,1}(p|q)$. Equations (5.20) and (5.25) yield[9]

$$F^{\mathcal{O}}_{1,1}(p|q) = F^{\mathcal{O}}_2(\bar{p},q) + 2\pi E_p\,\delta(p-q)\,F^{\mathcal{O}}_0\,, \tag{5.30}$$

$$\operatorname*{Res}_{p=q} F^{\mathcal{O}}_2(\bar{p},q) = 0\,. \tag{5.31}$$

It follows that in the limit $R\to\infty$ implied in (5.15) we obtain

$$A_\Phi = F^\Phi_0 = \langle 0|\Phi|0\rangle\,. \tag{5.32}$$

We see that the pre-quench value on the excited state coincides with that on the ground state[10]. On the other hand, since the post-quench state (5.9) differs from that obtained from a quench from the ground state, the time evolution is in general different in the two cases. In particular, recalling also (5.17), for the asymptotic offset we obtain

$$E_\Phi \equiv A_\Phi + D_\Phi = \langle 0|\Phi|0\rangle - \lambda\,B_\Phi(0) + O(\lambda^2)\,, \tag{5.33}$$

which differs at order λ from that in (5.2). Equations (5.29) and (5.33) lead to the large time result

$$\langle\Phi(x,t)\rangle_1 = E_\Phi + \lambda\left[\frac{6-4\sqrt{2}}{M^2}\,F^\Psi_1 F^\Phi_1\,\cos Mt + O(t^{-1})\right] + O(\lambda^2)\,. \tag{5.34}$$

Comparing this result with (5.2) we see that, although the amplitude of the undamped oscillations has changed, the condition for their presence continues to be $F^\Psi_1 F^\Phi_1 \neq 0$. The offset E_Φ in general differs at order λ from $\langle\Phi\rangle^{\rm eq}_\lambda$ in (5.2). Actually, as we will see, E_Φ can differ from $\langle\Phi\rangle^{\rm eq}_\lambda$ at order 1 for a quench in a spontaneously broken phase, for which the first excited state is a topological excitation.

5.4 Topological quasiparticles

Some additional considerations are needed if the quench is performed within a phase with spontaneously broken symmetry. In the one-dimensional case we are considering this means that there are degenerate ground states $|0_a\rangle$ labeled by $a = 1,2,\ldots,N$, and that the fundamental quasiparticle excitations have a topological nature, namely they are kinks $|K_{ab}(q)\rangle$ interpolating between $|0_a\rangle$ and $|0_b\rangle$, with $a\neq b$. It follows that the first excited

[9] It can be noted that, although the limit $R\to\infty$ in (5.15) ensures that $p,q\to 0$, eqs. (5.30) and (5.31) hold for generic momenta. Indeed, the annihilation which produces the disconnected part requires no permutation, and no consideration on low-energy statistics.

[10] This result requires a generalization in the case of topological quasiparticles, to be discussed in the next section.

state we consider in this chapter as the pre-quench state now corresponds to such a kink. Then, when considering the pre-quench expectation value (5.15), eq. (5.30) still holds with

$$F_0^{\mathcal{O}} = \langle 0_a|\mathcal{O}(0,0)|0_a\rangle \equiv \langle \mathcal{O}\rangle_a \,, \tag{5.35}$$

and

$$F_2^{\mathcal{O}}(\bar{p},q) = \langle 0_a|\mathcal{O}(0,0)|K_{ab}(\bar{p})K_{ba}(q)\rangle \,. \tag{5.36}$$

Now, however, (5.31) is replaced by[11] [86]

$$\operatorname*{Res}_{p=q} F_2^{\mathcal{O}}(\bar{p},q) = iM[\langle \mathcal{O}\rangle_a - \langle \mathcal{O}\rangle_b] \,. \tag{5.37}$$

The pole associated to (5.37) now gives an additional contribution when (5.15) is evaluated using (5.28), with the result that the pre-quench expectation value becomes

$$A_\Phi = \frac{\langle \Phi\rangle_a + \langle \Phi\rangle_b}{2} \,. \tag{5.38}$$

The meaning of this result is quite clear. In the kink state, the system is in the ground state $|0_a\rangle$ on one side of the spatial location of the kink, and in the ground state $|0_b\rangle$ on the other side. Since the kink has a definite momentum q, it is completely delocalized in space, so that the expectation value of the field is given by the average (5.38).

With this new expression for A_Φ, the post-quench one-point function is still given by (5.18) and (5.16). Concerning its large time behavior, an undamped oscillating term would be again proportional to $F_1^\Psi F_1^\Phi$. However, the physically relevant cases correspond to a topologically neutral quench operator Ψ, and this implies that $F_1^\Psi = \langle 0_a|\Psi(0,0)|K_{ba}(q)\rangle$ vanishes. It follows that the large time result (5.34) now becomes

$$\langle \Phi(x,t)\rangle_1 = \frac{\langle \Phi\rangle_a + \langle \Phi\rangle_b}{2} - \lambda\left[B_\Phi(0) + O(t^{-1})\right] + O(\lambda^2) \,. \tag{5.39}$$

It is interesting to compare this result with that obtained in [87], where the time evolution in a non-equilibrium state interpolating between the degenerate ground states $|0_a\rangle$ and $|0_b\rangle$ was studied in a "no-quench" setting[12]. We mean by this that, instead of considering the non-equilibrium state produced by a quench as in the present case, in [87] an infinite-dimensional space of interpolating non-equilibrium states was considered. Hence, the two results for the one-point function at large time, while referring to the same topological setting, have a significantly different origin. It is then nontrivial that they turn out to exhibit similar features[13]. In both cases undamped oscillations are absent and the approach to the asymptotic offset is through terms decaying as t^{-1}. In both cases the offset involves the average (5.38): in (5.39) the expectation values $\langle \Phi\rangle_a$ and $\langle \Phi\rangle_b$ refer to the $t<0$ Hamiltonian, and there is the correction $-\lambda B_\Phi(0)$ due to the quench; in [87] the offset is (5.38) with $\langle \Phi\rangle_a$ and $\langle \Phi\rangle_b$ referring to the $t>0$ Hamiltonian.

[11] While (5.37) was considered in [86] in the context of an integrable theory, the derivation given there is general, since involves no scattering.

[12] See the following chapter for a detailed discussion.

[13] For the case of [87] we refer to $t\to\infty$ with x fixed.

5.5 Final remarks

In this chapter we studied analytically the dependence on the initial condition of the late time dynamics following a quantum quench of a generic homogeneous one-dimensional system. More precisely, we considered the case in which before the quench the system is in the first excited state of its Hamiltonian H_0, at variance with the case of quenches from the ground state (see chapter 4). We overcame the technical difficulties related to the non-normalizability of the excited state working in presence of a regulator which, once removed at the end of the calculations, leaves a finite result for the observables. In this way we showed, in particular, that the condition for the presence of persistent oscillations of one-point functions is not affected by the change of the initial condition and remains that first found in [56] for quenches from the ground state: persistent oscillations of one-point functions arise if the post-quench spectrum of excitations includes neutral quasiparticles, and if the observable couples to these quasiparticles. The argument of [58] pointing to oscillations persisting beyond the perturbative scale of our calculations – a circumstance indeed numerically observed in [63] – applies also to the present case. At the same time, the comparison with the case of quenches from the ground state also shows quantitative differences in the amplitude of the oscillations, as well as in the value of the asymptotic offset. Another difference with the case of quenches from the ground state is that those from the excited state heavily involve, already at first order in the quench parameter λ, the connectedness structure of the matrix elements, with disconnected parts playing a substantial role. The role of disconnected parts in non-equilibrium quantum dynamics was already pointed out in [69], where it was generally shown that they are responsible for the lightcone propagation of two-point correlations.

We also illustrated the implications of our results for quenches performed within a spontaneously broken phase, for which the first excited state corresponds to a topological excitation: a kink, or domain wall. We observed how the results for one-point functions at late times share quantitative properties with those obtained in [87] in a very different way, namely considering an infinite-dimensional space of initial conditions of domain wall type, not necessarily produced by a quench (see the following chapter).

Chapter 6

Space of initial conditions and universality

We study analytically the role of initial conditions in non-equilibrium quantum dynamics considering the one-dimensional ferromagnets in the regime of spontaneously broken symmetry. We analyze the expectation value of local operators for the infinite-dimensional space of initial conditions of domain wall type, generally intended as initial conditions spatially interpolating between two different ground states. In systems with more than two ground states the tuning of an interaction parameter can induce a transition which is the non-equilibrium quantum analogue of the interfacial wetting transition occurring in classical systems at equilibrium.

6.1 Introduction

Universality is a central paradigm of statistical physics. In the equilibrium setting, in which it originated and is well established [2], it says that systems possessing a continuous phase transition exhibit a number of quantitative properties that do not depend on the microscopic details of the Hamiltonian, for example the range of the interaction as long as it is short. In a given space dimensionality, these *universal* properties depend instead on the group G of internal transformations that leave the Hamiltonian invariant, so that G is the label of the different universality classes (see chapter 1).

The extension of such a notion of universality to the non-equilibrium framework is a nontrivial task. In the quantum case, a time independent Hamiltonian H generates unitary time evolution as in equilibrium. However, observables are now expectation values on a non-equilibrium state $|\psi\rangle$ that is not an eigenstate of H, but rather, in the physically interesting cases, a superposition of infinitely many eigenstates. The question then arises of whether the notion of universality is compatible with the presence of the infinitely many coefficients of the superposition, which in turn correspond to infinitely many possible initial

conditions of the time evolution. Since at the mathematical level these coefficients can be arbitrary, it is essential to refer to well defined physical problems.

We discussed in previous chapters the case on non-equilibrium states generated by quantum quenches. A physical problem involving no quench but still leading to a non-equilibrium state $|\psi\rangle$ is that in which H is the Hamiltonian of a translation invariant system, but the initial condition of the time evolution is spatially inhomogeneous. In this chapter we will study this problem for the case of the one-dimensional ferromagnets with interaction parameters in the range in which the spontaneous breaking of a discrete symmetry G leads to degenerate ground states that we denote $|0_a\rangle$, $a = 1, 2, \ldots, N$. We are interested in the expectation value $\langle \Phi(x,t) \rangle_{ab}$ of a local operator Φ (e.g. the order parameter operator), for initial ($t = 0$) conditions that interpolate between a ground state $|0_a\rangle$ as $x \to -\infty$, and a different ground state $|0_b\rangle$ as $x \to +\infty$. This interpolation is chosen to preserve the symmetry G of the system, but still can be realized in infinitely many ways, meaning that the corresponding non-equilibrium states $|\psi\rangle$ form an infinite-dimensional space $\mathcal{W}$. We refer to $\mathcal{W}$ as the space of domain wall states or, equivalently, of domain wall initial conditions.

6.2 Space of domain wall initial conditions

The elementary excitation modes of a one-dimensional ferromagnet in the regime of spontaneously broken symmetry are kinks interpolating between two degenerate ground states. In the proximity of the quantum critical point these are relativistic quasiparticles with energy and momentum

$$(E, p) = (M \cosh\theta, M \sinh\theta)\,, \tag{6.1}$$

where θ is called rapidity, and the mass M is a measure of the deviation from criticality. The interpolating initial conditions we are interested in correspond to non-equilibrium states of the form

$$|\psi\rangle = \sum_{n=1}^{\infty} |\psi_n\rangle = \sum_{n=1}^{\infty} \int d\theta_1 \ldots d\theta_n \, f_n(\theta_1, \ldots, \theta_n) \, |\theta_1, \ldots, \theta_n\rangle\,, \tag{6.2}$$

where $|\theta_1, \ldots, \theta_n\rangle$ is a n-kink state starting in $|0_a\rangle$ and ending in[1] $|0_b\rangle$. The different choices of the functions f_n span the space $\mathcal{W}$ of the domain wall states $|\psi\rangle$ and allow for arbitrary spatial interpolation in the initial condition. Since we consider initial conditions that do not introduce any explicit breaking of the symmetry of the system under the group G, the functions f_n are required to preserve this property. They are also required to decay for $\theta_i \to \pm\infty$ sufficiently rapidly to ensure convergence of the integrals over rapidities, and to be free of singularities for real values of the rapidities. The expectation value of a local

[1] It is understood that for $N > 2$ degenerate ground states and $n > 1$ the expansion (6.2) includes a sum over the intermediate ground states visited in the n-step path from $|0_a\rangle$ to $|0_b\rangle$.

operator with such a general symmetry preserving domain wall initial condition is given by

$$\langle\Phi(x,t)\rangle_{ab} = \frac{\langle\psi|\Phi(x,t)|\psi\rangle}{\langle\psi|\psi\rangle}\,. \tag{6.3}$$

6.2.1 Time evolution

We will now investigate the properties of the dynamics in the infinite-dimensional subspace $\mathcal{W}_1$ of initial conditions corresponding to one-kink states

$$|\psi_1\rangle = \int d\theta\, f(\theta)\,|\theta\rangle\,, \tag{6.4}$$

where we have simplified the notation setting $f_1 = f$. In this subspace the expectation value (6.3) reads

$$\begin{aligned} G_\Phi(x,t) &= \frac{1}{N_f}\,\langle\psi_1|\Phi(x,t)|\psi_1\rangle \\ &= \frac{1}{N_f}\int d\theta_1 d\theta_2\, f^*(\theta_1) f(\theta_2)\, F_\Phi(\theta_1-\theta_2)\, e^{i[(p_1-p_2)x+(E_1-E_2)t]}\,, \end{aligned} \tag{6.5}$$

where we defined[2]

$$N_f = \langle\psi_1|\psi_1\rangle = 2\pi\int d\theta\,|f(\theta)|^2\,, \tag{6.6}$$

$$F_\Phi(\theta_1-\theta_2) = \langle\theta_1|\Phi(0,0)|\theta_2\rangle\,, \tag{6.7}$$

and used

$$\Phi(x,t) = e^{i(Px+Ht)}\,\Phi(0,0)\,e^{-i(Px+Ht)}\,, \tag{6.8}$$

with P the momentum operator. The operators Φ of our interest are invariant under relativistic transformations and, since such a transformation shifts rapidities by a constant, the matrix element (6.7) depends on the rapidity difference. It can be written as [86]

$$F_\Phi(\theta) = i\frac{\langle\Phi\rangle_a - \langle\Phi\rangle_b}{\theta - i\epsilon} + \sum_{k=0}^{\infty} C_k^\Phi\,\theta^k + 2\pi\,\delta(\theta)\langle\Phi\rangle_a\,, \tag{6.9}$$

where

$$\langle\Phi\rangle_a = \langle 0_a|\Phi(x,t)|0_a\rangle \tag{6.10}$$

is the equilibrium expectation value in the ground state $|0_a\rangle$, the term containing $\delta(\theta)$ is the disconnected part corresponding to the annihilation of the particle on the left with the particle on the right, while the connected part has been expanded in powers of θ. The pole

[2]We use the state normalization $\langle\theta|\theta'\rangle = 2\pi\,\delta(\theta-\theta')$.

term is a remnant in the connected part of the annihilation configuration[3] $\theta = 0$, and the infinitesimal imaginary part $i\epsilon$ specifies the regularization prescription for the integral in (6.5).

Let us call $G_\Phi^{\rm sing}$ the contribution to (6.5) of (6.9) without the regular part $\sum_{k=0}^\infty C_k^\Phi\,\theta^k$. Defining $\theta_\pm = \theta_1 \pm \theta_2$ we write this contribution in the form

$$G_\Phi^{\rm sing}(x,t) = \langle\Phi\rangle_a + i\frac{\langle\Phi\rangle_a - \langle\Phi\rangle_b}{2N_f}\int d\theta_+ d\theta_-\,\frac{f^*(\theta_1)f(\theta_2)}{\theta_- - i\epsilon}\,e^{2iMt\,B(x/t,\theta_+)\sinh\frac{\theta_-}{2}}\,, \qquad (6.11)$$

where

$$B(x/t,\theta_+) = \frac{x}{t}\cosh\frac{\theta_+}{2} + \sinh\frac{\theta_+}{2}\,. \qquad (6.12)$$

We can set $\sinh\frac{\theta_-}{2} = p$ and consider the integral over p in which we close the contour in the upper (lower) complex half-plane if B is positive (negative). In particular, we can close the contour along the line with constant imaginary part $\mathrm{Im}\,p = c$. When $t \to \infty$, the contribution coming from the integral on this line is suppressed as $e^{-2M|cB|t}$ and can be neglected. On the other hand, we can reduce $|c|$ in such a way that the closed integration contour contains only the singularity at $p = i\epsilon/2$ for $c > 0$, and no singularity at all for $c < 0$. Hence, Cauchy's residue integration tells us that for t large

$$G_\Phi^{\rm sing}(x,t) \simeq \langle\Phi\rangle_a - \frac{\langle\Phi\rangle_a - \langle\Phi\rangle_b}{N_f}\,2\pi\int_{\theta_0}^\infty d\theta\,|f(\theta)|^2\,, \qquad (6.13)$$

where θ_0 is the value of θ above which $\tanh\theta > -x/t$. Since θ_0 is equal to $+\infty$ when $x/t < -1$ and to $-\infty$ when $x/t > 1$, we have

$$G_\Phi^{\rm sing}(x,t) \simeq \begin{cases}\langle\Phi\rangle_a\,, & x < -t\,,\\ \langle\Phi\rangle_b\,, & x > t\,,\end{cases} \qquad (6.14)$$

for t large. On the other hand, $\theta_0 \simeq -x/t$ when $|x|/t \ll 1$, and we can break the integration over θ into that on the small interval between $-x/t$ and 0, in which $f(\theta) \simeq f(0)$, and that for $\theta > 0$. Since the ground states $|0_a\rangle$ and $|0_b\rangle$ are exchanged by the symmetry G of the Hamiltonian and play a symmetric role preserved by the initial condition, $|f(\theta)|^2$ is an even function. As a consequence $2\pi\int_0^\infty d\theta\,|f(\theta)|^2 = N_f/2$ and we have

$$G_\Phi^{\rm sing}(x,t) \simeq \frac{\langle\Phi\rangle_a + \langle\Phi\rangle_b}{2} - 2\pi A_f\,[\langle\Phi\rangle_a - \langle\Phi\rangle_b]\,\frac{x}{t}\,, \qquad |x| \ll t\,, \qquad (6.15)$$

with $A_f = |f(0)|^2/N_f$.

[3]The pole is known to account for phase separation in the classical case at equilibrium [16], in which it yields, in particular, the exact order parameter profile originally obtained in [88,89] from the lattice solution of the two-dimensional Ising model. Annihilation poles are well known in the multiparticle matrix elements of integrable theories [85], but integrability plays no role in the determination of the residue for the matrix element (6.7) [86].

Now we consider the contribution to (6.5) coming from the regular part $\sum_{k=0}^{\infty} C_k^\Phi \, \theta^k$ of (6.9), namely

$$G_\Phi^{\rm reg}(x,t) = \frac{1}{N_f} \sum_{k=0}^{\infty} C_k^\Phi \int d\theta_1 d\theta_2 \, f^*(\theta_1) f(\theta_2) \, (\theta_1 - \theta_2)^k \, e^{i[(p_1-p_2)x + (E_1-E_2)t]} \, . \qquad (6.16)$$

We first observe that for t large enough the rapid oscillations of the integrand suppress the integral unless the phase is stationary, namely unless $E_j x + p_j t = 0$, $j = 1, 2$. Since $|p_j|/E_j = |\tanh\theta_j| < 1$, the stationarity condition is satisfied inside the lightcone[4] $|x| < t$. Hence, for t large we have

$$G_\Phi^{\rm reg}(x,t) \simeq 0 \, , \qquad |x| > t \, , \qquad (6.17)$$

where the corrections are small and rapidly vanishing as $|x|$ increases with t fixed.

On the other hand, the stationarity condition $\tanh\theta_j = -x/t$ implies that inside the lightcone small rapidities dominate the integral for $|x|/t \ll 1$. Hence in this limit we can write

$$G_\Phi^{\rm reg}(x,t) \simeq A_f \sum_{k=0}^{\infty} C_k^\Phi \int d\theta_1 d\theta_2 \, (\theta_1 - \theta_2)^k \, e^{iM[(\theta_1-\theta_2)x + \frac{1}{2}\theta_1^2(t+i\epsilon) - \frac{1}{2}\theta_2^2(t-i\epsilon)]} \, , \qquad (6.18)$$

where the infinitesimal imaginary parts added to t preserve the convergence of the integral. We can now rescale the rapidities and deduce that the k-th term decays at large times as $t^{-(k+2)/2}$. Hence the leading contribution comes from $k = 0$ and we have

$$\begin{aligned} G_\Phi^{\rm reg}(x,t) &\simeq A_f \, C_0^\Phi \left| \int d\theta \, e^{iM[\theta x + \frac{1}{2}\theta^2(t+i\epsilon)]} \right|^2 = A_f \, C_0^\Phi \, \frac{2\pi}{M|t+i\epsilon|} \, e^{-\frac{M\epsilon x^2}{t^2+\epsilon^2}} \\ &\to A_f \, C_0^\Phi \, \frac{2\pi}{Mt} \, , \qquad |x| \ll t \, . \end{aligned} \qquad (6.19)$$

Putting all together, since $G_\Phi(x,t)$ is the sum of $G_\Phi^{\rm sing}(x,t)$ and $G_\Phi^{\rm reg}(x,t)$, the results that we obtained for these two terms lead to the large time behaviors

$$G_\Phi(x,t) \simeq \begin{cases} \langle\Phi\rangle_a \, , & x < -t \, , \\ \frac{1}{2}\left[\langle\Phi\rangle_a + \langle\Phi\rangle_b\right] + \mathcal{A}\left\{\frac{C_0^\Phi}{M} - \left[\langle\Phi\rangle_a - \langle\Phi\rangle_b\right] x\right\} t^{-1} \, , & |x| \ll t \, , \\ \langle\Phi\rangle_b \, , & x > t \, , \end{cases} \qquad (6.20)$$

where C_0^Φ is determined by the equilibrium universality class, while the positive dimensionless amplitude

$$\mathcal{A} = 2\pi A_f = 2\pi \, \frac{|f(0)|^2}{N_f} \qquad (6.21)$$

[4]This mechanism leading to the lightcone can be compared with that for two-point functions in homogeneous systems out of equilibrium, in which the connectedness structure of matrix elements plays an essential role [69]. The presence of a lightcone was originally observed in the study of a free fermionic chain with a steplike initial condition [90].

is the only quantity depending on the specific initial condition.

When $\langle\Phi\rangle_a \neq \langle\Phi\rangle_b$, $G_\Phi(x,t)$ should tend as $t \to \infty$ to a non-constant limit shape as a function of x/t, since in this variable the edges of the lightcone are fixed at ± 1. To see this, we notice that if the large time analysis of the contribution (6.16) of regular terms is performed at a generic point x inside the lightcone, the stationarity condition $\tanh\theta_j = -x/t$ selects the rapidities around which to expand to evaluate the integral, and considerations analogous to those we just made for x small lead to the conclusion that again this contribution is suppressed at large times. It follows that (6.16) goes to zero for any x at large times, so that in this limit the dominant x-dependence is given by (6.13), as long as $\langle\Phi\rangle_a \neq \langle\Phi\rangle_b$. Hence, for $t \to \infty$ and $\langle\Phi\rangle_a \neq \langle\Phi\rangle_b$, $G_\Phi(x,t) \to G_\Phi^{\rm sing}(x,t)$ and is a function of x/t, since θ_0 in (6.13) depends on x/t. We also see that the large time limit of $G_\Phi(x,t)/\langle\Phi\rangle_a$ changes with the initial condition and depends on the universality class only through the "dilatation" factor $\langle\Phi\rangle_b/\langle\Phi\rangle_a$.

We saw that the generality of the large time result (6.20) for $|x| \ll t$ is due to the dominance in this region of the low-energy modes[5] and these are maximally insensitive to the details of the initial condition. Since the energy of a n-kink state is at least nM, this result should generically[6] hold in the whole space $\mathcal{W}$ of domain wall states, as long as the one-kink contribution from $\mathcal{W}_1$ is present, and we show in the appendix 6.A the mechanism through which this extension occurs. The one-kink state will naturally be present in the states (6.2) arising in physical applications, but an interesting exception occurs for systems with more than two degenerate ground states, where the tuning of an interaction parameter can induce a transition to a regime in which $\mathcal{W}_1$ is empty; we illustrate this phenomenon in section 6.3.3.

6.3 Some universality classes

6.3.1 Ising model

A first illustration of the results of the previous section is provided by the Ising universality class (symmetry group $G = \mathbb{Z}_2$), whose simplest lattice realization is the nearest neighbor transverse field Ising chain with Hamiltonian

$$H_{\rm Ising} = -J \sum_i \left(\sigma_i^x \sigma_{i+1}^x + g\, \sigma_i^z \right) , \tag{6.22}$$

where $\sigma_i^{x,z}$ are Pauli matrices at site i, and $J > 0$, $|g| < 1$ is the ferromagnetically ordered regime of our interest. Denoting the two degenerate ground states as $|0_+\rangle$ and $|0_-\rangle$, we

[5] The fact that the low-energy modes dominate the large time dynamics in the general case of interacting quasiparticles is known for quantum quenches (see chapters 4, 5).

[6] Fine tuning of the functions f_n can lead to peculiar states. These, however, will form some zero measure subset, and typically will not be physically relevant.

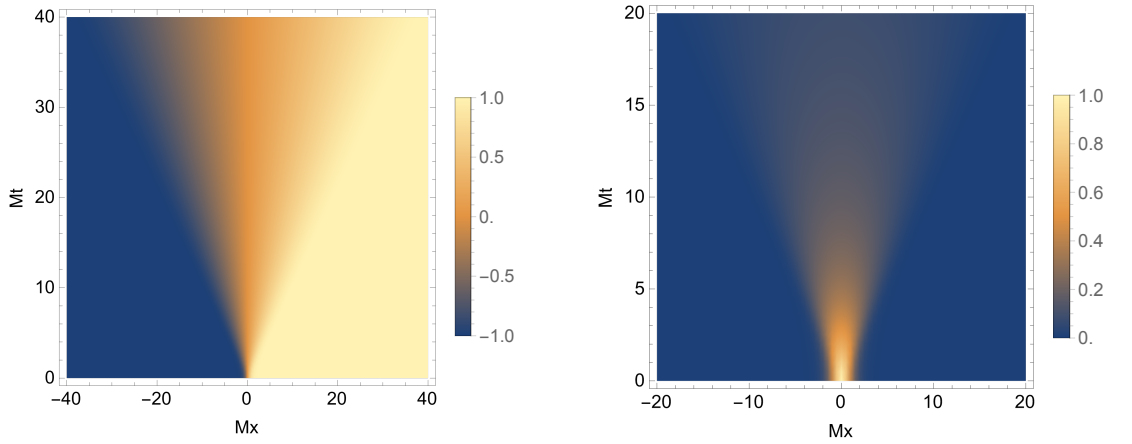

Figure 6.1: Ising magnetization components in the non-equilibrium state (6.27) with $MR = 1$. **Left:** Order parameter $\langle\sigma^x(x,t)\rangle_{-+}/\langle\sigma^x\rangle_+$. **Right:** Connected transverse magnetization $\langle\sigma^z(x,t)\rangle^c_{-+}/\langle\sigma^z(0,0)\rangle^c_{-+}$, with $\langle\sigma^z(x,t)\rangle^c_{-+} = \langle\sigma^z(x,t)\rangle_{-+} - \langle\sigma^z\rangle_+$.

have $\langle\sigma^x\rangle_- = -\langle\sigma^x\rangle_+$ and $\langle\sigma^z\rangle_- = \langle\sigma^z\rangle_+$. Hence, for the order parameter operator σ^x, the large time result (6.20) becomes

$$\frac{\langle\sigma^x(x,t)\rangle_{-+}}{\langle\sigma^x\rangle_+} \simeq \begin{cases} -1\,, & x < -t\,, \\ 2\mathcal{A}\,x/t\,, & |x| \ll t\,, \\ 1\,, & x > t\,. \end{cases} \tag{6.23}$$

Here we also took into account that $C_0^{\sigma^x} = 0$, as expected on symmetry grounds and explicitly following from [49] (see [23] for a review)

$$F_{\sigma^x}(\theta) = [i\coth(\theta/2) + 2\pi\,\delta(\theta)]\,\langle\sigma^x\rangle_-\,. \tag{6.24}$$

Recalling our result that $\mathcal{A}$ depends on the initial condition, (6.23) is consistent with the behavior displayed by the plots of [91,92] for the chain (6.22) with two different realizations of sharp (steplike) domain wall initial conditions. Similarly, our result that (6.23) tends at large times to a function of x/t depending on the initial condition explains the observations of [92] about the plots against x/t.

We already remarked that for $|x| \ll t$ the dependence on the initial condition in (6.20) is limited to the constant $\mathcal{A}$ because long wavelength modes dominate in this region. On the other hand, when moving towards the edges of the lightcone from inside, the fine structure of the initial condition becomes more and more relevant. For the chain (6.22) this feature is illustrated by the modulated behavior[7] of the order parameter observed in [91] zooming

[7]This type of behavior was originally observed in a free fermion chain with sharp domain wall initial condition [93].

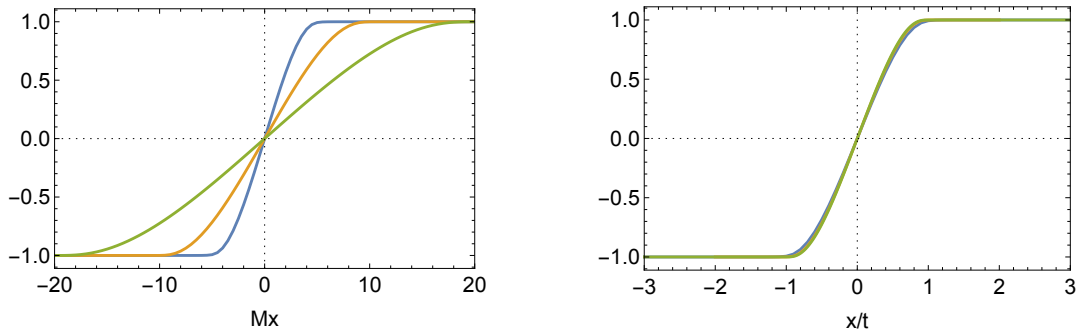

Figure 6.2: Ising order parameter $\langle\sigma^x(x,t)\rangle_{-+}/\langle\sigma^x\rangle_+$ in the non-equilibrium state (6.27) with $MR = 1$. **Left:** $Mt = 5$, 10, 20, in order of decreasing slope at $x = 0$. **Right:** In the variable x/t the three curves approach the large time limit given by (6.13).

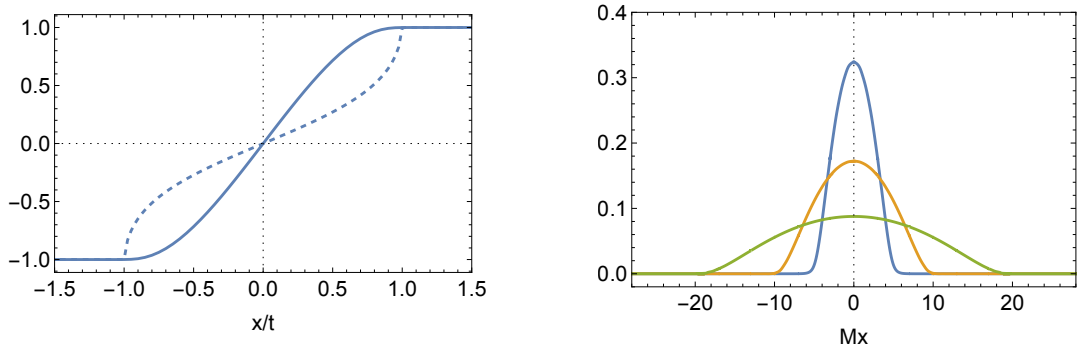

Figure 6.3: Ising magnetization components in the non-equilibrium state (6.27). **Left:** Large time limit (6.13) of the order parameter $\langle\sigma^x(x,t)\rangle_{-+}/\langle\sigma^x\rangle_+$ for $MR = 1$ (continuous line) and $MR = 0.1$ (dashed line). **Right:** Connected transverse magnetization $\langle\sigma^z(x,t)\rangle^c_{-+}/\langle\sigma^z(0,0)\rangle^c_{-+}$ (as defined in fig. 6.1) for $MR = 1$ and $Mt = 5$, 10, 20, in order of decreasing value at $x = 0$.

in close to the edges of the lightcone for the two sharp domain wall initial conditions.

For the transverse magnetization, the result [23, 49]

$$F_{\sigma^z}(\theta) = [\mathcal{C}\cosh(\theta/2) + 2\pi\,\delta(\theta)]\,\langle\sigma^z\rangle_+\,, \tag{6.25}$$

with $\mathcal{C}$ real and dimensionless, gives $C_0^{\sigma^z} = \mathcal{C}\langle\sigma^z\rangle_+$, and then

$$\frac{\langle\sigma^z(x,t)\rangle_{-+}}{\langle\sigma^z\rangle_+} \simeq \begin{cases} 1\,, & |x| > t\,, \\ 1 + \mathcal{A}\mathcal{C}/(Mt)\,, & |x| \ll t\,. \end{cases} \tag{6.26}$$

We show in figs. 6.1, 6.2 and 6.3 the expectation values $\langle\sigma^x(x,t)\rangle_{-+}$ and $\langle\sigma^z(x,t)\rangle_{-+}$

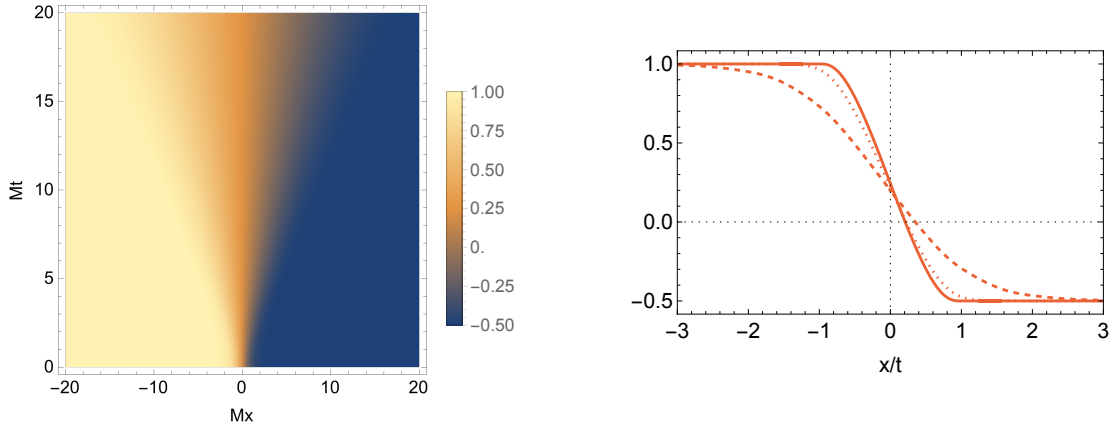

Figure 6.4: Potts order parameter component $\langle\sigma_1(x,t)\rangle_{12}/\langle\sigma_1\rangle_1$ in the non-equilibrium state (6.27) with $MR = 1$. On the right $Mt = 1$ (dashed), $Mt = 3$ (dotted) and $Mt = 20$ (continuous); the latter curve is indistinguishable from the large time limit shape (6.13).

for the state (6.4) with $f(\theta) = e^{-MR\theta^2}$, namely for the Gaussian wave packet

$$\int d\theta\, e^{-MR\theta^2}\, |\theta\rangle\,. \tag{6.27}$$

The distance over which the order parameter significantly differs from the asymptotic values in the initial condition grows with R. The large time regime corresponds to t much larger than $1/M$ and R. The state (6.27) conveniently illustrates some global features of the large time behavior as the initial condition varies. In particular, the change in the order parameter limit shape shown in the left panel of fig. 6.3 is essentially due to the fact that $\mathcal{A}$, and then the slope in the origin, decreases with MR.

6.3.2 Potts model

The three-state Potts universality class, characterized by invariance under the permutational group $G = S_3$, finds its simplest representative in the nearest neighbor chain [94]

$$H_{\rm Potts} = -J \sum_i \left[\sigma_i^\dagger \sigma_{i+1} + \sigma_i \sigma_{i+1}^\dagger + g(M_i + M_i^\dagger)\right]\,, \tag{6.28}$$

where σ_i and M_i are 3×3 matrices satisfying $\sigma_i^2 = \sigma_i^\dagger$, $\sigma_i^3 = M_i^3 = 1$, $M_i^2 = M_i^\dagger$, and $M_i\sigma_i = \omega\,\sigma_i M_i$, where $\omega = e^{2i\pi/3}$. Explicit representations are

$$\sigma = \begin{pmatrix} 1 & 0 & 0 \\ 0 & \omega & 0 \\ 0 & 0 & \omega^2 \end{pmatrix}\,, \qquad M = \begin{pmatrix} 0 & 1 & 0 \\ 0 & 0 & 1 \\ 1 & 0 & 0 \end{pmatrix}\,. \tag{6.29}$$

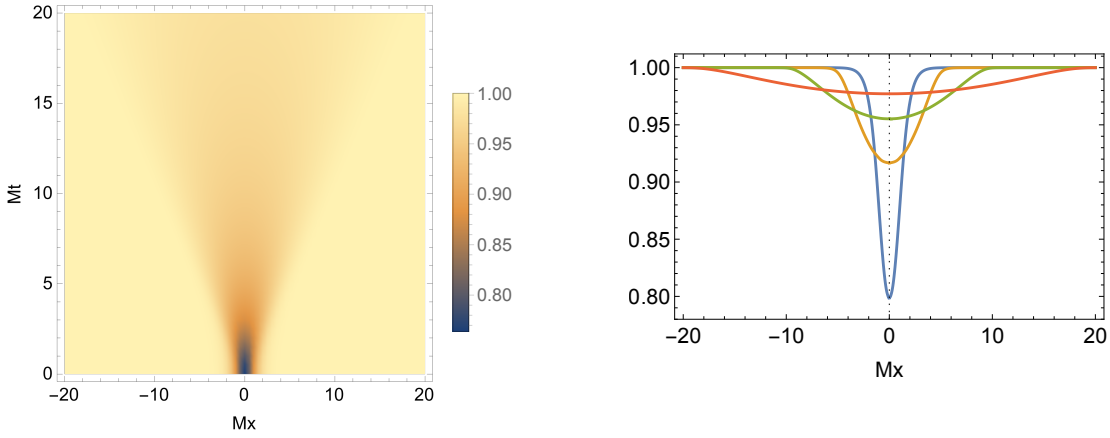

Figure 6.5: Potts order parameter component $\langle\sigma_3(x,t)\rangle_{12}/\langle\sigma_3\rangle_1$ in the non-equilibrium state (6.27) with $MR = 1$. On the right, $Mt = 1$, 5, 10, 20 in order of increasing value at $x = 0$. The deviation from 1 measures the presence of the phase not selected by the initial condition.

We refer to the ferromagnetically ordered regime $J > 0$, $|g| < 1$, in which there are three degenerate ground states $|0_a\rangle$, $a = 1, 2, 3$. The hermitian order parameter operator with components

$$\sigma_a = \omega^{-a}\,\sigma + \omega^a\,\sigma^\dagger\,, \qquad a = 1, 2, 3\,, \tag{6.30}$$

satisfies $\sum_{a=1}^{3}\sigma_a = 0$ and, by permutational symmetry,

$$\langle\sigma_a\rangle_b = \frac{1}{2}\,(3\delta_{ab} - 1)\,\langle\sigma_a\rangle_a\,. \tag{6.31}$$

Hence, σ_a detects phase a and does not distinguish between the other two phases. The matrix elements [86]

$$F_{\sigma_1}(\theta) = \left[-\frac{\sqrt{3}}{2}\,\frac{\sinh\left(\frac{\theta}{6} - \frac{i\pi}{3}\right)}{\sinh\frac{\theta}{2}}\,\mathcal{F}(\theta) + 2\pi\delta(\theta)\right]\langle\sigma_1\rangle_1\,, \tag{6.32}$$

and

$$F_{\sigma_3}(\theta) = \left[\frac{\sqrt{3}}{2}\,\frac{\sinh\left(\frac{\theta}{6} - \frac{i\pi}{3}\right) + \sinh\left(\frac{\theta}{6} + \frac{i\pi}{3}\right)}{\sinh\frac{\theta}{2}}\,\mathcal{F}(\theta) - \pi\delta(\theta)\right]\langle\sigma_1\rangle_1\,, \tag{6.33}$$

where

$$\mathcal{F}(\theta) = \exp\left\{\int_0^\infty dx\,\frac{2\sinh\frac{2x}{3}}{x\sinh^2 x}\,\sin^2\frac{\theta x}{2\pi}\right\}\,, \tag{6.34}$$

determine through (6.9) $C_0^{\sigma_1} = -\langle\sigma_1\rangle_1/(4\sqrt{3})$ and $C_0^{\sigma_3} = \langle\sigma_1\rangle_1/(2\sqrt{3})$, so that we have the large time behaviors

$$\frac{\langle\sigma_1(x,t)\rangle_{12}}{\langle\sigma_1\rangle_1} \simeq \begin{cases} 1\,, & x < -t\,, \\ 1/4 - \mathcal{A}\left(\frac{1}{4\sqrt{3}} + \frac{3}{2}Mx\right)/(Mt)\,, & |x| \ll t\,, \\ -1/2\,, & x > t\,, \end{cases} \tag{6.35}$$

and

$$\frac{\langle\sigma_3(x,t)\rangle_{12}}{\langle\sigma_3\rangle_1} \simeq \begin{cases} 1\,, & |x| > t\,, \\ 1 - \mathcal{A}/(\sqrt{3}Mt)\,, & |x| \ll t\,. \end{cases} \tag{6.36}$$

Figures 6.4 and 6.5 show the order parameter components $\langle\sigma_1(x,t)\rangle_{12}$ and $\langle\sigma_3(x,t)\rangle_{12}$ in the state (6.27). In (6.36) and fig. 6.5 the deviation from 1 measures the presence of phase 3. Although this phase is not selected by the initial condition, it is produced by quantum fluctuations.

6.3.3 Ashkin-Teller model

The Ashkin-Teller chain [94, 95] corresponds to two transverse field Ising chains with site variables $\sigma_{1,i}$ and $\sigma_{2,i}$ interacting via the Hamiltonian

$$H_{\rm AT} = -J\sum_i \left[\sigma^x_{1,i}\sigma^x_{1,i+1} + \sigma^x_{2,i}\sigma^x_{2,i+1} + \lambda\,\sigma^x_{1,i}\sigma^x_{1,i+1}\sigma^x_{2,i}\sigma^x_{2,i+1} + g(\sigma^z_{1,i} + \sigma^z_{2,i} + \lambda\,\sigma^z_{1,i}\sigma^z_{2,i})\right]. \tag{6.37}$$

The theory possesses a $\mathbb{Z}_2$ symmetry in each of the two Ising variables, as well as the symmetry under exchange of the two variables. It is characterized by the fact that $g = 1$ leads to a *line* of critical points as λ varies in an interval including the decoupling point $\lambda = 0$, with critical exponents varying continuously with λ [96]. In the ferromagnetically ordered regime there are four degenerate ground states $|0_{++}\rangle$, $|0_{+-}\rangle$, $|0_{-+}\rangle$, $|0_{--}\rangle$, labeled by the signs that the two Ising order parameters take in each of them. The vicinity of the critical line is described by the sine-Gordon theory [42], through a mapping that determines, in particular, the nature of the kinks interpolating between the different ground states [97]. A pair of ground states such as $|0_{++}\rangle$ and $|0_{-+}\rangle$ ($|0_{+-}\rangle$), related by spin reversal in the first (second) Ising copy, is connected by a kink A_1 (A_2) with mass M. For $\lambda > 0$, A_1 and A_2 form a bound state B with mass M_B that connects the ground states $|0_{++}\rangle$ and $|0_{--}\rangle$. Consider now $\langle\Phi(x,t)\rangle_{++,--}$. We deduced from the analysis of section 6.2 and the appendix 6.A that the leading behavior at large times for $|x| \ll t$ is determined by the n-kink states with minimal n among those connecting $|0_{++}\rangle$ and $|0_{--}\rangle$. For $\lambda > 0$, $n = 1$ and the relevant states are given by (6.4) with $|\theta\rangle = |B(\theta)\rangle$. However, when the decoupling point $\lambda = 0$ is approached, M_B tends to the unbinding threshold $2M$, and for $\lambda < 0$ the bound state B no longer exists. Hence, for $\lambda < 0$ the space $\mathcal{W}_1$ is empty and the dominant contribution comes from the $n = 2$ state A_1A_2. It follows that two-kink contributions that

in the appendix are neglected as subleading with respect to one-kink contributions become leading for $\lambda < 0$ and modify the result (6.20) for $|x| \ll t$. This same unbinding mechanism accounts for interfacial wetting in the theory of phase separation in classical systems at equilibrium [16, 17, 37, 98] (see chapter 2). Clearly, the mechanism requires at least three degenerate ground states. For the Potts chain of the previous section the existence of a single-kink excitation connecting any pair of ground states is ensured by the permutational symmetry.

6.4 Final remarks

We studied the role of initial conditions in non-equilibrium quantum dynamics in the framework of one-dimensional ferromagnets in the regime of spontaneously broken symmetry. We considered domain wall initial conditions, generally intended as initial conditions that spatially interpolate between two different ground states. The interpolation is arbitrary, with the only constraint of preserving the symmetry characteristic of the equilibrium universality class (e.g. the $\mathbb{Z}_2$ symmetry for Ising). In this setting we obtained analytical results for the one-point functions of local operators at large times. We showed that in this limit the time evolution takes place inside a lightcone produced by the spatial inhomogeneity of the initial condition, and that in the innermost region of the lightcone ($|x| \ll t$) the spacetime dependence is (up to an overall amplitude depending on the initial condition) universal, namely is determined by data of the equilibrium universality class. The origin of the universality is that the result in this region is determined by the excitations with the largest wavelength, which are maximally insensitive to the fine structure of the initial condition. This result should then hold also when the distance from the critical point is not small, in spite of the fact that it was derived in the continuum limit. We also showed that the large time limit curve in the variable x/t (which is nontrivial for operators that distinguish between the two ground states involved in the initial condition) changes with the initial condition. Our formalism also allowed us to show that in systems with more than two degenerate ground states the tuning of an interaction parameter (within the spontaneously broken regime) can change the structure of the space of non-equilibrium states, since the subspace of one-kink excitations disappears via the unbinding of a bound state. The corresponding transition is the non-equilibrium quantum analogue of the interfacial wetting transition observed at equilibrium in classical systems at phase coexistence.

6.A Composite excitations

This appendix is devoted to a generalization of the analysis performed in the present chapter. Let us consider the state

$$|\psi\rangle = |\psi_1\rangle + |\psi_2\rangle \,, \tag{6.38}$$

where $|\psi_1\rangle$ is the one-kink state (6.4) and $|\psi_2\rangle$ is a superposition of two-kink states $|K_{ac}(\theta_1)K_{cb}(\theta_2)\rangle$ with a, b, c all different. Since such a state requires at least three degenerate ground states, we will consider the three-state Potts universality class of section 6.3.2. It is convenient to exploit the fact that this model possesses a duality between the ferromagnetically ordered and the paramagnetic regime. One implication is the correspondence $A = K_{a,a+1\,(\mathrm{mod}\,3)}$, $\bar{A} = K_{a,a-1\,(\mathrm{mod}\,3)}$ between the kinks of the ordered phases and the elementary excitations A, $\bar{A}$ of the paramagnetic phase. A and $\bar{A}$ are charge conjugated quasiparticles and the theory is invariant under charge conjugation. It follows that a general superposition of states $|K_{12}K_{23}\rangle$ corresponds to

$$|\psi_2\rangle = \int d\theta_1 d\theta_2 \, f_2(\theta_1, \theta_2) \, |A(\theta_1)A(\theta_2)\rangle \, . \tag{6.39}$$

The Potts theory is integrable in the scaling limit we consider [99, 100], and we have[8]

$$\begin{aligned}
&\langle A(\theta_1') \dots A(\theta_m')|\tilde{\Phi}(0,0)|A(\theta_1)\dots A(\theta_n)\rangle = \\
&\langle A(\theta_2') \dots A(\theta_m')|\tilde{\Phi}(0,0)|\bar{A}(\theta_1' + i\pi)A(\theta_1)\dots A(\theta_n)\rangle \\
&+ \sum_{j=1}^{n} 2\pi\delta(\theta_1' - \theta_j) \left[\prod_{k=1}^{j-1} S_{AA}(\theta_k - \theta_1')\right] \\
&\times \langle A(\theta_2') \dots A(\theta_m')|\tilde{\Phi}(0,0)|A(\theta_1)\dots A(\theta_{j-1})A(\theta_{j+1})\dots A(\theta_n)\rangle \, ,
\end{aligned} \tag{6.40}$$

where $S_{AA}(\theta_1 - \theta_2)$ is the scattering amplitude[9] of $A(\theta_1)$ with $A(\theta_2)$; it satisfies crossing

$$S_{AA}(\theta) = S_{\bar{A}A}(i\pi - \theta) \, , \tag{6.41}$$

and unitarity

$$S_{AA}(\theta)S_{AA}(-\theta) = 1 \, . \tag{6.42}$$

We also took into account that when working in the paramagnetic phase we have to consider the dual $\tilde{\Phi}$ of the operator Φ of interest in the regime of spontaneously broken symmetry. Iterative use of (6.40) allows one to express any matrix element in terms of the form factors

$$F^{\tilde{\Phi}}_{\alpha_1\dots\alpha_n}(\theta_1, \dots, \theta_n) = \langle 0|\tilde{\Phi}(0,0)|\alpha_1(\theta_1)\dots\alpha_n(\theta_n)\rangle \, , \tag{6.43}$$

where $\alpha_i = A, \bar{A}$, and $|0\rangle$ is the unique ground state of the paramagnetic phase. We will consider operators whose expectation values $\langle\Phi\rangle_a$ in the ordered phases are a-independent. This introduces some simplifications in the equations satisfied by the form factors, which

[8] See [101] for an early advanced application of this formalism in the Potts paramagnetic phase.

[9] The scattering in the three-state Potts theory is completely elastic, meaning that the final state is identical to the initial one.

read [85]

$$F^{\tilde\Phi}_{\dots\alpha_j\alpha_{j+1}\dots}(\dots,\theta_j,\theta_{j+1},\dots)=S_{\alpha_j\alpha_{j+1}}(\theta_j-\theta_{j+1})F^{\tilde\Phi}_{\dots\alpha_{j+1}\alpha_j\dots}(\dots,\theta_{j+1},\theta_j,\dots)\,, \tag{6.44}$$

$$F^{\tilde\Phi}_{\alpha_1\dots\alpha_n}(\theta_1+2i\pi,\theta_2,\dots,\theta_n)=F^{\tilde\Phi}_{\alpha_2\dots\alpha_n,\alpha_1}(\theta_2,\dots,\theta_n,\theta_1)\,, \tag{6.45}$$

$$\begin{aligned}&\mathrm{Res}_{\theta'=\theta}F^{\tilde\Phi}_{\bar\alpha\beta\alpha_1\dots\alpha_n}(\theta'+i\pi,\theta,\theta_1,\dots,\theta_n)\\&\quad=i\delta_{\alpha\beta}\left[1-\prod_{j=1}^n S_{\alpha\alpha_j}(\theta-\theta_j)\right]F^{\tilde\Phi}_{\alpha_1\dots\alpha_n}(\theta_1,\theta_2,\dots,\theta_n)\,.\end{aligned} \tag{6.46}$$

Let us consider $\langle\Phi(x,t)\rangle_{13}=\langle\psi|\Phi(x,t)|\psi\rangle/\langle\psi|\psi\rangle$ with $|\psi\rangle$ given by (6.38). The contribution proportional to $\langle\psi_1|\Phi|\psi_1\rangle$ follows from the results of section 6.2. We now consider the contribution proportional to

$$\begin{aligned}\langle\psi_2|\Phi(x,t)|\psi_2\rangle=\int d\theta_1d\theta_2d\theta_3d\theta_4\,f_2^*(\theta_2,\theta_1)f_2(\theta_3,\theta_4)\\\times\langle A(\theta_2)A(\theta_1)|\tilde\Phi(0,0)|A(\theta_3)A(\theta_4)\rangle\,e^{i[(p_1+p_2-p_3-p_4)x+(E_1+E_2-E_3-E_4)t]}\,,\end{aligned} \tag{6.47}$$

where

$$\begin{aligned}&\langle A(\theta_2)A(\theta_1)|\tilde\Phi(0,0)|A(\theta_3)A(\theta_4)\rangle\\&=F^{\tilde\Phi}_{\bar AAA\bar A}(\theta_2+i\pi,\theta_3,\theta_4,\theta_1-i\pi)\\&+2\pi\Big[\delta(\theta_{14})S_{AA}(\theta_{12})S_{AA}(\theta_{31})F^{\tilde\Phi}_{\bar AA}(\theta_2+i\pi,\theta_3)+\delta(\theta_{13})S_{AA}(\theta_{12})F^{\tilde\Phi}_{\bar AA}(\theta_2+i\pi,\theta_4)\\&+\delta(\theta_{23})F^{\tilde\Phi}_{\bar AA}(\theta_1+i\pi,\theta_4)+\delta(\theta_{24})S_{AA}(\theta_{34})F^{\tilde\Phi}_{\bar AA}(\theta_1+i\pi,\theta_3)\Big]\\&+(2\pi)^2\left[\delta(\theta_{23})\delta(\theta_{14})+\delta(\theta_{24})\delta(\theta_{13})S_{AA}(\theta_{32})\right]\langle\tilde\Phi\rangle\,,\end{aligned} \tag{6.48}$$

with $\theta_{ij}=\theta_i-\theta_j$ and $\langle\tilde\Phi\rangle=\langle0|\tilde\Phi|0\rangle=\langle\Phi\rangle_a$.

Let us call G_4 the contribution to (6.47) of the term $F^{\tilde\Phi}_{\bar AAA\bar A}$ in (6.48). It follows from (6.46) that when integrating over θ_2 we have to deal with poles at $\theta_2=\theta_3,\theta_4$. Proceeding as in section 6.2, the contribution $G_4^{\rm pole}$ of these poles at large times is determined by the residues on the poles, which we know from (6.46), and reads

$$\begin{aligned}G_4^{\rm pole}(x,t)\simeq-2\pi\int_{\theta_0}^\infty d\theta\Big\{\int d\theta_1d\theta_4\,f_2^*(\theta,\theta_1)f_2(\theta,\theta_4)F^{\tilde\Phi}_{A\bar A}(\theta_4,\theta_1-i\pi)\\\times\left[1-S_{AA}(\theta_1-\theta)S_{AA}(\theta-\theta_4)\right]e^{i[p_{14}x+E_{14}t]}\\+\int d\theta_1d\theta_3\,f_2^*(\theta,\theta_1)f_2(\theta_3,\theta)S_{AA}(\theta_3-\theta)F^{\tilde\Phi}_{A\bar A}(\theta_3,\theta_1-i\pi)\\\times\left[1-S_{AA}(\theta_1-\theta)S_{AA}(\theta-\theta_3)\right]e^{i[p_{13}x+E_{13}t]}\Big\}\,,\end{aligned} \tag{6.49}$$

where $p_{ij} = p_i - p_j$ and $E_{ij} = E_i - E_j$. Since (6.46) shows that $F^{\tilde{\Phi}}_{A\bar{A}}(\theta_4, \theta_1 - i\pi)$ has no pole[10] on the integration path, the behavior of (6.49) at large times can now be analyzed as the contribution of regular terms along the lines already seen in section 6.2. The stationary phase condition yields the lightcone and the suppression of the integral outside it. Deeply inside the lightcone, namely for $|x|/t \ll 1$, small values of θ_1, θ_4 (θ_1, θ_3) dominate in the first (second) term, and the expressions in the square brackets become $1 - S_{AA}(-\theta)S_{AA}(\theta)$, which vanishes due to (6.42). Hence, $G_4^{\rm pole}$ can be ignored in the regions specified in (6.20). Concerning the contribution $G_4^{\rm reg}$ coming from the regular part of $F^{\tilde{\Phi}}_{\bar{A}AA\bar{A}}$, we have again suppression outside the lightcone and dominance of small rapidities $\theta_1, \ldots, \theta_4$ for $|x|/t \ll 1$. In this region, rescaling of rapidities in (6.47) yields that $G_4^{\rm reg}$ is suppressed at least as t^{-2}, and is then subleading with respect to the one-kink contribution.

Let us now call G_2 the contribution to (6.47) of the four terms in (6.48) containing $F^{\tilde{\Phi}}_{\bar{A}A}$. It will be sufficient to consider one of these terms, say $\delta(\theta_{14})S_{AA}(\theta_{12})S_{AA}(\theta_{31})F^{\tilde{\Phi}}_{\bar{A}A}(\theta_2 + i\pi, \theta_3)$. Since the form factor has no pole at $\theta_2 = \theta_3$, we have suppression of the integral outside the lightcone and dominance of small values of θ_2, θ_3 for $|x|/t \ll 1$. In this region $f_2^*(\theta_2, \theta_1) f_2(\theta_3, \theta_1) S_{AA}(\theta_{12}) S_{AA}(\theta_{31}) F^{\tilde{\Phi}}_{\bar{A}A}(\theta_2 + i\pi, \theta_3) \simeq |f_2(0, \theta_1)|^2 S_{AA}(\theta_1) S_{AA}(-\theta_1) F^{\tilde{\Phi}}_{\bar{A}A}(i\pi, 0)$, which reduces to $|f_2(0, \theta_1)|^2 C_0^{\Phi}$ using (6.9), (6.42) and duality. The integral over θ_2 and θ_3 is analogous to (6.18) and, taking into account that the other terms in G_2 behave in the same way, we get

$$G_2(x,t) \simeq B_{f_2} \frac{C_0^{\Phi}}{Mt}\,, \qquad |x|/t \ll 1\,. \tag{6.50}$$

The last contribution to (6.47) comes from the term in (6.48) proportional to $\langle\tilde{\Phi}\rangle$, and is equal to $G_0 = \langle\psi_2|\psi_2\rangle \langle\tilde{\Phi}\rangle = \langle\psi_2|\psi_2\rangle \langle\Phi\rangle_a$.

Finally, $\langle\Phi(x,t)\rangle_{13}$ includes the off-diagonal contribution proportional to $\langle\psi_1|\Phi|\psi_2\rangle + \langle\psi_2|\Phi|\psi_1\rangle$. It is sufficient to consider the first term, which involves

$$\langle \bar{A}(\theta_1)|\tilde{\Phi}(0,0)|A(\theta_2)A(\theta_3)\rangle = F^{\tilde{\Phi}}_{\bar{A}AA}(\theta_1 + i\pi, \theta_2, \theta_3)\,. \tag{6.51}$$

Since (6.46) shows that this matrix element yields no poles on the integration path, we have suppression outside the lightcone and dominance of small $\theta_1, \theta_2, \theta_3$ for $|x|/t \ll 1$. In this region rescaling of the rapidities shows at least a $t^{-3/2}$ suppression at large times, which is again subleading with respect to the one-kink contribution.

Putting all together, and recalling that $\langle\psi|\psi\rangle = \langle\psi_1|\psi_1\rangle + \langle\psi_2|\psi_2\rangle$, we see that inclusion in $|\psi\rangle$ of the two-kink contribution gives again the result (6.20), specialized to the case of a-independent $\langle\Phi\rangle_a$ that we considered in this appendix. The difference with respect to the one-kink result is a change of the constant $\mathcal{A}$ that encodes the dependence on the initial condition.

[10] This corresponds to the fact that (6.9) has no pole for $\langle\Phi\rangle_a = \langle\Phi\rangle_b$.

Chapter 7

Unitary time evolution in isolated systems

In this chapter we consider d-dimensional quantum systems which for positive times evolve with a time-independent Hamiltonian in a non-equilibrium state that we keep generic in order to account for arbitrary evolution at negative times. We show how the one-point functions of local operators depend on the coefficients of the expansion of the non-equilibrium state on the basis of energy eigenstates. We express in this way the asymptotic offset and show under which conditions oscillations around this value stay undamped at large times. We also show how, in the case of small quenches, the structure of the general results simplifies and reproduces that obtained perturbatively in chapter 4.

7.1 Problem and general setting

It is our present purpose to further investigate the properties of unitary non-equilibrium evolution at large times. To this end, we consider a quantum system in d spatial dimensions with Hamiltonian

$$\begin{cases} H_0(\mathbf{x},t)\,, & t<0\,, \\ H\,, & t\geq 0\,, \end{cases} \tag{7.1}$$

where H does not depend on time and is also translation invariant in space. We are interested in the time evolution of the system for $t>0$, and expand the non-equilibrium state on the basis of the quasiparticle states $|\mathbf{p}_1,\ldots,\mathbf{p}_n\rangle$ of the Hamiltonian H, with coefficient functions $f_n(\mathbf{p}_1,\ldots,\mathbf{p}_n)$ which know about the evolution of the system since $t=-\infty$. The main question we want to answer is how the one-point function of a local operator Φ depends on the coefficients f_n. Hence, in order to study the features of the generic case, these coefficients are not specified and we perform a non-perturbative analysis relying on the structural properties of unitary time evolution of quasiparticle modes.

We consider the expectation values $\langle\Phi(\mathbf{x},t)\rangle$ of local, scalar, hermitian operators $\Phi(\mathbf{x},t)$. If I denotes the identity operator, the normalization

$$\langle\Phi(\mathbf{x},t)\rangle = 1 \quad \text{if} \quad \Phi = I \tag{7.2}$$

is enforced at $t=-\infty$ and is then preserved by the time evolution. We have

$$\Phi(\mathbf{x},t) = e^{i(\boldsymbol{\mathcal{P}}\cdot\mathbf{x}+Ht)}\,\Phi(0,0)\,e^{-i(\boldsymbol{\mathcal{P}}\cdot\mathbf{x}+Ht)}\,, \qquad t\geq 0\,, \tag{7.3}$$

where $\boldsymbol{\mathcal{P}}$ denotes the momentum operator. We expand the non-equilibrium state on the basis of the quasiparticle states $|\mathbf{p}_1,\ldots,\mathbf{p}_n\rangle$ of the Hamiltonian H, with coefficient functions $f_n(\mathbf{p}_1,\ldots,\mathbf{p}_n)$ which know about the evolution of the system since $t=-\infty$. The main question we want to answer is how the one-point function $\langle\Phi(\mathbf{x},t)\rangle$ depends on the coefficients f_n. Hence, in order to study the features of the generic case, these coefficients are not specified and we perform a non-perturbative analysis relying on the structural properties of unitary time evolution of quasiparticle modes.

The state $|\psi\rangle$ of the system can be generally expanded on the basis of asymptotic quasiparticle states $|\mathbf{p}_1,\ldots,\mathbf{p}_n\rangle$ of the theory with Hamiltonian H, which are eigenstates of energy and momentum with eigenvalues

$$E = \sum_{i=1}^{n} E_{\mathbf{p}_i}\,, \qquad \mathbf{P} = \sum_{i=1}^{n}\mathbf{p}_i\,, \tag{7.4}$$

respectively. Energy and momentum of the quasiparticles are related as

$$E_{\mathbf{p}} = \sqrt{M^2+\mathbf{p}^2}\,, \tag{7.5}$$

where $M>0$ is the quasiparticle mass[1] and measures the distance from a quantum critical point; we also adopt the state normalization

$$\langle\mathbf{q}|\mathbf{p}\rangle = (2\pi)^d E_{\mathbf{p}}\,\delta(\mathbf{q}-\mathbf{p})\,. \tag{7.6}$$

The expansion of the state $|\psi\rangle$ on the basis of asymptotic quasiparticle states takes the form

$$|\psi\rangle = \sum_{n=0}^{\infty}\int_{-\infty}^{\infty}\prod_{i=1}^{n}\frac{d\mathbf{p}_i}{(2\pi)^d E_{\mathbf{p}_i}}\,f_n(\mathbf{p}_1,...,\mathbf{p}_n)\,|\mathbf{p}_1,...,\mathbf{p}_n\rangle\,, \tag{7.7}$$

where the coefficient functions $f_n(\mathbf{p}_1,\ldots,\mathbf{p}_n)$ give the probability amplitude that the state $|\mathbf{p}_1,...,\mathbf{p}_n\rangle$ is observed at $t=+\infty$.

The one-point function $\langle\Phi(\mathbf{x},t)\rangle$ is related to the expectation value

$$G_\Phi(\mathbf{x},t) = \langle\psi|\Phi(\mathbf{x},t)|\psi\rangle\,. \tag{7.8}$$

[1]For the sake of notational simplicity we refer to the case of a single quasiparticle species. Generalizations will be discussed when relevant.

$\langle\Phi(\mathbf{x},t)\rangle$ is continuous at $t=0$, although in general non-differentiable. $G_\Phi(\mathbf{x},0)$ does not automatically coincide with $\langle\Phi(\mathbf{x},0)\rangle$ and continuity at $t=0$ is ensured writing

$$\langle\Phi(\mathbf{x},t)\rangle = G_\Phi(\mathbf{x},t) - G_\Phi(\mathbf{x},0) + \langle\Phi(\mathbf{x},0)\rangle\,. \tag{7.9}$$

Recalling (7.7), we have

$$\begin{aligned} G_\Phi(\mathbf{x},t) = \sum_{n,m=0}^{\infty} \int \prod_{i=1}^{n} \frac{d\mathbf{p}_i}{(2\pi)^d E_{\mathbf{p}_i}} \prod_{j=1}^{m} \frac{d\mathbf{q}_j}{(2\pi)^d E_{\mathbf{q}_j}} f_n(\mathbf{p}_1,...,\mathbf{p}_n) f_m^*(\mathbf{q}_1,...,\mathbf{q}_m) \\ \times F^\Phi_{m,n}(\mathbf{q}_1,...,\mathbf{q}_m|\mathbf{p}_1,...,\mathbf{p}_n)\, e^{i[(\mathbf{Q}-\mathbf{P})\cdot\mathbf{x}+(\tilde{E}-E)t]}\,, \qquad t\geq 0\,, \end{aligned} \tag{7.10}$$

where we used (7.3) and defined

$$\tilde{E} = \sum_{j=1}^{m} E_{\mathbf{q}_j}\,, \qquad \mathbf{Q} = \sum_{j=1}^{m} \mathbf{q}_j\,, \tag{7.11}$$

and

$$F^\Phi_{m,n}(\mathbf{q}_1,...,\mathbf{q}_m|\mathbf{p}_1,...,\mathbf{p}_n) = \langle \mathbf{q}_1,...,\mathbf{q}_m|\Phi(0,0)|\mathbf{p}_1,...,\mathbf{p}_n\rangle\,. \tag{7.12}$$

The matrix elements (7.12) decompose into the sum of a connected term

$$F^{\Phi,c}_{m,n}(\mathbf{q}_1,...,\mathbf{q}_m|\mathbf{p}_1,...,\mathbf{p}_n) = \langle \mathbf{q}_1,...,\mathbf{q}_m|\Phi(0,0)|\mathbf{p}_1,...,\mathbf{p}_n\rangle_c\,, \tag{7.13}$$

plus disconnected terms containing delta functions associated to the annihilations of particles on the left with particles on the right, namely

$$\begin{aligned} &F^\Phi_{m,n}(\mathbf{q}_1,...,\mathbf{q}_m|\mathbf{p}_1,...,\mathbf{p}_n) = F^{\Phi,c}_{m,n}(\mathbf{q}_1,...,\mathbf{q}_m|\mathbf{p}_1,...,\mathbf{p}_n) \\ &+ \sum_{i=1}^{n}\sum_{j=1}^{m} (2\pi)^d E_{\mathbf{p}_i}\delta(\mathbf{p}_i-\mathbf{q}_j) F^{\Phi,c}_{m-1,n-1}(\mathbf{q}_1,...,\mathbf{q}_{j-1},\mathbf{q}_{j+1},...,\mathbf{q}_m|\mathbf{p}_1,...,\mathbf{p}_{i-1},\mathbf{p}_{i+1},...,\mathbf{p}_n) \\ &+ \sum_{\substack{i,l=1\\ i\neq l}}^{n}\sum_{\substack{j,k=1\\ j\neq k}}^{m} (2\pi)^{2d} E_{\mathbf{p}_i}E_{\mathbf{p}_l}\delta(\mathbf{p}_i-\mathbf{q}_j)\delta(\mathbf{p}_l-\mathbf{q}_k) \\ &\times F^{\Phi,c}_{m-2,n-2}(\mathbf{q}_1,...,\mathbf{q}_{j-1},\mathbf{q}_{j+1},...,\mathbf{q}_{k-1},\mathbf{q}_{k+1},...,\mathbf{q}_m|\mathbf{p}_1,...,\mathbf{p}_{i-1},\mathbf{p}_{i+1},...,\mathbf{p}_{l-1},\mathbf{p}_{l+1},...,\mathbf{p}_n) \\ &+ ...\,, \end{aligned} \tag{7.14}$$

where the final dots stay for all the terms with more than two annihilations[2].

[2]Clearly, the matrix elements $F^\Phi_{m,n}$ with m and/or n equal 0 coincide with the connected ones.

As a consequence of (7.14), the expectation value (7.10) expands as

$$
\begin{aligned}
G_\Phi(\mathbf{x},t) = {} & |f_0|^2 F^\Phi_{0,0} + \\
& + \int \frac{d\mathbf{p}_1}{(2\pi)^d E_{\mathbf{p}_1}} f_1(\mathbf{p}_1) f_0^* e^{-i(\mathbf{p}_1\cdot\mathbf{x}+E_{\mathbf{p}_1}t)} F^\Phi_{0,1}(|\mathbf{p}_1) + c.c. \\
& + \int \frac{d\mathbf{p}_1 d\mathbf{q}_1}{(2\pi)^{2d} E_{\mathbf{p}_1} E_{\mathbf{q}_1}} f_1(\mathbf{p}_1) f_1^*(\mathbf{q}_1) e^{i[(\mathbf{q}_1-\mathbf{p}_1)\cdot\mathbf{x}+(E_{\mathbf{q}_1}-E_{\mathbf{p}_1})t]} F^{\Phi,c}_{1,1}(\mathbf{q}_1|\mathbf{p}_1) \\
& + \int \frac{d\mathbf{p}_1}{(2\pi)^d E_{\mathbf{p}_1}} |f_1(\mathbf{p}_1)|^2 F^\Phi_{0,0} \\
& + \int \frac{d\mathbf{p}_1 d\mathbf{p}_2}{(2\pi)^{2d} E_{\mathbf{p}_1} E_{\mathbf{p}_2}} f_2(\mathbf{p}_1,\mathbf{p}_2) f_0^* e^{-i(\mathbf{P}\cdot\mathbf{x}+Et)} F^\Phi_{0,2}(|\mathbf{p}_1,\mathbf{p}_2) + c.c. \\
& + \int \frac{d\mathbf{p}_1 d\mathbf{p}_2 d\mathbf{q}_1}{(2\pi)^{3d} E_{\mathbf{p}_1} E_{\mathbf{p}_2} E_{\mathbf{q}_1}} f_2(\mathbf{p}_1,\mathbf{p}_2) f_1^*(\mathbf{q}_1) e^{i[(\mathbf{q}_1-\mathbf{P})\cdot\mathbf{x}+(E_{\mathbf{q}_1}-E)t]} F^{\Phi,c}_{1,2}(\mathbf{q}_1|\mathbf{p}_1,\mathbf{p}_2) + c.c. \\
& + 2\int \frac{d\mathbf{p}_1 d\mathbf{p}_2}{(2\pi)^{2d} E_{\mathbf{p}_1} E_{\mathbf{p}_2}} f_2(\mathbf{p}_1,\mathbf{p}_2) f_1^*(\mathbf{p}_2) e^{-i(\mathbf{p}_1\cdot\mathbf{x}+E_{\mathbf{p}_1}t)} F^\Phi_{0,1}(|\mathbf{p}_1) + c.c. \\
& + \int \frac{d\mathbf{p}_1 d\mathbf{p}_2 d\mathbf{q}_1 d\mathbf{q}_2}{(2\pi)^{4d} E_{\mathbf{p}_1} E_{\mathbf{p}_2} E_{\mathbf{q}_1} E_{\mathbf{q}_2}} f_2(\mathbf{p}_1,\mathbf{p}_2) f_2^*(\mathbf{q}_1,\mathbf{q}_2) e^{i[(\mathbf{Q}-\mathbf{P})\cdot\mathbf{x}+(\tilde{E}-E)t]} F^{\Phi,c}_{2,2}(\mathbf{q}_1,\mathbf{q}_2|\mathbf{p}_1,\mathbf{p}_2) \\
& + 4\int \frac{d\mathbf{p}_1 d\mathbf{p}_2 d\mathbf{q}_1}{(2\pi)^{3d} E_{\mathbf{p}_1} E_{\mathbf{p}_2} E_{\mathbf{q}_1}} f_2(\mathbf{p}_1,\mathbf{p}_2) f_2^*(\mathbf{q}_1,\mathbf{p}_2) e^{i[(\mathbf{q}_1-\mathbf{P})\cdot\mathbf{x}+(E_{\mathbf{q}_1}-E)t]} F^{\Phi,c}_{1,1}(\mathbf{q}_1|\mathbf{p}_1) \\
& + 2\int \frac{d\mathbf{p}_1 d\mathbf{p}_2}{(2\pi)^{2d} E_{\mathbf{p}_1} E_{\mathbf{p}_2}} |f_2(\mathbf{p}_1,\mathbf{p}_2)|^2 F^\Phi_{0,0} + \cdots ,
\end{aligned}
\tag{7.15}
$$

where the complex conjugated (*c.c.*) terms come from the relation

$$
F^{\Phi,c}_{n,m}(\mathbf{p}_1,...,\mathbf{p}_n|\mathbf{q}_1,...,\mathbf{q}_m) = [F^{\Phi,c}_{m,n}(\mathbf{q}_1,...,\mathbf{q}_m|\mathbf{p}_1,...,\mathbf{p}_n)]^* \tag{7.16}
$$

satisfied by the hermitian operators we consider. It follows that the expansion (7.10) can be re-expressed in terms of the connected matrix elements as

$$
\begin{aligned}
G_\Phi(\mathbf{x},t) = \sum_{n,m=0}^{\infty} \int \prod_{i=1}^{n} \frac{d\mathbf{p}_i}{(2\pi)^d E_{\mathbf{p}_i}} \prod_{j=1}^{m} \frac{d\mathbf{q}_j}{(2\pi)^d E_{\mathbf{q}_j}} \, g_{m,n}(\mathbf{q}_1,...,\mathbf{q}_m,\mathbf{p}_1,...,\mathbf{p}_n) \\
\times F^{\Phi,c}_{m,n}(\mathbf{q}_1,...,\mathbf{q}_m|\mathbf{p}_1,...,\mathbf{p}_n)\, e^{i[(\mathbf{Q}-\mathbf{P})\cdot\mathbf{x}+(\tilde{E}-E)t]} ,
\end{aligned}
\tag{7.17}
$$

where the coefficient functions $g_{m,n}(\mathbf{q}_1,...,\mathbf{q}_m,\mathbf{p}_1,...,\mathbf{p}_n)$ expand in terms of the coefficients of (7.10) as

$$
\begin{aligned}
& g_{m,n}(\mathbf{q}_1,...,\mathbf{q}_m,\mathbf{p}_1,...,\mathbf{p}_n) = \\
& \sum_{k=0}^{\infty} \frac{(m+k)!\,(n+k)!}{m!\,n!\,k!} \int \prod_{i=1}^{k} \frac{d\mathbf{a}_i}{(2\pi)^d E_{\mathbf{a}_i}} \, f^*_{m+k}(\mathbf{q}_1,...,\mathbf{q}_m,\mathbf{a}_1,...,\mathbf{a}_k)\, f_{n+k}(\mathbf{p}_1,...,\mathbf{p}_n,\mathbf{a}_1,...,\mathbf{a}_k) .
\end{aligned}
\tag{7.18}
$$

Notice that the contribution to (7.17) with $m = n = 0$ has, in particular, $E = \tilde{E} = 0$, and is then time-independent. If we subtract it from (7.17) defining

$$G^s_\Phi(\mathbf{x},t) = \sum_{\substack{m,n=0\\(m,n)\neq(0,0)}}^{\infty} \int \prod_{i=1}^{n} \frac{d\mathbf{p}_i}{(2\pi)^d E_{\mathbf{p}_i}} \prod_{j=1}^{m} \frac{d\mathbf{q}_j}{(2\pi)^d E_{\mathbf{q}_j}}\, g_{m,n}(\mathbf{q}_1,...,\mathbf{q}_m,\mathbf{p}_1,...,\mathbf{p}_n) \\ \times F^{\Phi,c}_{m,n}(\mathbf{q}_1,...,\mathbf{q}_m|\mathbf{p}_1,...,\mathbf{p}_n)\, e^{i[(\mathbf{Q}-\mathbf{P})\cdot\mathbf{x}+(\tilde{E}-E)t]}\,, \tag{7.19}$$

the one-point function (7.9) can be rewritten as

$$\langle\Phi(\mathbf{x},t)\rangle = G^s_\Phi(\mathbf{x},t) - G^s_\Phi(\mathbf{x},0) + \langle\Phi(\mathbf{x},0)\rangle\,, \qquad t \geq 0\,. \tag{7.20}$$

7.2 Translation invariant case

So far we allowed for $t > 0$ the presence of spatial inhomogeneities inherited from the time evolution at negative times. We now consider the case in which such inhomogeneities are absent and the state of the system is translation invariant. This is a particular case in which the coefficient functions in (7.7) take the form[3]

$$f_n(\mathbf{p}_1,...,\mathbf{p}_n) = \delta(\mathbf{P})\,\hat{f}_n(\mathbf{p}_1,...,\mathbf{p}_n)\,, \tag{7.21}$$

so that we have

$$|\psi\rangle = \sum_{n=0}^{\infty} \int_{-\infty}^{\infty} \prod_{i=1}^{n} \frac{d\mathbf{p}_i}{(2\pi)^d E_{\mathbf{p}_i}}\, \delta(\mathbf{P})\,\hat{f}_n(\mathbf{p}_1,...,\mathbf{p}_n)\,|\mathbf{p}_1,...,\mathbf{p}_n\rangle\,, \tag{7.22}$$

and the expression (7.10) for the expectation value becomes

$$G_\Phi(t) = \sum_{n,m=0}^{\infty} \int \prod_{i=1}^{n} \frac{d\mathbf{p}_i}{(2\pi)^d E_{\mathbf{p}_i}} \prod_{j=1}^{m} \frac{d\mathbf{q}_j}{(2\pi)^d E_{\mathbf{q}_j}}\, \delta(\mathbf{P})\delta(\mathbf{Q}) \\ \times \hat{f}_n(\mathbf{p}_1,...,\mathbf{p}_n)\,\hat{f}^*_m(\mathbf{q}_1,...,\mathbf{q}_m)\,F^{\Phi}_{m,n}(\mathbf{q}_1,...,\mathbf{q}_m|\mathbf{p}_1,...,\mathbf{p}_n)\,e^{i(\tilde{E}-E)t}\,. \tag{7.23}$$

[3]For $n = 0$ there are no momenta and (7.21) reduces to $f_0 = \hat{f}_0$.

Use of (7.14) now leads to an expansion in terms of connected matrix elements which for the subtracted expectation value (7.19) reads

$$
\begin{aligned}
G^s_\Phi(t) = &\int \frac{d\mathbf{p}_1}{(2\pi)^d E_{\mathbf{p}_1}} \delta(\mathbf{p}_1) \hat{f}_1(\mathbf{p}_1) \hat{f}_0^* e^{-iE_{\mathbf{p}_1} t} F^\Phi_{0,1}(|\mathbf{p}_1) + c.c. \\
&+ \int \frac{d\mathbf{p}_1 d\mathbf{q}_1}{(2\pi)^{2d} E_{\mathbf{p}_1} E_{\mathbf{q}_1}} \delta(\mathbf{p}_1)\delta(\mathbf{q}_1) \hat{f}_1(\mathbf{p}_1) \hat{f}_1^*(\mathbf{q}_1) e^{i(E_{\mathbf{q}_1} - E_{\mathbf{p}_1})t} F^{\Phi,c}_{1,1}(\mathbf{q}_1|\mathbf{p}_1) \\
&+ \int \frac{d\mathbf{p}_1 d\mathbf{p}_2}{(2\pi)^{2d} E_{\mathbf{p}_1} E_{\mathbf{p}_2}} \delta(\mathbf{p}_1 + \mathbf{p}_2) \hat{f}_2(\mathbf{p}_1, \mathbf{p}_2) \hat{f}_0^* e^{-iEt} F^\Phi_{0,2}(|\mathbf{p}_1, \mathbf{p}_2) + c.c. \\
&+ \int \frac{d\mathbf{p}_1 d\mathbf{p}_2 d\mathbf{q}_1}{(2\pi)^{3d} E_{\mathbf{p}_1} E_{\mathbf{p}_2} E_{\mathbf{q}_1}} \delta(\mathbf{p}_1 + \mathbf{p}_2)\delta(\mathbf{q}_1) \hat{f}_2(\mathbf{p}_1, \mathbf{p}_2) \hat{f}_1^*(\mathbf{q}_1) e^{i(E_{\mathbf{q}_1} - E)t} F^{\Phi,c}_{1,2}(\mathbf{q}_1|\mathbf{p}_1, \mathbf{p}_2) + c.c. \\
&+ 2 \int \frac{d\mathbf{p}_1}{(2\pi)^{2d} E_{\mathbf{p}_1} M} \delta(\mathbf{p}_1) \hat{f}_2(\mathbf{p}_1, 0) \hat{f}_1^*(0) e^{-iE_{\mathbf{p}_1} t} F^\Phi_{0,1}(|\mathbf{p}_1) + c.c. \\
&+ \int \frac{d\mathbf{p}_1 d\mathbf{p}_2 d\mathbf{q}_1 d\mathbf{q}_2}{(2\pi)^{4d} E_{\mathbf{p}_1} E_{\mathbf{p}_2} E_{\mathbf{q}_1} E_{\mathbf{q}_2}} \delta(\mathbf{p}_1 + \mathbf{p}_2)\delta(\mathbf{q}_1 + \mathbf{q}_2) \hat{f}_2(\mathbf{p}_1, \mathbf{p}_2) \hat{f}_2^*(\mathbf{q}_1, \mathbf{q}_2) e^{i(\tilde{E} - E)t} \\
&\times F^{\Phi,c}_{2,2}(\mathbf{q}_1, \mathbf{q}_2|\mathbf{p}_1, \mathbf{p}_2) \\
&+ 4 \int \frac{d\mathbf{p}_1 d\mathbf{q}_1}{(2\pi)^{3d} E_{\mathbf{p}_1} E^2_{\mathbf{q}_1}} \delta(\mathbf{q}_1 - \mathbf{p}_1) \hat{f}_2(\mathbf{p}_1, -\mathbf{q}_1) \hat{f}_2^*(\mathbf{q}_1, -\mathbf{q}_1) e^{i(E_{\mathbf{q}_1} - E_{\mathbf{p}_1})t} F^{\Phi,c}_{1,1}(\mathbf{q}_1|\mathbf{p}_1) \\
&+ \cdots .
\end{aligned}
\tag{7.24}
$$

Notice that the terms coming from the connected part of the original matrix elements (7.12) contain delta functions that do not mix the momenta $\{\mathbf{p}_i\}$ and $\{\mathbf{q}_j\}$, while the terms coming from the disconnected parts involve delta functions of differences of these momenta. Hence, the expansion in terms of the connected matrix elements can be written in the form

$$
\begin{aligned}
G^s_\Phi(t) = \sum_{\substack{m,n=0 \\ (m,n)\neq(0,0)}}^{\infty} &\int \prod_{i=1}^{n} \frac{d\mathbf{p}_i}{(2\pi)^d E_{\mathbf{p}_i}} \prod_{j=1}^{m} \frac{d\mathbf{q}_j}{(2\pi)^d E_{\mathbf{q}_j}} \big[\delta(\mathbf{P})\delta(\mathbf{Q})\, h_{m,n}(\mathbf{q}_1, ..., \mathbf{q}_m, \mathbf{p}_1, ..., \mathbf{p}_n) \\
&+ \delta(\mathbf{Q} - \mathbf{P})\, \tilde{h}_{m,n}(\mathbf{q}_1, ..., \mathbf{q}_m, \mathbf{p}_1, ..., \mathbf{p}_n)\big]\, F^{\Phi,c}_{m,n}(\mathbf{q}_1, ..., \mathbf{q}_m|\mathbf{p}_1, ..., \mathbf{p}_n)\, e^{i(\tilde{E} - E)t},
\end{aligned}
\tag{7.25}
$$

with coefficient functions $h_{m,n}(\mathbf{q}_1, ..., \mathbf{q}_m, \mathbf{p}_1, ..., \mathbf{p}_n)$ and $\tilde{h}_{m,n}(\mathbf{q}_1, ..., \mathbf{q}_m, \mathbf{p}_1, ..., \mathbf{p}_n)$ related to the coefficients $\hat{f}_n$ of (7.23) as

$$
h_{m,n}(\mathbf{q}_1, ..., \mathbf{q}_m, \mathbf{p}_1, ..., \mathbf{p}_n) = \hat{f}_n(\mathbf{p}_1, ..., \mathbf{p}_n) \hat{f}_m^*(\mathbf{q}_1, ..., \mathbf{q}_m)\,, \tag{7.26}
$$

and[4]

$$\tilde{h}_{m,n}(\mathbf{q}_1,...,\mathbf{q}_m,\mathbf{p}_1,...,\mathbf{p}_n)=\sum_{k=1}^{\infty}\frac{(m+k)!\,(n+k)!}{m!\,n!\,k!\,(2\pi)^d}\int\prod_{i=1}^{k-1}\frac{d\mathbf{a}_i}{(2\pi)^d E_{\mathbf{a}_i}}\,\frac{1}{E_{\mathbf{A}+\mathbf{Q}}}$$
$$\times\,\hat{f}_{n+k}(\mathbf{p}_1,...,\mathbf{p}_n,\mathbf{a}_1,...,\mathbf{a}_{k-1},-\mathbf{A}-\mathbf{Q})\,\hat{f}^*_{m+k}(\mathbf{q}_1,...,\mathbf{q}_m,\mathbf{a}_1,...,\mathbf{a}_{k-1},-\mathbf{A}-\mathbf{Q})\,, \quad (7.27)$$

where

$$\mathbf{A}=\sum_{i=1}^{k-1}\mathbf{a}_i\,. \quad (7.28)$$

7.2.1 Large time behavior

For $t\to\infty$ the integrand of (7.25) rapidly oscillates because of the exponential factor $e^{i(\tilde{E}-E)t}$ and suppresses the integrals unless the phase is stationary, namely unless the momenta are small. The coefficient functions and the matrix elements in (7.25) generically go to constants in this limit[5]. The behavior for t large enough of the contribution to (7.25) with (m,n) quasiparticles is then obtained using the non-relativistic expression of the energies and rescaling the momentum components by $\sqrt{t}$; this gives

$$\left[B^{\Phi}_{m,n}\,t^{-(m+n-2+\delta_{n,0}+\delta_{m,0})d/2}+\tilde{B}^{\Phi}_{m,n}\,t^{-(m+n-1-\delta_{n,1}\delta_{m,1})d/2}\right]e^{i(m-n)Mt}, \quad (7.29)$$

where $B^{\Phi}_{m,n}$ and $\tilde{B}^{\Phi}_{m,n}$ are constants and we took into account that the term $(m,n)=(0,0)$ is not present in (7.25). We see that the leading time dependence comes from (m,n) equal $(1,0)$ and $(0,1)$ and corresponds to undamped oscillations. Notice that in absence of the delta function in (7.22) (i.e. in the generic inhomogeneous case of previous section) the oscillations coming from the $(1,0)$ and $(0,1)$ contributions would be damped as $t^{-d/2}$.

Since the only relativistic invariant that can be formed from the energy and momentum of a single particle is a constant, $F^{\Phi}_{m,n}$ with $m+n=1$ is a constant. Besides (7.16), the matrix elements $F^{\Phi}_{m,n}$ with m and n interchanged are related by crossing symmetry [8], which amounts to analytic continuation in the momenta; this leads to the real constant

$$F^{\Phi}_{0,1}=F^{\Phi}_{1,0}\equiv F^{\Phi}_1\,. \quad (7.30)$$

Putting all together, the large time limit of the one-point function (7.20) is given by

$$\langle\Phi(t)\rangle=A_\Phi+\frac{F^{\Phi}_1}{(2\pi)^d M}(h_1\,e^{-iMt}+h_1^*\,e^{iMt})+O(t^{-d/2})\,,\qquad t\to\infty\,, \quad (7.31)$$

with

$$h_1=h_{0,1}(0)+\tilde{h}_{0,1}(0)\,, \quad (7.32)$$

[4]For $m=0$ and $k=1$ there no momenta $\mathbf{q}_i$ and $\mathbf{a}_i$. In this case $E_{\mathbf{A}+\mathbf{Q}}=E_0=M$.

[5]The case $d=1$ involves some additional consideration that we postpone to section 7.3.

and

$$A_\Phi = \langle\Phi(0)\rangle - \sum_{\substack{m,n=0\\(m,n)\neq(0,0),(1,1)}}^{\infty} \int \prod_{i=1}^{n} \frac{d\mathbf{p}_i}{(2\pi)^d E_{\mathbf{p}_i}} \prod_{j=1}^{m} \frac{d\mathbf{q}_j}{(2\pi)^d E_{\mathbf{q}_j}} \left[\delta(\mathbf{P})\delta(\mathbf{Q}) \right.$$
$$\left. \times\, h_{m,n}(\mathbf{q}_1,...,\mathbf{q}_m,\mathbf{p}_1,...,\mathbf{p}_n) + \delta(\mathbf{Q}-\mathbf{P})\,\tilde{h}_{m,n}(\mathbf{q}_1,...,\mathbf{q}_m,\mathbf{p}_1,...,\mathbf{p}_n)\right]$$
$$\times\, F^{\Phi,c}_{m,n}(\mathbf{q}_1,...,\mathbf{q}_m|\mathbf{p}_1,...,\mathbf{p}_n)\,. \tag{7.33}$$

In the physical dynamical problems we consider, the $\hat{f}_n$'s in (7.22) are nonzero unless an internal symmetry[6] forces some of them to vanish. In the current case of a single particle species, a $\mathbb{Z}_2$ symmetry may lead to the vanishing of the $\hat{f}_n$'s with n even or of those with n odd. Since h_1 is a sum of terms containing $\hat{f}^*_n\hat{f}_{n+1}$, we have $h_1 \neq 0$ unless $\hat{f}_0\hat{f}_1 = 0$. Hence, the condition for the presence of undamped oscillations in (7.31) is $\hat{f}_0\hat{f}_1F^\Phi_1 \neq 0$.

Notice that the asymptotic offset (7.33) differs from the constant $\langle\Phi(0)\rangle - G^s_\Phi(0)$ entering (7.20) for the subtraction of the term $(m,n) = (1,1)$ in the sum; the reason is that in (7.20) this term is canceled by the $(1,1)$ contribution to (7.25), which has $\tilde{E} = E$ and is time-independent. Equation (7.29) shows that the first subleading contributions to (7.31) come from (m,n) equal $(0,2)$, $(2,0)$, $(1,2)$ and $(2,1)$ and correspond to damped oscillations.

The analysis we performed above is easily generalized along the same lines to the case of several quasiparticle species $a = 1,2,...,k$ with masses M_a. In particular, the oscillations that remain undamped at large times take the form

$$\sum_{a=1}^{k} \frac{F^\Phi_{1a}}{(2\pi)^d M_a}(h_{1a}\,e^{-iM_at} + h^*_{1a}\,e^{iM_at}) + \sum_{\substack{a,b\\M_a\neq M_b}} \frac{F^\Phi_{1b,1a}(0|0)}{(2\pi)^{2d}} \frac{h_{1b,1a}(0,0)}{M_aM_b} e^{i(M_b-M_a)t}, \tag{7.34}$$

where the first sum generalizes the term present in (7.31), with F^Φ_{1a} and h_{1a} corresponding to (7.30) and (7.32) with the specification of the species of the particle. The second sum, on the other hand, is a contribution arising from the fact that the term $(m,n) = (1,1)$ is no longer time-independent when the two particles have different masses; $h_{1b,1a}$ corresponds to $h_{1,1}$ of (7.26) with the specification of the quasiparticle species[7]. We also see that the condition for the presence of this second type of undamped oscillations is $\hat{f}_{1b}\hat{f}_{1a}F^\Phi_{1b,1a} \neq 0$. Once again this condition involves one-quasiparticle states and is satisfied unless an internal symmetry causes the vanishing of one of the three factors. This clarifies the role of symmetries for undamped oscillations, a role that had been debated in the literature (see [102] and references therein). In the perturbative theory of quantum quenches, the undamped oscillations with frequencies $M_b - M_a$ arise at second order in the quench size [58], as will also be seen in the next section.

[6]The symmetry can also be topological, see the example of [87] (chapter 6).

[7]For $a \neq b$, $F^\Phi_{1b,1a} = F^{\Phi,c}_{1b,1a}$ follows from the fact that particles of different species cannot annihilate each other. The contribution multiplying $\tilde{h}_{1b,1a}$ is damped at large times.

7.3 Comparison with perturbative results

The Hamiltonian (7.1) includes as a particular case that in which the negative and positive time Hamiltonians differ for the change of an interaction parameter, namely the homogeneous quench

$$\begin{cases} H_0\,, & t<0\,, \\ H=H_0+\lambda\int_{-\infty}^{\infty} d\mathbf{x}\,\Psi(\mathbf{x})\,, & t\geq 0\,. \end{cases} \tag{7.35}$$

We then refer to $\Psi(x)$ as the quench operator and to λ as the quench size. As seen in chapter 4, a general perturbative analysis can be performed in the quench size [56], in any dimension d [59] and for arbitrarily strong interaction among the quasiparticles. When the system is in the ground state of H_0 for negative times, the post-quench state is given by (7.22) with[8] [56, 59]

$$\hat{f}_0 = 1 + O(\lambda^2)\,, \tag{7.36}$$

$$\hat{f}_{n\geq 1}(\mathbf{p}_1,...,\mathbf{p}_n) = \lambda\,\frac{(2\pi)^d}{n!E}\,F^{\Psi}_{n,0}(\mathbf{p}_1,...,\mathbf{p}_n|) + O(\lambda^2)\,. \tag{7.37}$$

It then follows from (7.32), (7.26), (7.27) and (7.30) that

$$h_1 = h_{0,1}(0) + O(\lambda^2) = \hat{f}_1(0) + O(\lambda^2) = \frac{\lambda}{M}(2\pi)^d F_1^{\Psi} + O(\lambda^2)\,, \tag{7.38}$$

and from (7.31) that undamped oscillations

$$\lambda\,\frac{2}{M^2} F_1^{\Psi} F_1^{\Phi}\cos Mt + O(\lambda^2) \tag{7.39}$$

show up already at leading order in the quench size, as originally shown in [56]. Notice also that (7.26) leads to

$$h_{1b,1a}(0,0) = \lambda^2\,\frac{(2\pi)^{2d}}{M_a M_b}\,F^{\Psi}_{1a}F^{\Psi}_{1b} + O(\lambda^3)\,, \tag{7.40}$$

so that in perturbation theory the undamped oscillations with frequencies $M_a - M_b$ in (7.34) arise at second order in the quench size, as observed in [58].

While the expressions (7.39) and (7.40) coincide with those of the perturbative calculations of [56, 58], a subtlety has to be pointed out: those perturbative calculations were performed in the basis of the quasiparticle states of the pre-quench theory (i.e. the unperturbed theory $\lambda = 0$), while the basis we use in this chapter is that of the $t > 0$ theory. The

[8] The result (7.37) shows the peculiarity of the case of non-interacting quasiparticles, for which H_0 and the quench operator are quadratic in the excitation modes and $F^{\Psi}_{n,0}$ vanishes for $n \neq 2$. As a consequence the post-quench state is made of pairs of quasiparticles with opposite momenta, a structure that does not occur for interacting quasiparticles.

point, however, is that the difference between the two bases can be ignored when working at leading order in perturbation theory[9].

We see from (7.36), (7.37), (7.26) and (7.27) that $h_{m,n}$ are of order λ^2 unless m or n vanish, and that $\tilde{h}_{m,n}$ are in any case of order λ^2. It follows that the asymptotic offset (7.33) takes the form

$$A_\Phi = \langle \Phi(0) \rangle - \sum_{n=1}^{\infty} \int \prod_{i=1}^{n} \frac{d\mathbf{p}_i}{(2\pi)^d E_{\mathbf{p}_i}} \, \delta(\mathbf{P}) \left[h_{0,n}(\mathbf{p}_1, ..., \mathbf{p}_n) \, F^{\Phi}_{0,n}(|\mathbf{p}_1, ..., \mathbf{p}_n) + c.c. \right] + O(\lambda^2) \,, \tag{7.41}$$

where $\langle \Phi(0) \rangle$ is now the expectation value on the ground state of the pre-quench theory, and

$$h_{0,n}(\mathbf{p}_1, ..., \mathbf{p}_n) = \hat{f}_0^* \hat{f}_n(\mathbf{p}_1, ..., \mathbf{p}_n) = \lambda \, \frac{(2\pi)^d}{n! E} \, [F^{\Psi}_{0,n}(|\mathbf{p}_1, ..., \mathbf{p}_n)]^* + O(\lambda^2) \,. \tag{7.42}$$

It was shown in [57] that (7.41), (7.42) lead to

$$A_\Phi = \langle \Phi \rangle_\lambda + O(\lambda^2) \,, \tag{7.43}$$

where $\langle \Phi \rangle_\lambda$ is the expectation value on the ground state of the post-quench theory. The non-perturbative expression (7.33) suggests that in general there is no simple way of expressing the offset.

In our analysis of the large time behavior of one-point functions in the previous section we used the fact that the matrix elements (7.13) generically go to some finite constant when the momenta tend to zero. In $d = 1$, however, the quasiparticles often possess a fermionic statistics[10], and for the matrix elements (7.13) this leads to a zero when $\mathbf{q}_i = \mathbf{q}_j$ or $\mathbf{p}_i = \mathbf{p}_j$, as well as to a pole[11] when $\mathbf{q}_i = \mathbf{p}_j$. The combined effect of these poles and zeros in the matrix elements (7.13) and in the coefficient functions which multiply them in the expressions such as (7.25) can affect the powers of time in (7.29), but not the undamped oscillations in (7.31) which are generally derived in any dimension. The perturbative results recalled above are of course consistent with this fact, and indicate that fermionic statitistics in $d = 1$ affects the decay of the remainder in (7.31) ($t^{-3/2}$ instead of $t^{-1/2}$) [56, 59]. If the quasiparticles have fermionic statistics the suitable sign factors have to be introduced in (7.14) and will affect the combinatorial prefactor in (7.27).

7.4 Final remarks

In this chapter we studied the non-equilibrium dynamics of quantum statistical systems in d spatial dimensions which for positive times evolve with a Hamiltonian H which is time-

[9] This is true in the generic case for which the quasiparticle content does not change when passing from $\lambda = 0$ to λ small. See [57] for the discussion and examples of the special case in which this condition is not fulfilled.

[10] The basic example is provided by the Ising chain, see [23] for a review.

[11] The residues on such annihilation poles are generally known in the case of integrable theories, see [85].

independent and translation invariant in space. The non-equilibrium state was expanded on the basis of energy eigenstates (asymptotic quasiparticle states) of H, with coefficient functions f_n which were left generic in order to account for arbitrary evolution for $t < 0$ under some Hamiltonian $H_0(\mathbf{x}, t)$. We then showed how the evolution for positive times of the one-point functions of local operators (e.g. the order parameter) depends on the f_n's.

While the theory shows that the large time dynamics is determined by low-energy modes, our framework ensures that the results hold also in the vicinity of quantum critical points. It also allows to appreciate the role played by the connectedness structure of matrix elements, a circumstance noted since [69], where this structure was shown to account for the lightcone spreading of correlations in two-point functions.

In the generic case (7.1), in which translation invariance is absent, the theory leads to oscillations of the one-point functions that normally decay as $t \to \infty$. This is the case, in particular, when the system is confined in a finite region of space before this spatial constraint is removed for $t > 0$ (release from a trap[12]). In such a situation, the energy density carried by the quasiparticle excitations goes to zero in any point of space as $t \to \infty$ (local dissipation) and is insufficient to sustain the oscillations at large enough times. A first illustration of this phenomenon was given perturbatively in [58, 59] in the framework of inhomogeneous quantum quenches.

On the other hand, when the analysis is specialized to the case in which no spatial inhomogeneity is inherited from negative times, the theory shows that one-point functions exhibit undampend oscillations when no internal symmetry prevents a one-quasiparticle contribution to the non-equilibrium state or the coupling of the operator to this contribution. This result confirms the one obtained perturbatively since [56, 58] for the case of the instantaneous change of an interaction parameter. Since the theory shows the role of translation invariance in keeping the oscillations undamped, observing no damping in the cases predicted by the theory can be used to test up to which timescale numerical simulations remain reliable (i.e. insensitive to finite size or other undesired effects).

We also obtained the expression (7.33) of the asymptotic offset of one-point functions in terms of the matrix elements of the operator and of the coefficients specifying the non-equilibrium state. We showed how the structure of this result simplifies in the particular case of a small quench from the ground state and allows, up to higher order corrections in the quench size, the resummation originally shown in [57]. While no similar resummations seem likely for the full result (7.33), it is known that expansions over quasiparticles modes often converge rapidly providing very good approximations from the first few terms[13]. It will be interesting to investigate to which extent this happens in the present case.

[12] See the early experimental realization of [103], where oscillations were observed.

[13] This has been checked in detail for integrable models, see [23].

Bibliography

[1] L. Landau and E. Lifshitz, *Statistical Physics*, vol. 5. Elsevier Science, 1980.

[2] K. G. Wilson and J. Kogut, "The renormalization group and the ϵ expansion," *Physics Reports*, vol. 12, no. 2, pp. 75–199, 1974.

[3] K. G. Wilson, "The renormalization group: Critical phenomena and the Kondo problem," *Reviews of modern physics*, vol. 47, no. 4, p. 773, 1975.

[4] J. Zinn-Justin, *Quantum Field Theory and Critical Phenomena*. International series of monographs on physics, Oxford University Press, 2021.

[5] J. Cardy, *Scaling and Renormalization in Statistical Physics*, vol. 5 of *Cambridge Lecture Notes in Physics*. Cambridge University Press, 1996.

[6] G.-C. Wick, "Properties of Bethe-Salpeter wave functions," *Physical Review*, vol. 96, no. 4, p. 1124, 1954.

[7] S. Weinberg, *The Quantum Theory of Fields: Volume 2, Modern Applications*. Cambridge University Press, 1996.

[8] R. Eden, P. Landshoff, D. Olive, and J. Polkinghorne, *The Analytic S-Matrix*. Cambridge University Press, 1966.

[9] C. Itzykson and J.-M. Drouffe, *Statistical Field Theory*. Cambridge Monographs on Mathematical Physics, Cambridge University Press, 1991.

[10] F. Buff, R. Lovett, and F. Stillinger Jr, "Interfacial density profile for fluids in the critical region," *Physical Review Letters*, vol. 15, no. 15, p. 621, 1965.

[11] T. Gotō, "Relativistic quantum mechanics of one-dimensional mechanical continuum and subsidiary condition of dual resonance model," *Progress of Theoretical Physics*, vol. 46, no. 5, pp. 1560–1569, 1971.

[12] Y. Nambu, "Strings, monopoles, and gauge fields," *Physical Review D*, vol. 10, no. 12, p. 4262, 1974.

[13] G. Delfino, W. Selke, and A. Squarcini, "Particles, string and interface in the three-dimensional Ising model," *Nuclear Physics B*, vol. 958, p. 115139, 2020.

[14] G. Delfino, M. Sorba, and A. Squarcini, "Interface in presence of a wall. Results from field theory," *Nuclear Physics B*, vol. 967, p. 115396, 2021.

[15] L. H. Ryder, *Quantum field theory*. Cambridge University Press, 1996.

[16] G. Delfino and J. Viti, "Phase separation and interface structure in two dimensions from field theory," *Journal of Statistical Mechanics: Theory and Experiment*, vol. 2012, no. 10, p. P10009, 2012.

[17] G. Delfino and A. Squarcini, "Exact theory of intermediate phases in two dimensions," *Annals of Physics*, vol. 342, pp. 171–194, 2014.

[18] G. Delfino and A. Squarcini, "Phase separation in a wedge: exact results," *Physical Review Letters*, vol. 113, no. 6, p. 066101, 2014.

[19] M. Caselle, M. Hasenbusch, and M. Panero, "The interface free energy: comparison of accurate Monte Carlo results for the 3D Ising model with effective interface models," *Journal of High Energy Physics*, vol. 2007, no. 09, p. 117, 2007.

[20] D. B. Abraham, "Capillary waves and surface tension: an exactly solvable model," *Physical Review Letters*, vol. 47, no. 8, p. 545, 1981.

[21] D. B. Abraham, "Surface structures and phase transitions - Exact results," in *Phases Transitions and Critical Phenomena* (C. Domb and J. L. Lebowitz, eds.), vol. 10, p. 1, Academic Press, London, 1986.

[22] B. M. McCoy and T. T. Wu, "Two-dimensional Ising field theory in a magnetic field: breakup of the cut in the two-point function," *Physical Review D*, vol. 18, no. 4, p. 1259, 1978.

[23] G. Delfino, "Integrable field theory and critical phenomena: the Ising model in a magnetic field," *Journal of Physics A: Mathematical and General*, vol. 37, no. 14, p. R45, 2004.

[24] D. B. Abraham and M. Issigoni, "Phase separation at the surface of an Ising ferromagnet," *Journal of Physics A: Mathematical and General*, vol. 13, no. 4, p. L89, 1980.

[25] G. Delfino and A. Squarcini, "Interfaces and wetting transition on the half plane. Exact results from field theory," *Journal of Statistical Mechanics: Theory and Experiment*, vol. 2013, no. 05, p. P05010, 2013.

[26] G. Delfino and A. Squarcini, "Long range correlations generated by phase separation. Exact results from field theory," *Journal of High Energy Physics*, vol. 2016, no. 11, pp. 1–31, 2016.

[27] P.-G. De Gennes, "Wetting: statics and dynamics," *Reviews of modern physics*, vol. 57, no. 3, p. 827, 1985.

[28] S. Dietrich, "Wetting phenomena," in *Phase transitions and critical phenomena* (C. Domb and J. L. Lebowitz, eds.), vol. 12, pp. 1–218, Academic Press, London, 1988.

[29] D. Bonn, J. Eggers, J. Indekeu, J. Meunier, and E. Rolley, "Wetting and spreading," *Reviews of modern physics*, vol. 81, no. 2, p. 739, 2009.

[30] L. D. Landau and E. M. Lifshitz, *Quantum mechanics: non-relativistic theory*, vol. 3. Elsevier, 2013.

[31] S. Ghoshal and A. Zamolodchikov, "Boundary S-matrix and boundary state in two-dimensional integrable quantum field theory," *International Journal of Modern Physics A*, vol. 9, no. 21, pp. 3841–3885, 1994.

[32] K. Binder, D. Landau, and D. Kroll, "Critical wetting with short-range forces: is mean-field theory valid?," *Physical review letters*, vol. 56, no. 21, p. 2272, 1986.

[33] K. Binder and D. Landau, "Wetting and layering in the nearest-neighbor simple-cubic Ising lattice: a Monte Carlo investigation," *Physical Review B*, vol. 37, no. 4, p. 1745, 1988.

[34] K. Ragil, J. Meunier, D. Broseta, J. O. Indekeu, and D. Bonn, "Experimental observation of critical wetting," *Physical review letters*, vol. 77, no. 8, p. 1532, 1996.

[35] D. Ross, D. Bonn, and J. Meunier, "Observation of short-range critical wetting," *Nature*, vol. 400, no. 6746, pp. 737–739, 1999.

[36] A. Parry and R. Evans, "Comment on simple scaling theory for three-dimensional critical wetting with short-ranged forces," *Physical Review B*, vol. 39, no. 16, p. 12336, 1989.

[37] G. Delfino, "Interface localization near criticality," *Journal of High Energy Physics*, vol. 2016, no. 5, pp. 1–11, 2016.

[38] D. B. Abraham, "Solvable model with a roughening transition for a planar Ising ferromagnet," *Physical Review Letters*, vol. 44, no. 18, p. 1165, 1980.

[39] S. Coleman, *Aspects of Symmetry: Selected Erice lectures*. Cambridge University Press, 1988.

[40] S. Coleman, "Quantum sine-Gordon equation as the massive Thirring model," *Physical Review D*, vol. 11, no. 8, p. 2088, 1975.

[41] S. Mandelstam, "Soliton operators for the quantized sine-Gordon equation," *Physical Review D*, vol. 11, no. 10, p. 3026, 1975.

[42] A. B. Zamolodchikov and A. B. Zamolodchikov, "Factorized S-matrices in two dimensions as the exact solutions of certain relativistic quantum field theory models," *Annals of physics*, vol. 120, no. 2, pp. 253–291, 1979.

[43] G. Delfino, "Order parameter profiles in presence of topological defect lines," *Journal of Physics A: Mathematical and Theoretical*, vol. 47, no. 13, p. 132001, 2014.

[44] G. Delfino, W. Selke, and A. Squarcini, "Vortex mass in the three-dimensional O(2) scalar theory," *Physical Review Letters*, vol. 122, no. 5, p. 050602, 2019.

[45] J. Lipa, D. Swanson, J. Nissen, T. Chui, and U. Israelsson, "Heat capacity and thermal relaxation of bulk helium very near the lambda point," *Physical review letters*, vol. 76, no. 6, p. 944, 1996.

[46] M. Panero and A. Smecca, "Topological excitations in statistical field theory at the upper critical dimension," *Journal of High Energy Physics*, vol. 2021, no. 3, pp. 1–14, 2021.

[47] A. Smecca and M. Panero, "Monopole-like configurations in the O(3) spin model at the upper critical dimension," *PoS*, vol. LATTICE2021, p. 121, 2022.

[48] G. Delfino and M. Sorba, "Mass of quantum topological excitations and order parameter finite size dependence," *Journal of Physics A: Mathematical and Theoretical*, vol. 57, no. 8, p. 085003, 2024.

[49] B. Berg, M. Karowski, and P. Weisz, "Construction of Green's functions from an exact S-matrix," *Physical Review D*, vol. 19, no. 8, p. 2477, 1979.

[50] G. Derrick, "Comments on nonlinear wave equations as models for elementary particles," *Journal of Mathematical Physics*, vol. 5, no. 9, pp. 1252–1254, 1964.

[51] A. Squarcini and A. Tinti, "Correlations and structure of interfaces in the ising model: theory and numerics," *Journal of Statistical Mechanics: Theory and Experiment*, vol. 2021, no. 8, p. 083209, 2021.

[52] A. Polkovnikov, K. Sengupta, A. Silva, and M. Vengalattore, "Nonequilibrium dynamics of closed interacting quantum systems," *Reviews of Modern Physics*, vol. 83, no. 3, p. 863, 2011.

[53] C. Gogolin and J. Eisert, "Equilibration, thermalisation, and the emergence of statistical mechanics in closed quantum systems," *Reports on Progress in Physics*, vol. 79, no. 5, p. 056001, 2016.

[54] L. D'Alessio, Y. Kafri, A. Polkovnikov, and M. Rigol, "From quantum chaos and eigenstate thermalization to statistical mechanics and thermodynamics," *Advances in Physics*, vol. 65, no. 3, pp. 239–362, 2016.

[55] E. Barouch, B. M. McCoy, and M. Dresden, "Statistical mechanics of the XY model. I," *Physical Review A*, vol. 2, no. 3, p. 1075, 1970.

[56] G. Delfino, "Quantum quenches with integrable pre-quench dynamics," *Journal of Physics A: Mathematical and Theoretical*, vol. 47, no. 40, p. 402001, 2014.

[57] G. Delfino and J. Viti, "On the theory of quantum quenches in near-critical systems," *Journal of Physics A: Mathematical and Theoretical*, vol. 50, no. 8, p. 084004, 2017.

[58] G. Delfino, "Persistent oscillations after quantum quenches: The inhomogeneous case," *Nuclear Physics B*, vol. 954, p. 115002, 2020.

[59] G. Delfino and M. Sorba, "Persistent oscillations after quantum quenches in d dimensions," *Nuclear Physics B*, vol. 974, p. 115643, 2022.

[60] G. Delfino and M. Sorba, "Quantum quenches from an excited state," *Nuclear Physics B*, vol. 994, p. 116312, 2023.

[61] K. Sengupta, S. Powell, and S. Sachdev, "Quench dynamics across quantum critical points," *Physical Review A*, vol. 69, no. 5, p. 053616, 2004.

[62] P. Calabrese and J. Cardy, "Evolution of entanglement entropy in one-dimensional systems," *Journal of Statistical Mechanics: Theory and Experiment*, vol. 2005, no. 04, p. P04010, 2005.

[63] O. A. Castro-Alvaredo, M. Lencsés, I. M. Szécsényi, and J. Viti, "Entanglement oscillations near a quantum critical point," *Physical Review Letters*, vol. 124, no. 23, p. 230601, 2020.

[64] M. C. Bañuls, J. I. Cirac, and M. B. Hastings, "Strong and weak thermalization of infinite nonintegrable quantum systems," *Physical review letters*, vol. 106, no. 5, p. 050405, 2011.

[65] M. Kormos, M. Collura, G. Takács, and P. Calabrese, "Real-time confinement following a quantum quench to a non-integrable model," *Nature Physics*, vol. 13, no. 3, pp. 246–249, 2017.

[66] H. Bernien, S. Schwartz, A. Keesling, H. Levine, A. Omran, H. Pichler, S. Choi, A. S. Zibrov, M. Endres, M. Greiner, *et al.*, "Probing many-body dynamics on a 51-atom quantum simulator," *Nature*, vol. 551, no. 7682, pp. 579–584, 2017.

[67] F. Liu, R. Lundgren, P. Titum, G. Pagano, J. Zhang, C. Monroe, and A. V. Gorshkov, "Confined quasiparticle dynamics in long-range interacting quantum spin chains," *Physical review letters*, vol. 122, no. 15, p. 150601, 2019.

[68] P. Emonts and I. Kukuljan, "Reduced density matrix and entanglement of interacting quantum field theories with Hamiltonian truncation," *Physical Review Research*, vol. 4, no. 3, p. 033039, 2022.

[69] G. Delfino, "Correlation spreading and properties of the quantum state in quench dynamics," *Physical Review E*, vol. 97, no. 6, p. 062138, 2018.

[70] G. Barton, *Introduction to dispersion techniques in field theory.* Lecture notes and supplements in physics, W.A. Benjamin, New York, 1965.

[71] G. Delfino, G. Mussardo, and P. Simonetti, "Non-integrable quantum field theories as perturbations of certain integrable models," *Nuclear Physics B*, vol. 473, no. 3, pp. 469–508, 1996.

[72] P. Calabrese, F. H. Essler, and M. Fagotti, "Quantum quench in the transverse field Ising chain: I. time evolution of order parameter correlators," *Journal of Statistical Mechanics: Theory and Experiment*, vol. 2012, no. 07, p. P07016, 2012.

[73] D. Schuricht and F. H. Essler, "Dynamics in the Ising field theory after a quantum quench," *Journal of Statistical Mechanics: Theory and Experiment*, vol. 2012, no. 04, p. P04017, 2012.

[74] G. Delfino and P. Grinza, "Confinement in the q-state Potts field theory," *Nuclear Physics B*, vol. 791, no. 3, pp. 265–283, 2008.

[75] L. Lepori, G. Z. Toth, and G. Delfino, "The particle spectrum of the three-state Potts field theory: a numerical study," *Journal of Statistical Mechanics: Theory and Experiment*, vol. 2009, no. 11, p. P11007, 2009.

[76] M. Caselle and M. Hasenbusch, "Universal amplitude ratios in the three-dimensional Ising model," *Journal of Physics A: Mathematical and General*, vol. 30, no. 14, p. 4963, 1997.

[77] D. Lee, N. Salwen, and M. Windoloski, "Introduction to stochastic error correction methods," *Physics Letters B*, vol. 502, no. 1-4, pp. 329–337, 2001.

[78] M. Caselle, M. Hasenbusch, P. Provero, and K. Zarembo, "Bound states and glueballs in three-dimensional Ising systems," *Nuclear Physics B*, vol. 623, no. 3, pp. 474–492, 2002.

[79] S. Dusuel, M. Kamfor, K. P. Schmidt, R. Thomale, and J. Vidal, "Bound states in two-dimensional spin systems near the Ising limit: A quantum finite-lattice study," *Physical Review B*, vol. 81, no. 6, p. 064412, 2010.

[80] Y. Nishiyama, "Magnon-bound-state hierarchy for the two-dimensional transverse-field Ising model in the ordered phase," *Physica A: Statistical Mechanics and its Applications*, vol. 463, pp. 303–309, 2016.

[81] F. Rose, F. Benitez, F. Léonard, and B. Delamotte, "Bound states of the ϕ^4 model via the nonperturbative renormalization group," *Physical Review D*, vol. 93, no. 12, p. 125018, 2016.

[82] K. Hódsági, M. Kormos, and G. Takács, "Quench dynamics of the Ising field theory in a magnetic field," *SciPost Physics*, vol. 5, no. 3, p. 027, 2018.

[83] T. Hashizume, J. C. Halimeh, and I. P. McCulloch, "Hybrid infinite time-evolving block decimation algorithm for long-range multidimensional quantum many-body systems," *Physical Review B*, vol. 102, no. 3, p. 035115, 2020.

[84] T. Hashizume, I. P. McCulloch, and J. C. Halimeh, "Dynamical phase transitions in the two-dimensional transverse-field Ising model," *Physical Review Research*, vol. 4, no. 1, p. 013250, 2022.

[85] F. A. Smirnov, *Form factors in completely integrable models of quantum field theory*, vol. 14. World Scientific, 1992.

[86] G. Delfino and J. L. Cardy, "Universal amplitude ratios in the two-dimensional q-state Potts model and percolation from quantum field theory," *Nuclear Physics B*, vol. 519, no. 3, pp. 551–578, 1998.

[87] G. Delfino and M. Sorba, "Space of initial conditions and universality in nonequilibrium quantum dynamics," *Nuclear Physics B*, vol. 983, p. 115910, 2022.

[88] D. Abraham and P. Reed, "Phase separation in the two-dimensional Ising ferromagnet," *Physical Review Letters*, vol. 33, no. 6, p. 377, 1974.

[89] D. B. Abraham and P. Reed, "Interface profile of the Ising ferromagnet in two dimensions," *Communications in Mathematical Physics*, vol. 49, pp. 35–46, 1976.

[90] T. Antal, Z. Rácz, A. Rákos, and G. M. Schütz, "Transport in the XX chain at zero temperature: Emergence of flat magnetization profiles," *Physical Review E*, vol. 59, no. 5, p. 4912, 1999.

[91] V. Zauner, M. Ganahl, H. G. Evertz, and T. Nishino, "Time evolution within a comoving window: scaling of signal fronts and magnetization plateaus after a local quench in quantum spin chains," *Journal of Physics: Condensed Matter*, vol. 27, no. 42, p. 425602, 2015.

[92] V. Eisler, F. Maislinger, and H. G. Evertz, "Universal front propagation in the quantum Ising chain with domain-wall initial states," *SciPost Physics*, vol. 1, no. 2, p. 014, 2016.

[93] V. Hunyadi, Z. Rácz, and L. Sasvári, "Dynamic scaling of fronts in the quantum XX chain," *Physical Review E*, vol. 69, no. 6, p. 066103, 2004.

[94] J. Sólyom, "Duality of the block transformation and decimation for quantum spin systems," *Physical Review B*, vol. 24, no. 1, p. 230, 1981.

[95] J. C. Bridgeman, A. O'Brien, S. D. Bartlett, and A. C. Doherty, "Multiscale entanglement renormalization ansatz for spin chains with continuously varying criticality," *Physical Review B*, vol. 91, no. 16, p. 165129, 2015.

[96] R. Baxter, *Exactly Solved Models in Statistical Mechanics*. Academic Press, 1982.

[97] G. Delfino and P. Grinza, "Universal ratios along a line of critical points. the Ashkin-Teller model," *Nuclear Physics B*, vol. 682, no. 3, pp. 521–550, 2004.

[98] G. Delfino, W. Selke, and A. Squarcini, "Structure of interfaces at phase coexistence. theory and numerics," *Journal of Statistical Mechanics: Theory and Experiment*, vol. 2018, no. 5, p. 053203, 2018.

[99] R. Köberle and J. A. Swieca, "Factorizable Z(n) models," *Physics Letters B*, vol. 86, no. 2, pp. 209–210, 1979.

[100] A. Zamolodchikov, "Integrals of motion in scaling 3-state Potts model field theory," *International Journal of Modern Physics A*, vol. 3, no. 03, pp. 743–750, 1988.

[101] M. Caselle, G. Delfino, P. Grinza, O. Jahn, and N. Magnoli, "Potts correlators and the static three-quark potential," *Journal of Statistical Mechanics: Theory and Experiment*, vol. 2006, no. 03, p. P03008, 2006.

[102] M. Medenjak, B. Buča, and D. Jaksch, "Isolated Heisenberg magnet as a quantum time crystal," *Physical Review B*, vol. 102, no. 4, p. 041117, 2020.

[103] T. Kinoshita, T. Wenger, and D. S. Weiss, "A quantum Newton's cradle," *Nature*, vol. 440, no. 7086, pp. 900–903, 2006.